

MODERN DEVELOPMENT OF MAGNETIC RESONANCE

abstracts

2013

KAZAN * RUSSIA



MODERN DEVELOPMENT OF MAGNETIC RESONANCE

ABSTRACTS OF THE
INTERNATIONAL CONFERENCE

Editor:
KEV M. SALIKHOV

KAZAN, SEPTEMBER 24–28, 2013

Prof. Kev M. Salikhov
Zavoisky Physical-Technical Institute,
Russian Academy of Sciences, Kazan, Russian Federation
Phone: 7 (843) 2720503
E-mail: salikhov@kfti.knc.ru

This work is subject to copyright.

All rights are reserved, whether the whole or part of the material is concerned, specifically those of translation, reprinting, re-use of illustrations, broadcasting, reproduction by photocopying machines or similar means, and storage in data banks.

© 2013 Zavoisky Physical-Technical Institute, Kazan

© 2013 Igor A. Aksenov, graphic design

Printed in the Russian Federation

Published by Zavoisky Physical-Technical Institute, Kazan
www.kfti.knc.ru

CHAIRMAN

Kev Salikhov,
Full Member of the Russian Academy of Sciences

PROGRAM COMMITTEE

Albert Aganov (Russia)
Vadim Atsarkin (Russia)
Pavel Baranov (Russia)
Marina Bennati (Germany)
Bernhard Blümich (Germany)
Michael Bowman (USA)
Marina Brustolon (Italy)
Sabine Van Doorslaer (Belgium)
Jack Freed (USA)
Ilgiz Garifullin (Russia)
Graeme Hanson (Australia)
Martina Huber (The Netherlands)
Walter Kockenberger (UK)
Wolfgang Lubitz (Germany)
Klaus Möbius (Germany)
Hitoshi Ohta (Japan)
Igor Ovchinnikov (Russia)
Kev Salikhov (Russia)
Vladimir Skirda (Russia)
Murat Tagirov (Russia)
Takeji Takui (Japan)
Valery Tarasov (Russia)
Dmitrii Tayurskii (Russia)
Yurii Tsvetkov (Russia)
Violeta Voronkova (Russia)

LOCAL ORGANIZING COMMITTEE

Tarasov V.F., chairman

Adzhaliev Yu.A.

Akhmin S.M.

Falin M.L.

Gavrilova T.P.

Gerasimov K.I.

Goleneva V.M.

Gubaidulina A.Z.

Guseva R.R.

Kupriyanova O.O.

Kurkina N.G.

Lvov S.G.

Mosina L.V.

Petrushkin S.V.

Voronkova V.K.

Voronova L.V.

Yanduganova O.B.

SCIENTIFIC SECRETARY

Violeta K. Voronkova

The conference is organized under the auspices of the AMPERE Society

ORGANIZERS

Kazan E. K. Zavoisky Physical-Technical Institute
of the Kazan Scientific Center of the Russian Academy of Sciences
The Academy of Sciences of the Republic of Tatarstan

SUPPORTED BY

The Government of the Republic of Tatarstan
The Russian Foundation for Basic Research
Bruker BioSpin GmbH, Germany

CONFERENCE LOCATION

The Academy of Sciences of the Republic of Tatarstan
Kazan, ul. Baumana 20

CONTENTS

PLENARY LECTURES

Zavoisky Award Lecture. Pulsed EPR Dipolar Spectroscopy and its Applications <i>Yu. D. Tsvetkov</i>	2
The Water Splitting Machine of Photosynthesis Studied by EPR Techniques <i>W. Lubitz</i>	3
Multi-Extreme THz ESR: Its Developments and Applications <i>H. Ohta, S. Okubo, E. Ohmichi, T. Sakurai, T. Shimokawa</i>	4
EPR Methods for Characterizing Disorder and Structural Changes of Membrane Proteins <i>G. Jeschke, B. Joseph, E. Bordignon, M. Yulikov, Ye. Polyhach, T. von Hagens, V. Korkhov, C. Dietz, H. Paulsen</i>	5
PELDOR of Spin Labeled DNA <i>Yu. D. Tsvetkov, A. D. Milov, N. A. Kuznetsov, O. S. Fedorova</i>	7
Probing Conformational Changes in Photosynthetic Protein Complexes – News and Views from High-Field Dipolar EPR Spectroscopy <i>K. Möbius</i>	8
Uncovering a Complex Interplay of Spins, Orbitals and Charges in LaSrMnO ₄ by Sub-THz Spectroscopy in Ultra-Strong Magnetic Fields <i>V. Kataev</i>	10
High-Frequency EPR Evidence of Heisenberg Localized Magnetic Moments in MnSi <i>S. V. Demishev, A. V. Semeno, V. V. Glushkov, I. I. Lobanova, A. N. Samarina, N. E. Sluchanko</i>	11
Low-Temperature Electron Spin Dynamics and DNP <i>M. K. Bowman, A. G. Maryasov, V. M. Tormyshev</i>	13
Asymmetry of Electron Transfer in Photosystem I as Studied by Pump-Probe Femtosecond Absorption Spectrometry and W-band Transient EPR Spectroscopy <i>A. Yu. Semenov, A. Savitsky, K. Möbius, J. Golbeck, V. Nadochenko</i>	15
Multifunctional <i>in vivo</i> EPR Spectroscopy and Imaging Using Advanced Nitroxide and Trityl Paramagnetic Probes <i>V. V. Khramtsov</i>	17

SECTION 1
DEDICATION TO THE MEMORY OF THE LATE
YURII V. YABLOKOV

Invited Talks

- In memory of Yurii V. Yablokov
B. I. Kochelaev 20
- ESR in Combination with Luminescence and Mössbauer Methods
as a Tool for Investigation of Structure, Molecular Dynamics and
Redox Status of Biosystems
G. I. Likhtenshtein 21
- EPR Evidence of Molecular Photoeffect for Multiwall Carbon
Nanotubes
I. Geru 23
- Dedicated to Prof. Yu. V. Yablokov. Peculiarities of Interaction between
Jahn-Teller Centers
M. V. Eremin 25
- From Jahn-Teller Effect via Mixed Valence Clusters to Carbon
Materials – the Poznan’s Period
M. A. Augustyniak-Jablokow 26
- EPR of Clusters Containing Dysprosium Ions
V. K. Voronkova, A. A. Sukhanov, A. Baniodeh, A. K. Powell 28

SECTION 2
CHEMICAL AND BIOLOGICAL SYSTEMS

Invited Talks

- EPR of Switchable Magneto-Active Materials with Nitroxides
*E. G. Bagryanskaya, M. V. Fedin, S. L. Veber, I. Yu. Drozdyuk,
E. V. Tretyakov, V. I. Ovcharenko, A. M. Sheveleva, D. I. Kolokolov,
A. G. Stepanov* 30
- Structural Studies of Biological Membranes Using ESEEM Spectroscopy
of Spin Labels and Deuterium Substitution
S. A. Dzuba 32
- Oral Talks
- Short Nitroxide Biradicals: Comparison of EPR Data with
Quantum-Chemical Calculations
A. I. Kokorin, E. N. Golubeva, B. Y. Mladenova-Kattinig, G. Grampp 33
- Spin Relaxation and Magnetic Interactions in Light-Induced
Spin-Correlated Radical Pairs in P3HT:PC60BM Composite
L. V. Kulik, M. N. Uvarov, A. A. Popov, E. A. Lukina 35

SECTION 3
 CHEMICAL AND BIOLOGICAL SYSTEMS.
 ELECTRON SPIN BASED METHODS FOR ELECTRONIC
 AND SPATIAL STRUCTURE DETERMINATION

Invited Talks

- EPR Study on Mechanism of Catalyzed Reactions from Arylboronic
 Acids to Phenols
H. Yang, Y. Li, M. Jiang, H. Fu 38

Oral Talks

- Continuous-Wave and Time-Resolved Electron Paramagnetic Resonance
 Study of Dimerized Aza-Crown Copper Porphyrins
Yu. E. Kandrashkin, V. S. Iyudin, V. K. Voronkova, E. A. Mikhailitsyna,
V. S. Tyurin 40
- The Molten Globule State of Maltose Binding Protein: DEER
 Measurements at pH 3
M. Chakour, J. Reichenwallner, B. Selmke, C. Chen, S. Theison,
R. Chakraborty, S. Indu, R. Varadarajan, D. Hinderberger,
W. E. Trommer 42
- Investigation of C60 Derivatives with Two and Four Nitroxide Groups
 by Time-Resolved and Pulse EPR Spectroscopy
R. B. Zaripov, A. E. Mambetov, V. K. Voronkova, K. M. Salikhov,
V. P. Gubskaya, I. A. Nuretdinov 43

SECTION 4
 THEORY OF MAGNETIC RESONANCE,
 MODERN METHODS OF MAGNETIC RESONANCE

Invited Talks

- Molecular Dynamics and Electron Spin Relaxation
M. Brustolon, A. Barbon 46
- PELDOR Theory Revisited
K. M. Salikhov 47

Oral Talks

- Bruker BioSpin: Latest Developments in EPR Instrumentation
D. A. Kuznetsov 50
- Vector Models in Echo Detected EPR, ESEEM, and PELDOR
 of Anisotropic Paramagnetic Centers
A. G. Maryasov, M. K. Bowman, Yu. D. Tsvetkov 51
- Magnetic Resonance of Nd³⁺ Nanostructures in Perovskite Type Crystals
M. L. Falin, V. A. Latypov, M. M. Zaripov 52

Combined Magneto-Electric Spin Resonance of Impurity Ho Ions in Synthetic Forsterite <i>V. F. Tarasov, N. K. Solovarov, A. A. Sukhanov, R. B. Zaripov, E. V. Zharikov</i>	53
Manipulating Spin Hyper-Polarization by means of Adiabatic Switching of a Spin-Locking RF-Field <i>A. S. Kiryutin, K. L. Ivanov, A. V. Yurkovskaya, H.-M. Vieth, N. N. Lukzen</i>	54
Distance and Orientation Measurements with DEER/PELDOR at 95 and 263 GHz <i>I. Tkach, M. Bennati</i>	55
 SECTION 5 STRONGLY CORRELATED ELECTRON SYSTEMS	
Oral Talks	
Magnetic Order and Excitations in Iridium Oxides <i>G. Khaliullin</i>	58
NMR and High-Field ESR Study of the Low-Dimensional Quantum Magnet BaAg ₂ Cu[VO ₄] ₂ <i>E. L. Vavilova, V. Kataev, M. Schäpers, Y. Krupskaya, A. U. B. Wolter-Giraud, H.-J. Grafe, A. Möller, B. Büchner</i>	59
NMR Evidence for a Strong in Plane Electronic Anisotropy of Cobalt Ions in Sodium Cobaltates Na _{2/3} CoO ₂ <i>I. R. Mukhamedshin, H. Alloul</i>	60
EPR Study of Magnetic Anomalies in the La _{2-x} Sr _x CuO ₄ Single Crystals above the Critical Temperature <i>V. O. Sakhin, Yu. I. Talanov, L. F. Salakhutdinov, T. Adachi, T. Noji, Y. Koike</i>	61
 SECTION 6 OTHER APPLICATIONS OF MAGNETIC RESONANCE	
Oral Talks	
NQR Cross Relaxation of N-14 Nuclei in Low Magnetic Field <i>G. V. Mozzhukhin, B. Z. Rameev, G. S. Kupriyanova, P. Aksu, B. Aktaş</i>	64
The T ₁ and T ₂ Relaxation Times Distribution for the ³⁵ Cl and ¹⁴ N NQR in Microcomposites and in Porous Materials <i>N. Ya. Sinyavsky, G. S. Kupriyanova, F. N. Dolinenkov</i>	65
Characterization of Porous and Nanostructured Solid-Phase Systems by EPR of pH-sensitive Probes and Labels <i>E. G. Kovaleva, L. S. Molochnikov</i>	66

Application of Spin-Probe Method To Study the Effect of Antioxidants on Biological Membranes <i>in vitro</i> <i>E. L. Maltseva, V. V. Belov, T. E. Chasovskaya, N. P. Palmira</i>	68
Hyperfine Structure of EPR Spectra of Eu^{2+} in SrMoO_4 . The Determination of Sign b_2^0 and P_2^0 at all Temperatures <i>A. D. Gorlov</i>	70
Electron Spin Density Distribution in Cu(II)-(bis)Oxamate Complexes: an ESR Study <i>A. Aliabadi, A. Petr, M. A. Abdulmalic, T. Ruffer, V. Kataev, B. Büchner</i>	72
EPR-Based Evaluation of the Oxidative Status Using Cyclic Dinitrones as Spin Probe Precursors <i>T. V. Kobzeva, G. G. Dultseva</i>	73
EPR Study of the Impurity Defects in Diamonds Grown in Carbonate Medium <i>A. Y. Komarovskikh, V. A. Nadolinny, Y. N. Pal'yanov, I. N. Kupriyanov</i>	74
New Compact Coherent Heterodyne EPR-Spectrometer <i>A. N. Tcherepanov, A. N. Tararkov</i>	76

SECTION 7

SPIN-BASED INFORMATION PROCESSING

Invited Talks

Recent Trends in Open Shell Chemistry: Can Chemistry Contribute to Electron Spin Science/Spin Technology of QC/QIP? <i>T. Takui</i>	78
--	----

Oral Talks

Light-induced Generation and Coherent Manipulation of Entangled Quantum States in Molecular Crystals <i>G. Kothe, T. Yago, M. Lukaschek, J.-U. Weidner, G. Link, T.-S. Lin</i>	79
Electron Spin Echo Memory Realized in a Native Atomic Frequency Combs Structure at Room Temperature <i>K. I. Gerasimov, S. A. Moiseev, V. I. Morosov, R. B. Zaripov</i>	80
Point Defects in Silicon Carbide as a Perspective Basis for Quantum Electronics Operating at Room Temperature <i>V. A. Soltamov, A. A. Soltamova, P. G. Baranov, F. Fuchs, G. V. Astakhov, V. Dyakonov</i>	82

SECTION 8 LOW-DIMENSIONAL SYSTEMS AND NANO-SYSTEMS

Invited Talks

- High Field NMR Studies of Magnetic Field Driven Quantum
Criticality in $S = 1/2$ Antiferromagnetic Spin Chains
H.-H. Klauss 86

Oral Talks

- Size-Dependent Lattice Distortions in Nanocrystalline Ceria Doped with
 Gd^{3+} and Y^{3+} : an EPR Study
R. M. Rakhmatullin, L. K. Aminov, I. N. Kurkin, R. Böttcher,
A. Pöpl, S. Sen 87
- Electronic and Magnetic Properties of Three Dimensional Disordered
Network of Nanographites: ESR and Magnetic Susceptibility Data
A. M. Ziatdinov, N. S. Saenko 88
- Spin-Crossover Like Transitions in Quasi 1D Compounds of Cu(II)
Based Exchange Clusters
V. A. Morozov 89
- Spin Dynamics in a New Quasi 1D Sodium Cobalt Tellurate
E. A. Zvereva, M. I. Stratan, T. M. Vasilchikova, A. N. Vasiliev,
V. B. Nalbandyan, I. L. Shukaev, M. A. Evstigneeva, B. Büchner 91
- A Multi-Frequency EPR and ENDOR study of NO_3^{2-} Defect in
Nanosized Hydroxyapatite
T. B. Biktagirov, M. R. Gafurov, G. V. Mamin, S. B. Orlinskii,
A. A. Rodionov, B. V. Yavkin, E. S. Klimashina, V. I. Putlayev 93
- Uncovering Heterogeneous Metal-Ion Coordination in Aggregating
Peptides
S. Saxena 95

POSTERS

- Quantum Chemistry Calculations of EPR Parameters of a Reduced
[4Fe4S]⁺ Cluster: Hyperfine Constants of Hydrogen Atoms
L. I. Savostina, W. Lubitz, M. van Gastel 98
- The Transformation of the Copper Centres in $Pb_5Ge_3O_{11}$ Crystals at
Annealing in Halogen Atmosphere
V. A. Vazhenin, M. Yu. Artyomov, A. P. Potapov, A. V. Fokin 100
- Magnetic Features of Spin-Crossover Dendrimeric Iron(III) Complex
N. E. Domracheva, A. V. Pyataev, V. E. Vorobeva, E. M. Zueva 102
- Suspended Long-Lived NMR Echo in Solids
A. N. Turanov, A. K. Khitrin 103

EPR Study of Non-Resonance Microwave Absorption of $\text{Cu}(\text{aetkpz})_2\text{Br}_2$ <i>A. S. Berezin, V. A. Nadolinny, L. G. Lavrenova, E. V. Lider</i>	104
Investigation of Healthy and Infected (Brucellosis, Mastitis) Blood and Milk Samples: an ESR Spin Labeling Study <i>U. Sayin, L. Palali, Z. Sayin, R. Tapramaz, E. Ergun, G. Bakkal, A. Ozmen</i>	107
Magnetic Properties of Gamma Irradiated 2,3-Butanedione Monoxime: an Experimental and Theoretical ESR Study <i>L. Ates, H. U. Taşdemir, U. Sayin, E. Türkkkan, A. Ozmen</i>	108
Research of Two-Circuit System of Surface Type of the Receiving Sensor of MRI-Tomography <i>A. A. Bayazitov, Ya. V. Fattakhov</i>	109
Superparamagnetic Behavior in LaSrMnZnO Systems <i>R. M. Eremina, K. R. Sharipov, L. V. Mingalieva</i>	110
Density Functional Computations of the EPR, NMR Spectra and Spatial Molecular Structure of Ortho-Nitrophenol <i>S. Gündoğdu, H. U. Taşdemir, E. Türkkkan, Ö. Dereli</i>	112
Electron Magnetic Resonance Technique in the Study of Macromolecule Adsorption on Magnetic Nanoparticle Surface on Dispersion <i>A. V. Bychkova, O. N. Sorokina, A. V. Shapiro, M. Rosenfeld, A. L. Kovarski, V. Berendyaev</i>	113
The Edge Magnetism of Monolayer Graphene and Nanographite <i>M. A. Augustyniak-Jabłokow, M. Maćkowiak, R. Strzelczyk, K. Tadzyszak</i>	115
Detection of Explosive Precursors Using Low-Field Magnetic Resonance Imaging and Spectroscopy <i>N. A. Krylatykh, Ya. V. Fattakhov, A. R. Fakhrutdinov, V. N. Anashkin, V. A. Shagalov, I. A. Nurmamyatov, R. Sh. Khabipov</i>	117
EPR of the Narrow-Gap Semiconductor PbS Doped Highly by Manganese Ions <i>V. A. Ulanov, A. M. Sinitsyn, R. R. Zainullin, E. R. Zhiteytsev</i>	118
Light-Induced EPR Study of Charge Recombination in P3HT/PC70BM Composite <i>E. A. Lukina, A. G. Popov, M. N. Uvarov, L. V. Kulik</i>	120
Abnormal Lines in EPR Spectra of Sportsmen's Serum Blood <i>M. I. Ibragimova, A. I. Chushnikov, G. V. Cherepnev, V. Yu. Petukhov, E. P. Zheglov</i>	121
EPR of Chromium Precipitates in BaF_2 Crystals <i>E. R. Zhiteytsev, R. R. Zainullin, A. M. Sinitsyn, V. A. Ulanov</i>	122
Spin Dynamics of ZnTPP in Room-Temperature Ionic Liquids $[\text{bmim}]\text{PF}_6$ and $[\text{bmim}]\text{BF}_4$ Studied by Time-Resolved EPR <i>M. Ivanov, S. L. Veber, M. V. Fedin</i>	123

Quantum Phase Transition in Eu-Zn Pnictides on the ESR Date <i>Y. V. Goryunov, A. N. Nateprov</i>	124
The Dependence of 4-Styrylpyridine Photoisomerization on Wavelength Radiation and on the Solvent. UV, NMN, and DFT Studies <i>L. G. Gafiyatullin, L. I. Savostina, O. I. Gnezdilov, O. A. Turanova, I. V. Ovchinnikov, A. N. Turanov</i>	126
FMR Investigation of Iron Silicide Films Ion Beam Synthesized in Magnetic Field <i>G. G. Gumarov, A. V. Alekseev, M. M. Bakirov, V. Yu. Petukhov, V. F. Valeev</i>	127
Unusual Anisotropy of the {g}-Tensor in Dimer Dysprosium (III) Complex. EPR Study <i>R. T. Galeev, A. A. Sukhanov, R. M. Eremina, V. K. Voronkova, A. Baniodeh, A. K. Powell</i>	129
The Kinetic EPR Spectroscopy of Diamines Protolytic Reactions <i>A. S. Masalimov, A. A. Tur, S. N. Nikolskiy</i>	130
EPR Study of Nitric Oxide Production in Heart and Spinal Cord of Rats under Hypokinesia and Condition of Spinal Cord Injury <i>Kh. L. Gainutdinov, V. V. Andrianov, V. S. Iyudin, I. I. Shaikhutdinov, F. G. Sitdikov, R. F. Tumakaev, G. G. Yafarova, R. Kh. Yagudin, R. I. Zaripova, T. L. Zefirov</i>	132
ESR Study of Critical Fluctuations at N-Sa Phase Transition <i>B. M. Khasanov</i>	134
Electron Spin Resonance in Thin Film GdMnO ₃ /SrTiO ₃ <i>T. P. Gavrilova, I. V. Yatsyk, R. M. Eremina, D. V. Mamedov, I. I. Fazlizhanov, A. A. Rodionov, V. I. Chichkov, N. V. Andreev, Ya. M. Mukovskii</i>	136
Electron Spin Echo of Light-Induced Spin Correlated Radical Pairs in PCBM/P3HT Composite <i>A. A. Popov, L. V. Kulik</i>	139
The Synthesis, EPR and Magnetic Properties of Fe(III) Complexes with Tetradentate N ₂ O ₂ Donating Schiff-Base Ligand Bridged by Pirazine <i>T. A. Ivanova, L. V. Mingalieva, I. V. Ovchinnikov, I. F. Gilmutdinov, O. A. Turanova, G. I. Ivanova</i>	140
EPR Investigation of Cu (II) Complexes with Hyperbranched Polyesterpolyols Modified by Amines <i>S. V. Yurtaeva, I. V. Ovchinnikov, M. P. Kuttyreva, A. R. Gataulina, N. A. Ulakhovich, V. I. Muravyev</i>	142
Electron Magnetic Resonance in Biological Systems <i>S. V. Yurtaeva, V. N. Efimov</i>	144
Asymmetric Stochastic Resonance in a System of Ferromagnetic Nanoparticles <i>A. G. Isavnin, I. I. Mirgazov</i>	146

Magnetic Resonance and Optical Spectroscopy of Yb ³⁺ in the CsCaF ₃ and CaF ₂ Single Crystals <i>M. L. Falin, K. I. Gerasimov, V. A. Latypov</i>	147
Separation of the Contributions of Dipole-Dipole and Exchange Interactions to the Shape of Epr Spectra of Free Radicals in Diluted Solutions <i>M. M. Bakirov, K. M. Salikhov, R. T. Galeev</i>	148
Modeling of PELDOR Signal for Three Spin Systems <i>I. T. Khairuzhdinov, K. M. Salikhov</i>	149
Tunable High-Frequency EPR Spectroscopy of the Clay and Plasticine <i>G. S. Shakurov, V. A. Shustov</i>	150
Chiral Spin-Liquid State in Mn _{1-x} Fe _x Si Solid Solutions <i>V. V. Glushkov, S. V. Grigoriev, S. V. Demishev, T. V. Ischenko, I. I. Lobanova, A. N. Samarina, A. V. Semeno, N. E. Sluchanko</i>	151
EPR Study on Mechanism of <i>ipso</i> -Nitration of Arylboronic Acids <i>H. Yang, Y. Li, M. Jiang, H. Fu</i>	153
Magnon BEC in CsMnF ₃ <i>R. Gazizulin</i>	155
Measurement of the <i>g</i> -factors of Ground and Excited States in the Zero dc Magnetic Field by the Photon Echo Method <i>V. N. Lisin, A. M. Shegeda</i>	156
EPR Study of New Spin Labels Based on 2,5-Bis(Spirocyclohexane)-Substituted Nitroxides of Pyrroline and Pyrrolidine Series <i>O. A. Krumkacheva, I. A. Kirilyuk, Y. F. Polienko, I. A. Grigor'ev, R. K. Strizhakov, E. S. Babailova, A. V. Ivanov, M. A. Vorobjeva, A. G. Venyaminova, A. A. Malygin, G. G. Karpova, M. V. Fedin, E. G. Bagryanskaya</i>	158
Validation of the MRI Based Fiber Tracking Results on a Numerical Phantom <i>O. V. Nedopekin, L. V. Konopleva, K. A. Il'yasov</i>	159
CPMG Echo Amplitudes with Arbitrary Refocusing Angle: Explicit Expressions, Asymptotic Behavior, Approximations <i>M. V. Petrova, A. B. Doktorov, N. N. Lukzen</i>	160
Comparison of X-, Q- and G-band Stimulated Electron Spin Echo Data on Molecular Motions of Spin Labels <i>N. P. Isaev, M. V. Fedin, V. Denysenkov, T. Prisner, S. A. Dzuba</i>	161
Pulsed ENDOR Study of the Nitrogen Donors in 6H SiC Crystals Grown under Carbon-Rich Conditions <i>D. Savchenko, E. Kalabukhova, A. Pöppel, B. Shanina, E. Mokhov</i>	162
AUTHOR INDEX	164

PLENARY LECTURES

Zavoisky Award Lecture.
Pulsed EPR Dipolar Spectroscopy and its Applications

Yu. D. Tsvetkov

Voevodsky Institute of Chemical Kinetics and Combustion, SB RAS

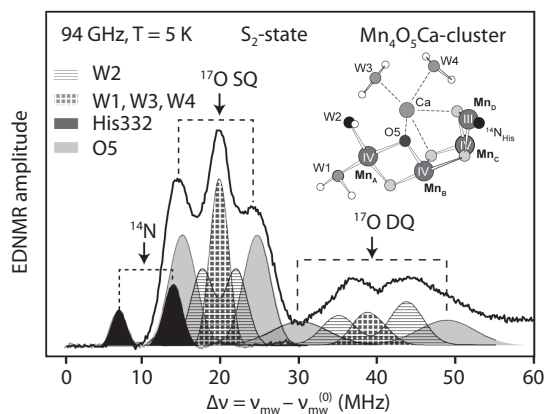
Introduction. Pulsed S-S ESE spectroscopy EPR. Radical tracks in irradiated solids. Pulsed S-I ESE spectroscopy EPR (ESEEM). Applications for electron, atom and ions traps structure determination. PELDOR-EPR spectroscopy for interspin distance and distance distribution determinations. Applications for spin labeled peptides. Conclusions.

The Water Splitting Machine of Photosynthesis Studied by EPR Techniques

W. Lubitz

Max Planck Institute for Chemical Energy Conversion, Mülheim/Ruhr 45470, Germany,
wolfgang.lubitz@cec.mpg.de

The process of light-induced water oxidation in photosynthesis occurs in a single biological supercomplex called photosystem II at a protein-bound $\text{Mn}_4\text{O}_5\text{Ca}$ cluster, which passes through 5 intermediate states (S_n -state cycle) [1]. A detailed electronic model of the catalytic center has been developed based on structural data from X-ray crystallography [2] and magnetic resonance (EPR and ENDOR) techniques [3–5]. Based on ^{55}Mn ENDOR spin and oxidation states and coupling of the Mn ions could be determined and a model of the catalytic center developed. High field ELDOR-detected NMR (EDNMR) at 94 GHz (see Figure) has been applied to detect the interaction of the cluster with magnetic nuclei of surrounding amino acids (^{14}N) and attached water molecules. In samples exchanged with H_2^{17}O , ^{17}O hyperfine couplings of three different types of water molecules were detected [6], see figure. They could be assigned based on the X-ray crystallographic model [2] which has been refined using density functional theory [5] and comparison with model complexes [1]. These data further refine the reaction pathway for O-O bond formation supporting an oxo/oxyl coupling mechanism in the catalytically active state (S_4) of the cycle [7, 1]. A mechanistic model for water oxidation in photosynthesis is proposed.



1. Cox N. *et al.*: *Acc. Chem. Res.*, doi: 10.1021/ar3003249 (2013), in press.
2. Umena Y., Kawakami K., Shen J.-R., Kamiya N.: *Nature* **473**, 55 (2011)
3. Kulik L.V., Epel B., Lubitz W., Messinger J.: *J. Am. Chem. Soc.* **129**, 13421 (2007)
4. Cox N. *et al.*: *J. Am. Chem. Soc.* **133**, 3635 (2011)
5. Ames W. *et al.*: *J. Am. Chem. Soc.* **133**, 19743 (2011)
6. Rapatskiy L. *et al.*: *J. Am. Chem. Soc.* **134**, 16619 (2012)
7. Siegbahn P.E.M.: *Acc. Chem. Res.* **42**, 1871 (2009)

Multi-Extreme THz ESR: Its Developments and Applications

H. Ohta^{1,2}, S. Okubo¹, E. Ohmichi², T. Sakurai³, and T. Shimokawa⁴

¹ Molecular Photoscience Research Center, Kobe University, Kobe 657-8501, Japan,
hohta@kobe-u.ac.jp

² Graduate School of Science, Kobe University, Kobe 657-8501, Japan

³ Center for Supports to Research and Education Activities, Kobe University,
Kobe 657-8501, Japan

⁴ Center for Collaborative Research and Technology Development, Kobe University,
Kobe 657-8501, Japan

Recent developments and some applications of our multi-extreme THz ESR will be presented. Our multi-extreme THz ESR covers, 1) frequency region between 0.03 and 7 THz; 2) temperature region between 1.8 and 300 K [1]; 3) magnetic field region up to 55 T using the pulsed magnetic field [1, 2]; 4) pressure region up to 2.7 GPa [3]; 5) measurements of micrometer size single crystal using a micro-cantilever [4], magnetization detected ESR using SQUID magnetometer (SQUID ESR) [5]. Finally its application to kagome lattice antiferromagnet Cr-jarosite will be presented.

1. Ohta H., Okubo S., Kawakami K., Fukuoka D., Inagaki Y., Kunimoto T., Hiroi Z.: *J. Phys. Soc. Jpn.* **72** (Suppl. B), 26–35 (2003); Ohta H., Tomoo M., Okubo S., Sakurai T., Fujisawa M., Tomita T., Kimata M., Yamamoto T., Kawachi M., Kindo K.: *J. Phys.: Conf. Series* **51**, 611–614 (2006)
2. Ohta H., Okubo S., Souda N., Tomoo M., Sakurai T., Yoshida T., Ohmichi E., Fujisawa M., Tanaka H., Kato R.: *Appl. Magn. Reson.* **35**, 399–410 (2009)
3. Sakurai T., Taketani A., Tomita T., Okubo S., Ohta H., Uwatoko Y.: *Rev. Sci. Instr.* **78**, 065107/pp. 1–6 (2007); Sakurai T., Horie T., Tomoo M., Kondo K., Matsumi N., Okubo S., Ohta H., Uwatoko Y., Kudo K., Koike Y., Tanaka H.: *J. Phys.: Conf. Series* **215**, 012184/pp. 1–4 (2010)
4. Ohta H., Kimata M., Okubo S., Ohmichi E., Osada T.: *AIP Conference Proceedings* **850**, 1643–1644 (2006); Ohmichi E., Mizuno N., Kimata M., Ohta H.: *Rev. Sci. Instrum.* **79**, 103903/pp. 1–5 (2008); Ohmichi E., Mizuno N., Kimata M., Ohta H., Osada T.: *Rev. Sci. Instrum.* **80**, 013904/pp. 1–5 (2009); Ohta H., Ohmichi E.: *Appl. Magn. Reson.* **37**, 881–891 (2010); Ohmichi E., Mizuno N., Hirano S., Ohta H.: *J. Low Temp. Phys.* **159**, 276–279 (2010); Tokuda Y., Hirano S., Ohmichi E., Ohta H.: *J. Phys. Conf.* **400**, 032103/pp. 1–4, 2012; Ohmichi E., Hirano S., Ohta H.: *J. Mag. Res.* **227**, 9–13 (2013)
5. Sakurai T., Goto R., Takahashi N., Okubo S., Ohta H.: *J. Phys.: Conf. Series* **334**, 012058/pp. 1–4 (2011); Sakurai T., Fujimoto K., Goto R., Okubo S., Ohta H., Uwatoko Y.: *J. Mag. Res.* **233**, 41–45 (2012)

EPR Methods for Characterizing Disorder and Structural Changes of Membrane Proteins

**G. Jeschke¹, B. Joseph¹, E. Bordignon¹, M. Yulikov¹, Ye. Polyhach¹,
T. von Hagens¹, V. Korkhov², C. Dietz³, and H. Paulsen³**

¹ Lab. Phys. Chem., ETH Zürich, Zürich CH-8093, Switzerland, gjeschke@ethz.ch

² Inst. for Molecular Biology and Biophysics, ETH Zürich, Zürich CH-8093, Switzerland

³ Inst. of General Botany, Universität Mainz, Mainz D-55099, Germany

Although knowledge on membrane proteins is still lagging knowledge on soluble proteins, X-ray crystallography and NMR spectroscopy by now provide a steady flow of new structures at atomic resolution. These structures and biochemical evidence point to the existence of membrane protein molecules and complexes in several conformational states and to the importance of flexible, disordered domains in regulation cascades. In such a picture, the atomistic structure snapshots obtained by X-ray crystallography and NMR spectroscopy provide very valuable starting points for further work, but are not sufficient for full understanding of protein function. Because of the structural flexibility of membrane proteins interpretation of the high-resolution structures may also be complicated by the fact that they are usually obtained in highly artificial environments.

The combination of an arsenal of EPR techniques with site-directed spin labeling can provide information on membrane proteins that nicely complements the information from high resolution structures. In many cases this information can be obtained on membrane proteins reconstituted into liposomes, which better mimic cell membranes than detergent micelles or the packing in crystal structures. Average water accessibility parameters and distance distributions can be

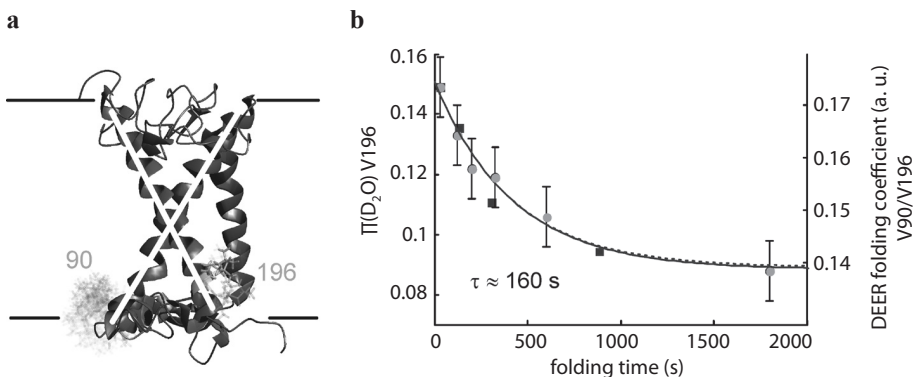


Fig. 1. Folding kinetics of LHCII assessed by pulse EPR. **a** Ribbon model of the LHCII protein, label sites, predicted conformational distributions of the spin labels (light grey), boundaries of the lipid bilayer (horizontal black lines), and substructure tested by the DEER experiment (white lines). **b** Folding parameters as a function of time for the water accessibility of residue 196 (circle) and for the distance distribution between residues 90 and 196 (square).

obtained for sites in disordered domains, where X-ray crystallography fails for lack of electron density and NMR spectroscopy may fail for lack of resolution.

These concepts are illustrated on the examples of the major light harvesting complex LHCII of green plants and of the vitamin B₁₂ ABC importer of *Escherichia coli*. For LHCII, water accessibility assessed by deuterium electron spin echo envelope (ESEEM) spectroscopy and distance distributions obtained from double electron electron resonance (DEER) experiments provide site-resolved information on folding [1, 2] (Fig. 1) and insight into the conformation and conformational distribution of the disordered N-terminal domain [3]. For the vitamin B₁₂ ABC transporter, a combination of DEER, orthogonal spin labeling with nitroxides and a Gd(III) complex, and water accessibility measurements by Overhauser dynamic nuclear polarization [4] sheds light on the correlation between binding of nucleotides and of the substrate-binding protein to the complex on the one hand and movements of the outer and inner gates of the substrate translocation pathway on the other hand.

The lecture will also emphasize the semi-quantitative character of the information that we obtain and will explain why such semi-quantitative information may be fully adequate for the questions to be answered.

1. Volkov A., Dockter C., Polyhach Y., Paulsen H., Jeschke G.: *J. Phys. Chem. Lett.* **1**, 663 (2010)
2. Dockter C., Volkov A., Bauer C., Polyhach Ye., Joly-Lopez Z., Jeschke G., Paulsen H.: *Proc. Natl. Acad. Sci. USA* **106**, 18485 (2009)
3. Dockter C., Müller A.H., Dietz C., Volkov A., Polyhach Ye., Jeschke G., Paulsen H.: *J. Biol. Chem.* **287**, 2915 (2012)
4. Doll A., Bordignon E., Joseph B., Tschaggelar R., Jeschke G.: *J. Magn. Reson.* **222**, 34 (2012)

PELDOR of Spin Labeled DNA

Yu. D. Tsvetkov, A. D. Milov, N. A. Kuznetsov, and O. S. Fedorova

Voevodsky Institute of Chemical Kinetics and Combustion, SB RAS
Institute of Chemical Biology and Fundamental Medicine, SB RAS

This report presents the main results, including literature data, of the studies on spin-labeled DNA and RNA using PELDOR method [1–3]. The time traces of PELDOR signals have been obtained experimentally and analyzed to determine intermolecular and intramolecular dipole interactions. The Tikhonov regularization method has been employed to estimate both the distances between spin labels and a distance distribution function for various, linear and spatially complex DNA structures using data on intramolecular dipole contribution. The major part of the report is devoted to the results obtained by studying damaged nucleotides and DNA/enzyme systems.

1. Kuznetsov N.A., Milov A.D., Koval V.V., Samoilova R.I., Grishin Y.A., Knorre D.G., Tsvetkov Yu.D., Fedorova O.S., Dzuba S.A.: *Phys.Chem.Chem.Phys.* **11**, 6826–6832 (2009)
2. Kuznetsov N.A., Milov A.D., Isaev N.P., Vorobjev Yu.N., Koval V.V., Dzuba S.A., Fedorova O.S., Tsvetkov Yu.D.: *Mol. BioSystems.* **7**, 2670–2680 (2011)
3. Fedorova O.S., Tsvetkov Yu.D.: *Acta Naturae* **4**, 52–75 (2012)

Probing Conformational Changes in Photosynthetic Protein Complexes – News and Views from High-Field Dipolar EPR Spectroscopy

K. Möbius^{1,2}

¹ Dept. of Physics, Free University Berlin, Berlin 14195, Germany

² Max Planck Institute for Chemical Energy Conversion, Mülheim (Ruhr) 45470, Germany

To understand key structural and dynamical characteristics of the light-initiated electron-transfer (ET) steps of photosynthesis on the molecular level, the initial, intermediate and final cofactor states of the reaction center protein complex are of paramount interest in the bio-energy community. The primary photochemical events power the solar-energy conversion in photosynthetic organisms by inducing charge separation between the primary donor, P, and the primary quinone acceptor, Q. Distance and relative orientation of functional cofactor groups within protein domains and their conformational changes and fluctuations during the reaction determine the efficiency of the biological process. Under physiological conditions, protein function is based on structural fluctuations, thereby the protein is sampling a large number of different conformational substates in a highly structured energy landscape. An extremely important role for the biological efficiency of the protein is played by its matrix, i.e., the micro-environment of the redox cofactors in their protein binding sites. At cryogenic temperatures, the conformational fluctuations die out and the protein stops its biological function.

Orientation-selective high-field pulsed dipolar EPR spectroscopy, such as PELDOR and related techniques, is particularly well-suited to elucidate molecular characteristics of transient radical and radical-pair redox states to great detail, even from disordered frozen-solution samples. Such information is often not available from other spectroscopic or diffraction techniques, for instance NMR or X-ray crystallography.

We employed a variety of EPR techniques at high microwave frequencies and Zeeman fields (95 GHz, 3.4 T) with their superior orientational selectivity and time resolution (as compared to standard X-band EPR techniques) to determine the 3D-structure of transient spin-polarized correlated radical pairs, $P^{+\bullet}Q^{-\bullet}$, and to explore the nature of postulated conformational changes upon light-induced electron transfer. The combined transient EPR, ENDOR and PELDOR experiments reveal that distance and relative orientation of $P^{+\bullet}$ and $Q^{-\bullet}$ do not change under charge separation in bacterial photosynthetic RCs from *Rhodobacter sphaeroides*. These experiments have been extended recently to Photosystem I of oxygenic *Synechocystis* revealing the 3D structure of the redox cofactors in their binding sites.

When embedding the RC into dehydrated disaccharide trehalose sugar, which has a rather unique capability to form glass matrices with hydrogen-bond networks with the protein, the photosynthetic function is strongly retarded at room temperature. Trehalose sugar as protein matrix exhibits an extraordinary

efficacy in the preservation of biostructures under adverse environmental conditions of extreme drought and high temperatures. Large amounts of trehalose are accumulated in organisms that can survive such conditions by entering for a long time (years) a state of reversibly suspended metabolism (“anhydrobiosis”). Our high-field EPR and laser-flash experiments show that the dry trehalose glass matrix rigidly coats the RC protein surface already at room temperature, thereby shifting the correlation time of thermal conformational fluctuations into the non-biological time domain.

This work has been done in collaboration with A. Savitsky², M. Flores², W. Lubitz², Y Grishin (Novosibirsk), A. Dubinskii (Moscow), G. Venturoli (Bologna), and A. Semenov (Moscow).

Uncovering a Complex Interplay of Spins, Orbitals and Charges in LaSrMnO_4 by Sub-THz Spectroscopy in Ultra-Strong Magnetic Fields

V. Kataev

Leibniz Institute for Solid State and Materials Research IFW Dresden, Dresden D-01171, Germany,
v.kataev@ifw-dresden.de

In this talk high-field ESR (HF-ESR) and a very peculiar anomalous magnetic field driven absorption of sub-THz radiation in single crystals of the single layer manganite $\text{La}_1\text{Sr}_1\text{MnO}_4$ (LSMO) in magnetic fields up to 40 T will be discussed

The LSMO crystallizes in the K_2NiF_4 -tetragonal structure type. The $\text{Mn}^{3+}\text{O}^{2-}$ -octahedra are strongly elongated along the tetragonal c -axis implying that at all $\text{Mn}(3d^4)$ -sites the $3z^2-r^2$ orbital from the e_g set is occupied. This ferro-orbital order completes with the collinear C-type antiferromagnetic order at $T_N = 127$ K. There is however a growing number of observations suggesting that the physics of LSMO is not confined to the spin sector only. Remarkably, LSMO shows anisotropic anomalies in the thermal expansion indicating a T -dependent redistribution of the electron density between the e_g orbitals, i.e. that the orbital degrees of freedoms are not completely quenched. Furthermore, the observation of small ferromagnetic moments in mSR and magnetization experiments is incompatible with the collinear spin structure and the completed ferro-orbital order.

Indeed, our HF-ESR measurements of a high-quality single crystal of LSMO in the paramagnetic regime at $T > T_N$ reveal a specific T -dependence of the g -factors and the single-ion anisotropy gap D which gives evidence for a progressive occupation of the out-of-plane $3z^2-r^2$ orbital with lowering T . At the magnetic phase transition a well-defined ESR signal transforms into extremely broad field dependent absorption bands with very peculiar properties. In particular, at $T \ll T_N$, with increasing the magnetic field strength B above 15 T the transmission signal $Tr(B)$ strongly reduces and exhibits a non-monotonous frequency dependence in a range $90 \text{ GHz} < \nu < 1.2 \text{ THz}$. A broad step in $Tr(B)$ shows a strong hysteresis for $B \parallel c$ -axis but is reversible for the $B \perp c$ geometry. Though LSMO nominally contains no holes we have found a significant negative magnetoresistance at $T < T_N$ in magnetic fields up to 30 T. The unusual field driven microwave absorption in LSMO bears striking similarity with the B -dependence of the dielectric constants found in the multiferroic manganites GdMnO_3 and TbMnO_3 and presented as a possible evidence for electromagnons. Our observations may indicate that a dynamic interplay between spins, orbitals and charges is not exceptional for the pseudocubic perovskites but may also occur in the layered manganites such as LSMO.

This work has been done in collaboration with U. Schaufuß, B. Büchner (IFW Dresden), R. Klingeler (Kirchhoff Institute for Physics, University of Heidelberg, Heidelberg), M. Goiran, B. Raquet, H. Rakoto, J.-M. Broto (Laboratoire National des Champs Magnétiques Pulsés, Toulouse), P. Reutler and A. Revcolevschi (Laboratoire de Chimie des Solides, Université Paris-Sud, Orsay).

High-Frequency EPR Evidence of Heisenberg Localized Magnetic Moments in MnSi

**S. V. Demishev, A. V. Semeno, V. V. Glushkov, I. I. Lobanova,
A. N. Samarin, and N. E. Sluchanko**

Prokhorov General Physics Institute of RAS, Moscow 119991, Russian Federation,
demis@lt.gpi.ru

In the recent years EPR became a powerful tool for studying strongly correlated metals like YbRh_2Si_2 , CeB_6 , EuB_6 and others. Studying of the dynamic magnetic properties opens new opportunities for probing of the ground state in these materials and provides information unavailable in the static magnetic measurements [1, 2]. In the present work we have investigated high-frequency (60 GHz) EPR in manganese monosilicide, MnSi, single crystals. This material is believed to be an archetypical itinerant magnet serving as important experimental confirmation of Moriya theory [3]. However, EPR experiments performed within the 4.2–300 K temperatures range at the applied magnetic field up to 7 T have demonstrated that the magnetic resonance in MnSi is due to localized magnetic moments of the Heisenberg type with the g -factor depending only slightly on temperature. At the same time, it has been found that the EPR linewidth is determined by spin fluctuations and can be quantitatively described in the wide temperature range ($4.2 \text{ K} < T < 60 \text{ K}$) in the framework of the Moriya theory using the $SL(T)$ function (Fig. 1). The revealed

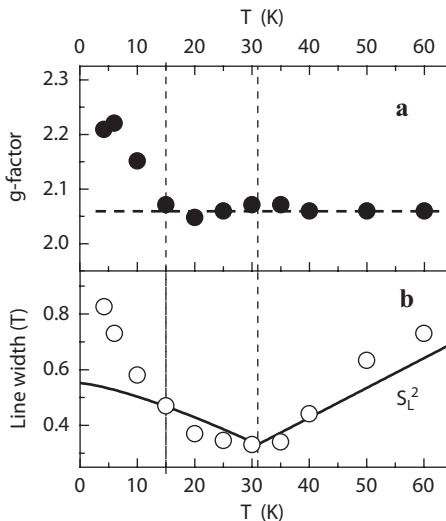


Fig. 1. The g -factor (a) and line width (b) for 60 GHz EPR in MnSi. In the panel (b) solid line represents approximation within Moriya theory of spin fluctuations.

deviations from the model of weak itinerant-electron magnetism commonly used for the description of the magnetic properties of MnSi indicate a possible spin-polaron nature of the unusual magnetic properties of this strongly correlated metal [4, 5].

The combination of EPR and magnetotransport measurements was found to be an essential tool for probing of the magnetic phase diagram of MnSi. It is shown that the phase boundary between paramagnetic (PM) phase and spin-polarized (SP) phase is well-defined, has no positive slope as it was suggested previously, and appears to be practically vertical corresponding to transition temperature $T_c \sim 30$ K. A low temperature anomaly at $T \sim 15$ K corresponding to magnetoresistance and g -factor changes is reported. The carried analysis of the transport and magnetic resonance data favors the explanation of magnetic properties of MnSi by localized magnetic moments rather than by itinerant magnetism approach. We argue that Heisenberg-type magnetism extension to spin-polaronic states can consistently explain the totality of the static and dynamic magnetic data for MnSi.

This work is supported by Program of RAS “Strongly correlated electrons” and by RFBR grant 13-02-00160.

1. Semeno A.V. *et al.*: Phys. Rev. B **79**, 014423 (2009)
2. Demishev S.V. *et al.*: Phys. Rev. B **80**, 245106 (2009)
3. Moriya T.: Spin Fluctuations in Itinerant Electron Magnetism. Berlin, Heidelberg, New York, Tokyo, Springer-Verlag, 1985.
4. Demishev S.V. *et al.*: JETP Lett. **93**, 213 (2011)
5. Demishev S.V. *et al.*: Phys. Rev. B **85**, 045131 (2012)

Low-Temperature Electron Spin Dynamics and DNP

M. K. Bowman¹, A. G. Maryasov², and V. M. Tormyshev³

¹ Department of Chemistry, The University of Alabama, Tuscaloosa, Alabama 35487, USA, mkbowman@as.ua.edu

² The V. V. Voevodsky Institute of Chemical Kinetics and Combustion, Novosibirsk 630090, Russian Federation, maryasov@kinetics.nsc.ru

³ Vorozhtsov Novosibirsk Institute of Organic Chemistry, Novosibirsk 630090, Russian Federation, torm@nioch.nsc.ru

The recent surge in low-temperature dynamic nuclear polarization (DNP) for the enhancement of NMR spectra has been aided by the development of a new family of stable triaryl methyl radicals (TAM or trityl). The trityl radicals can have a single, intense EPR line only fractions of a MHz wide, and very long relaxation times. Efforts to model the DNP process are underway in several labs in order to optimize both the efficiency and speed of DNP. The approaches can be characterized as: *ab initio*, starting with the fundamental properties of the electrons and nuclear spins; semi-empirical, based on the observed dynamics of the spins involved; and phenomenological, based on spin temperature and thermodynamics. Yet, the electron spin dynamics of trityl radicals at the concentrations, temperatures and magnetic fields used for DNP is largely unexplored and not available for validating or parameterizing the modeling.

We have measured the spin dynamics of the symmetric or “Finland” trityl radical, Fig. 1, at X-band and W-band at concentrations below 0.1 M between 3–100 K. The electron spin-lattice relaxation (T_{1e}) shows a strong concentration dependence at low temperature caused by spin diffusion. The decay of the dipolar echo shows that T_{1D} is largely temperature independent and very non-exponential, occurring over three orders of magnitude in time. Both of these relaxation modes suggest that the EPR frequency of a trityl radical should be a dynamic function of time, either because the spin moves from one radical to another by electron spin flip-flops, or because the local dipolar fields change as they relax and shift the frequency of a radical. This dynamic frequency is characterized

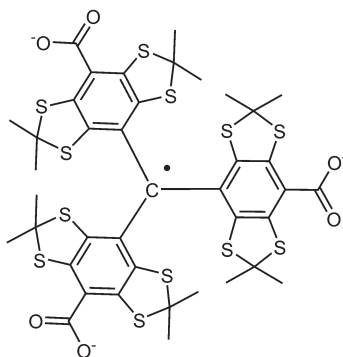


Fig. 1. Finland trityl radical.

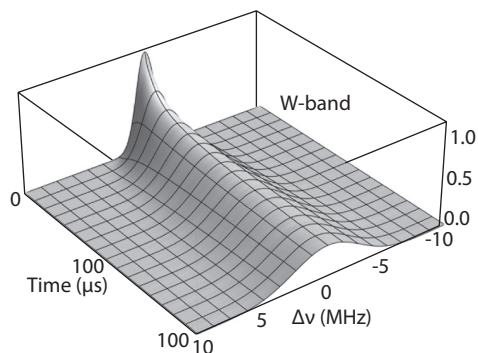


Fig. 2. Spectral Diffusion Kernel for 2.5 mM trityl at W-band at 50 K for times delays of 1–100 μ s.

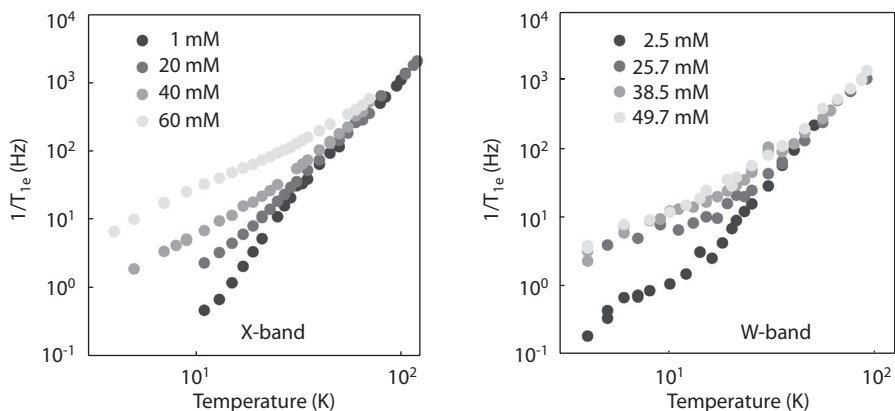


Fig. 3. Temperature and concentration dependence of electron spin-lattice relaxation rate of Finland trityl radical.

by the spectral diffusion kernel, Fig. 2. It shows how the EPR frequency of a trityl radical changes as a function of time from its original value. The starting frequency broadens to about 1 MHz wide in less than 1 ms and spreads over a range of about 10 MHz after 100 μ s.

Spectral diffusion has a rapid contribution from nuclear flip-flops and takes place in the first few ms. Other contributions depend on trityl concentration. Instantaneous diffusion occurs during microwave pulses and electron spin flip-flops and trityl T_{1e} contribute on the 10's of ms to seconds range.

The electron spin state of a trityl radical, its EPR frequency and the dipolar field it sees all depend on trityl concentration and vary with timescales ranging from 1 μ s to over 1 second. The dynamics are surprisingly similar at X-band and W-band. In particular the T_{1e} does not show the dependence on field anticipated for the direct process, Fig. 3. Our measurements suggest that electron spin dynamics are important parameters for understanding and optimizing DNP at low temperatures.

This work was supported by The Ministry of Education and Science of Russian Federation, project 8466, and P41EB002034 from NIBIB (NIH).

Asymmetry of Electron Transfer in Photosystem I as Studied by Pump-Probe Femtosecond Absorption Spectrometry and W-band Transient EPR Spectroscopy

**A. Yu. Semenov^{1,2}, A. Savitsky³, K. Möbius³, J. Golbeck⁴,
and V. Nadochenko²**

¹ A. N. Belozersky Institute of Physical-Chemical Biology, Moscow State University, Moscow, Russian Federation, semenov@genebee.msu.ru

² N. N. Semenov Institute of Chemical Physics, Russian Academy of Sciences, Moscow, Russian Federation

³ Max Planck Institute for Chemical Energy Conversion, Muelheim an der Ruhr, Germany;

⁴ The Pennsylvania State University, University Park, USA

The photosystem I (PS I) reaction center complex contains two symmetrical branches of redox cofactors (A and B) associated with heterodimeric protein subunits (PsaA/PsaB). According to the conventional viewpoint, in PS I the dimeric chlorophyll molecules (Chl) Chl1A/Chl1B were considered as a primary donor P700; the monomeric Chls (the third pair of Chl molecules Chl3A/Chl3B or A_0), as a primary acceptor; and the quinone(s) A_{1A}/A_{1B} as secondary acceptor(s). Our recent femtosecond pump-probe experiment in PS I complexes isolated from cyanobacteria *Synechocystis sp.* PCC 6803 revealed very fast (<100 fs) conversion of delocalized exciton into charge separated state $P700^+A_0^-A_1^-$; the secondary radical pair $P700^+A_0A_1^-$ was formed within 25 ps (Shelaev et al., *Biochim. Biophys. Acta* **1797**, 1410–1420 (2010)). Therefore the sequence of the primary electron transfer reactions in PS I can be presented as follows: $P700 \rightarrow A_{0A}/A_{0B} \rightarrow A_{1A}/A_{1B}$. The pump-probe femtosecond flash spectrometry with excitation maximum at 720 nm was employed for the study of kinetics of the primary and secondary ion-radical pair formation in PS I isolated from the *Synechocystis sp.* PCC 6803 mutants (M688HPsaA, M688LPsaA, M668HPsaB and M668LPsaB) with substituted axial ligands to the primary acceptor A_0 in both symmetrical A and B branches of redox-cofactors. It was demonstrated that replacement of methionine by leucine and histidine in the A-branch results in significant slowdown of kinetics of the secondary ion-radical pair $P700^+A_0A_1^-$ formation, but does not affect the formation of the primary radical pair $P700^+A_0^-A_1^-$. The analogous replacements in the B-branch do not influence the primary and secondary electron transfer reactions.

PS I mutants from the cyanobacterium *Synechocystis sp.* PCC 6803 bearing point mutations to the axial ligands of A_{0A} (M688NPsaA) and A_{0B} (M668NPsaB) were studied by high-field W-band electron paramagnetic resonance (EPR) spectroscopy. Because the geometries of the donor-acceptor radical pairs formed by electron transfer in the A- and B-branch differ, they have different spin-polarized EPR spectra and echo-modulation decay curves. Hence, time-resolved, multiple-frequency EPR spectroscopy, both in the direct-detection and pulse mode, can be used to probe the use of the two branches if electron transfer to the iron sulfur clusters is blocked. The analysis of the out-of-phase electron-electron dipolar electron spin echo envelope modulation shows that in the M668NPsaB mutant,

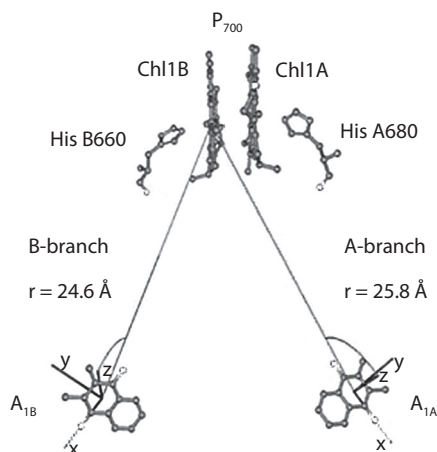


Fig. 1. Mutual arrangement of the primary electron donor P700 (the Chl1A and Chl1B special pair) and the phytylquinones A_{1A} and A_{1B} based on the X-ray crystal structure data (PDB entry 1JBO). The distances between P700 and A_{1A} and between P700 and A_{1B} correspond to distances between the spin density center in P700 and the geometrical centers of the benzoquinone fragments of A_{1A} and A_{1B} .

the estimated distance of $26.0 \pm 0.3 \text{ \AA}$ agrees well with the 25.8 \AA distance for the $P700^+A_{1A}^-$ radical pair measured in the X-ray crystal structure (Fig. 1). The other measured parameters of PS I from the M688NPsaB sample were virtually identical to those of the WT, and were clearly distinct from those of the M688NPsaA sample.

The same approach was employed for the study of the PS I complexes containing 2,3-dichloro-1,4-naphthoquinone (Cl_2NQ) in the A_{1A} and A_{1B} binding sites. The midpoint potential of Cl_2NQ is approximately 400 mV more positive than that of phytylquinone and these complexes are unable to transfer electrons to the iron-sulfur clusters. In these complexes no evidences for radical-pair formation in the B-branch were found.

The results obtained by both femtosecond pump-probe flash spectrometry and by high-field W-band EPR spectroscopy can be explained in terms of predominant A-branch electron transfer.

Multifunctional *in vivo* EPR Spectroscopy and Imaging Using Advanced Nitroxide and Trityl Paramagnetic Probes

V. V. Khramtsov

Department of Internal Medicine, the Ohio State University, Columbus OH 43210, USA,
Valery.Khramtsov@osumc.edu

Methods that monitor tissue oxygenation, pH, redox and major intracellular antioxidant, glutathione (GSH), *in vivo* are of critical importance for diagnostics and optimization of treatment strategies of various diseases including cancer and ischemic heart disease, two leading causes of mortality in the developed countries. The recent advances in low-field EPR-based techniques and chemistry of functional paramagnetic probes [1, 2] make multifunctional monitoring of tissue microenvironment (TME) feasible. The exemplified applications include concurrent monitoring of ischemia-induced myocardial oxygen depletion and acidosis in isolated rat hearts [3], and multifunctional monitoring of tumor TME [4]. Specifically we performed real-time longitudinal tumor pO_2 , pH_e , redox, and GSH monitoring in a mouse model of breast cancer. The L-band EPR studies using dual function paramagnetic probes show significant difference in pH_e and pO_2 between tumor and normal mammary gland tissues, as well as effect of treatment [1, 4]. Tumor tissue reducing capacity and GSH were elevated compared with normal mammary gland tissue [2, 3] and significantly affected by the treatment. In addition to spectroscopic studies pH_e mapping was performed using functional proton-electron double-resonance imaging [5]. The pH mapping superimposed with MRI supports probe localization in mammary gland/tumor tissue, shows high heterogeneity of pH_e and lower pH_e in tumor compared with mammary gland. The TME multifunctional profiling may provide biological markers for prediction of anti-cancer treatment and outcome and provides backgrounds for drug screening in animal preclinical models. Supported by NIH grant EB014542.

1. Dhimitruka *et al.*: *J. Am. Chem. Soc.* **135**, 5904–5910 (2013)
2. Khramtsov V.V. in: *Nitroxides – Theory, Experiment and Applications* (Kokorin A.I., ed.), p. 317–346. InTech, 2012.
3. Komarov D.A. *et al.*: *Magn. Reson. Med.* **68**, 649–55 (2012)
4. Bobko A.A. *et al.*: *Magn. Reson. Med.* **67**, 1827–1836 (2012)
5. Khramtsov V.V. *et al.*: *J. Magn. Reson.* **202**, 267–273 (2010)

SECTION 1

DEDICATION TO THE MEMORY OF
THE LATE YURII V. YABLOKOV

In memory of Yurii V. Yablokov

B. I. Kochelaev

Kazan (Volga Region) Federal University, Kazan 420008, Russian Federation

ESR in Combination with Luminescence and Mössbauer Methods as a Tool for Investigation of Structure, Molecular Dynamics and Redox Status of Biosystems

G. I. Likhtenshtein

Department of Chemistry, Ben-Gurion University of the Negev, Beer-Sheva 84105, Israel,
gertz@bgu.ac.il

Since 1960th the basic idea underlying our approach to solving a number of tasks in chemical biophysics and biomedicine is combining the classic ESR, as a basic method, with luminescence and Mössbauer techniques and the chemical kinetics [1–5]. Such an approach allowed us to markedly expand the potential of investigation in comparison with the each individual methods on its own.

Molecular dynamics and functional activity of proteins and enzymes. The physical labeling approach using radical pairs, nitroxide, fluorescence, dual nitroxide-phosphorescence and Mössbauer labels showed several general trends in dynamic behavior of labels incorporated in proteins and model systems: molecular motion of labels in the temporal range of seconds and amplitude of several angstrom and the parallel low amplitude fast wobbling were detected at temperature about 50 K. The dynamics gradually intensify as temperature increases, reaching nanosecond region at ambient temperatures. It was unambiguously found that the nanosecond range dynamics at ambient temperature is absolutely necessary for electron transfer from primary quinone acceptor to secondary one in the photosynthetic reaction center, electron transfer in the dual nitroxide-fluorescence probes incorporated in albumin, a substrate hydrolysis by α -chymotrypsin, myoglobin CO liganding and for some other processes in proteins.

Spin exchange and long-distance electron transfer. Analysis of empirical dependences of exchange integral for the triplet-triplet electron transfer (J_{TT}) on the distances between donor and acceptor allowed us to predict such a dependence for the spin exchange integral (J_{SE}) and, in turn, for resonance integral (V_2^{ET}) related to the long-distance electron transfer. All three integrals are dependent on the overlap integral (S_i), which quantitatively characterizes the degree of overlap of orbitals involved in these processes. Thus,

$$V_2^{ET}, J_{SE}, J_{TT} \propto S_n^i \propto \exp(-\beta_i R_i),$$

where R_i is the distance between the interacting centers and β_i is a coefficient which characterizes the degree of the integral decay. In the first approximation $n = 2$ for the ET and SE processes with the overlap of two orbitals and $n = 4$ for the TT process in which four orbitals overlap (of ground and triplet states of the donor and ground and triplet states of the acceptor). Therefore, $\beta_{ET} \approx 0.5\beta_{TT} = 1.3 \text{ \AA}^{-1}$. For a “conducting” bridge empirical $\beta_{ET}(c) = 0.3 \text{ \AA}^{-1}$. The value of β_{ET} (1.3 \AA^{-1}) is found to be close to that for V_2^{ET} obtained by analysis of k_{ET} on the distance R in model and biological systems.

Membranes molecular dynamics. Spin cascade method. To estimate encounters in a high range of rate constants and distances between interacting molecules in two-dimensional systems, membranes, a spin cascade method was proposed and implemented. The sensitised cascade triplet *cis-trans* photoisomerisation of the excited stilbene involves the use of a triplet sensitiser (Erythrosin B), a photochrome stilbene-derivative probe (4-dimethylamino-4'-aminostilbene) exhibiting the phenomenon of *trans-cis* photoisomerisation, and nitroxide radicals (5-doxyl stearic acid) to quench the excited triplet state of the sensitiser. Our data on diffusion rate constants together with the corresponding data obtained by methods utilising various characteristic times of about seven orders of magnitude and the experimental rate constants of about five orders of magnitude, were found to be in good agreement with the advanced theory of diffusion-controlled reactions in two dimensions.

Real time monitoring redox processes. Dual fluorescence nitroxide probes. In dual nitroxide-fluorescence supper molecules the nitroxide is a strong intramolecular quencher of the fluorescence from the chromophore fragment. Chemical or photo-reduction of this fragment to a corresponding hydroxylamine derivative, oxidation of the nitroxide fragment or addition of an active radical yield the fluorescence increase and the parallel decay of the fragment ESR signal. The ESR and fluorescence properties of the dual probes was intensively exploited as the basis of several methodologies which include a real time analysis of antioxidants, nitric oxide, superoxide and the establishment of antioxidant status of blood.

1. Likhtenshtein G.I.: Spin Labeling Method in Molecular Biology. N.Y., Wiley Interscience, 1976.
2. Likhtenshtein G.I.: Biophysical Labeling Methods in Molecular Biology. Cambridge, N.Y., Cambridge University Press, 1993.
3. Likhtenshtein G.I.: New Trends in Enzyme Catalysis and Mimicking Chemical Reactions. N.Y., Kluwer Academic/Plenum Publishers, 2003.
4. Likhtenshtein G.I., Yamauchi J, Nakatsuji S, Smirnov A., Tamura R.: Nitroxides: Application in Chemistry, Biomedicine, and Materials Science. Weinhem, WILEY-VCH, 2008.
5. Likhtenshtein G.I.: Solar Energy Conversion. Chemical Aspects. Weinhem, WILEY-VCH, 2012.

EPR Evidence of Molecular Photoeffect for Multiwall Carbon Nanotubes

I. Geru

Laboratory of Quantum Chemistry, Chemical Kinetics and Magnetic Resonance,
Institute of Chemistry of the Academy of Sciences of Moldova, Chisinau MD 2028, Moldova,
iongeru11@gmail.com

In the case of a few angstroms separation between the nanostructured surface of a solid body and the molecules of an adsorbed gas in a bounded state, these can become free under the action of photons. If the energy of the incident photon is equal or greater than the surface binding energy, then the emission of molecules under irradiation (molecular photoeffect) can be observed. However there is an essential difference between the “electronic” photoeffect and its molecular analogue. In the first case the photons penetrate the thin layer of the material surface (dependent on the light absorption coefficient) and impart their energy to the free electrons. If the energy of the photon $h\nu$ satisfies the condition $h\nu \geq A$ (A is the work required to remove the electron from the crystalline structure), then the electron is emitted under the influence of light. In the latter case the photons interact with the adsorbed molecules that are situated a short distance (a few angstroms) from the crystal (nanocrystal) surface. Their removal from the material surface, with which they interact, takes place when $h\nu \geq E_b$, where E_b is the surface binding energy of the molecule with the surface atoms.

We studied the EPR spectra for multiwalled carbon nanotubes (MW CNTs) at room temperature with and without laser irradiation ($\lambda = 532$ nm). The MW CNTs samples were purchased from SES Research (Houston, TX, USA), they are (short) S-Purified with an outer diameter of 10–30 nm. The ESR spectrum without laser radiation presents a wide asymmetric line with a width $\Delta H_p = 158$ mT and a g -factor $g = 2.3946$. The experimental data was used to calculate the second $\langle H^2 \rangle$ and fourth $\langle H^4 \rangle$ spectral moments of the line, taking into consideration its asymmetry with regards to the method described in [1], leading to the following result: $\langle H^4 \rangle / \langle H^2 \rangle^2 = 1.014$. Thus the EPR line shape for MW CNTs is approximately Gaussian (for which the ratio is 3), which demonstrates that the magnetic moments that contribute to the EPR spectrum are distributed randomly, and subject to dipole-dipole interactions. Given that the MW CNTs samples are pure, their magnetism is caused solely by the presence of O_2 molecules with integer spin $S = 1$ in the ground state, that are adsorbed on the nanotube surface, which have a much larger surface area than the single carbon nanotubes (SCNTs). According to [2] for SCNTs the binding of a triplet O_2 near the top of two adjacent zigzag bonds corresponds to a distance from the nanotube equal to 3.7 Å with binding energy of 27 meV (calculation on the basis of spin-polarized generalized gradient approximation). EPR data shown that the energy of photons emitted by laser MGL-450 used in our experiments (2.33 meV) is higher than

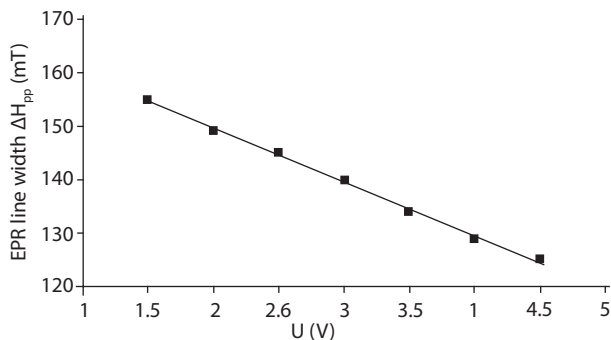


Fig. 1. Dependence of MW CNTs EPR line width on laser excitation level.

the binding energy of oxygen molecules adsorbed on the surface of MW CNTs and therefore under these conditions the molecular photoeffect must exist.

The linear narrowing of the MW CNTs EPR line with increasing laser irradiation intensity (which is linearly proportional to the applied laser excitation voltage U) is presented in Fig. 1. The observed narrowing is caused by the removal of O_2 molecule from the nanotube surface under the influence of laser radiation ($h\nu \geq E_b$), thus excluding their contribution to the ESR line width. The linear narrowing of the EPR line is a direct consequence of the linear growth of the number of removed O_2 molecules – the law of the molecular photoeffect is in full agreement with the Stoletov's law of the outer photoelectric effect.

The behavior under laser radiation of gas molecules adsorbed on nanostructure surfaces is independent of the nature of the molecules. The fact that the molecular photoeffect is observed for the first time for O_2 molecules with a magnetic moment is due to the applicability of EPR methods in this case.

1. Poole C.P., Jr.: Electron Spin Resonance: a Comprehensive Treatise on Experimental Techniques. New York-London-Sydney, Interscience Publishers, a division of John Wiley & Sons, 1967.
2. Tchernatinsky A., Desai S., Sumanasekera G.U. *et al.*: J. Appl. Phys. **99**, 034306 (2006)

**Dedicated to Prof. Yu. V. Yablokov.
Peculiarities of Interaction between Jahn-Teller Centers**

M. V. Eremin

Institute of Physics, Kazan Federal University, Kazan 420008, Russian Federation,
meremin@ksu.ru

My collaboration with Yu. V. Yablokov, and his nice scientific group, began with researches of three-nuclear complexes of copper. In the frame of Heisenberg – Dirac model the ground state of this complex has to be degenerate. The energy of low lying spin multiples ($S = 1/2$) are exactly equal. However, EPR experiments clear showed that this is not the case. Moreover, the effective q -value essentially deviated from its expected value 2. The group-theory analysis, which we carried out, showed that splitting of these states is caused by Dzyaloshinskii-Moriya interaction. The results and further progress of EPR studies of exchange couples complexes were summarized in the book [1].

The next stage of our cooperation was the study of crystals $K_2ZnF_4 \cdot Cu^{2+}$. Using EPR method the quasistatic long-range correlations of Cu^{2+} -centers via the phonon field were discovered at low temperatures [2]. Thus, it was very clear evidence for phonon mediates interaction [3] between paramagnetic ions. Peculiarities of anisotropic exchange coupled Cu^{2+} -ions were studied as well [4].

Among results of modern researches it is planned to discuss the orbital ordering pictures in $LaMnO_3$ [5] and Sr_2VO_4 [6] crystals.

1. Yablokov Yu.V., Voronkova V.K., Mosina L.V.: Paramagnetic Resonance of Exchange Clusters (in Russian). Moscow, Nauka, 1988.
2. Eremin M.V., Ivanova T.A., Yablokov Yu.V., Gumerov R.M. : JETP Lett. **37**, 226 (1983)
3. Aminov L.K., Kochelaev B.I.: Sov. Phys.: JETP **15**, 903 (1962)
4. Eremin M.V., Yablokov Yu.V., Ivanova T.A., Gumerov R.M.: Sov. Phys.: JETP **87**, 220–227 (1984)
5. Trokiner A., Verkhovskii S., Gerashenko A., Volkova Z., Anikeenok O., Mikhalev K., Eremin M., Pinsard-Gaudart L.: Phys. Rev. B **87**, 125142 (2013)
6. Eremin M.V., Deisenhofer J., Eremina R.M., Teyssier J., van der Marel D., Loidl A.: Phys. Rev. B **84**, 212407 (2011)

From Jahn-Teller Effect via Mixed Valence Clusters to Carbon Materials – the Poznan's Period

M. A. Augustyniak-Jablokow

Institute of Molecular Physics, Polish Academy of Sciences, Poznan 60-179, Poland,
aldona@ifmpan.poznan.pl

In the Institute of Molecular Physics Yurii V. Yablokov worked since March, 1999 till September, 2006. However he was scientifically active even after his formal retirement. During his Poznan period he published 30 scientific works. During these years I had the honor, luck and pleasure to work with him on various scientific projects.

Our cooperation started in 1996 and concerned the plasticity of the $\text{Cu}(\text{H}_2\text{O})_6^{2+}$ Jahn-Teller complex affected by lattice strains and cooperative interactions [1–3]. We have studied the systems in which hydrostatic pressure and temperature were able to switch the deformation of the $\text{Cu}(\text{H}_2\text{O})_6^{2+}$ octahedron. This problem was significant for me, but Yurii Yablokov had never limited himself to one problem. He continued working on Ni^{3+} and Cu^{2+} dynamics in ceramics [4–6] and searched for new problems as well. Among such new ones was the process of high spin – low spin transition in some compounds of Fe(III) [7, 8]. These interesting studies were interrupted by the death of Professor Zelentsov, who supplied us with the research material, and the reorganization of our laboratory, which limited our ability to work in this area. Another interesting problem concerned magnetic properties of mixed-valence vanadium clusters in $[\text{V}_4^{\text{IV}}\text{V}_2^{\text{V}}\text{O}_7(\text{OCH}_3)_{12}]$ and $[\text{V}_4^{\text{IV}}\text{V}_2^{\text{V}}\text{O}_7(\text{OC}_2\text{H}_5)_{12}]$ crystals [9, 10]. And again we were forced to abandon this interesting topic. The reason was the retirement of Professor Hartl, a German chemist, who gave us these interesting crystals. A few years earlier, on the initiative of Yurii Yablokov we were engaged to the research of shungite – a natural carbonaceous material, which, despite the amorphous structure, showed metallic type of conductivity. This problem required to explore the EPR of conduction electrons as well as to start in-depth study of the properties of the conductive carbon materials. We have published two papers devoted to the magnetic properties of shungite [11, 12], and to the last weeks of his live Yu. Yablokov worked on the third one devoted to the conductivity in these materials [13]. Shungites, or more precisely, the higher anthraxolites are interesting materials, but, at present, do not raise great scientific interest. But the study of this material allowed us to gain practice in the study of the conductive carbon materials and gave us background for the study of the properties of graphene. Yurii V. Yablokov cooperated with me and my PhD student working on this subject [14]. His remarks and deep understanding of the problem were essential both for this first publication and for the future direction of our research.

During his work in the Institute of Molecular Physics Yurii V. Yablokov worked with a group of young scientists and students. He never learnt to speak Polish sufficiently for common conversation, they did not know Russian, and often knew only little English, but in an astonishing way he was able to teach them physics and, in particular, to explain them in details the phenomenon of EPR. He taught them also a creative approach to research as well as the scientific integrity essential in work and life. They remember him and were supporting me in the hard year after Yurii Vasilevich Yablokov' death.

1. Augustyniak-Jabłokow M.A., Yablokov Y.V.: *Solid State Comm.* **115**, 439 (2000)
2. Augustyniak-Jabłokow M.A., Yablokov Y.V., Łukaszewicz K., Pietraszko A., Petrashen V.E., Ulanov V.A.: *Chem. Phys. Lett.* **344**, 345 (2001)
3. Hitchman M.A., Yablokov Y.V., Petrashen V.E., Augustyniak-Jabłokow M.A., Stratemeier H., Rile M.J., Łukaszewicz K., Tomaszewski P.E., Pietraszko A.: *Inorg. Chem.* **41**, 229 (2002)
4. Ivanova T.A., Jacyna-Onyszkiewicz I., Mrozinski J., Troc R., Yablokov Y.V., Zelentsov V.V.: *Physica B.* **304**, 246 (2001)
5. Ivanova T.A., Petrashen V.E., Chezhina N.V., Yablokov Y.V.: *Phys. Solid State* **44**, 1468 (2002)
6. Augustyniak-Jabłokow M.A., Yablokov Y.V., Jacyna-Onyszkiewicz I., Ivanova T.A., Shustov V.A.: *Acta Phys. Pol. A* **112**, 523 (2007)
7. Zelentsov V.V., Yablokov Y.V., Augustyniak-Jabłokow M.A., Krupska A., Mrozinski J., Ulanov V.A.: *Chem. Phys.* **301**, 15 (2004)
8. Yablokov Y.V., Zelentsov V.V., Augustyniak-Jabłokow M.A., Krupska A., Mrozinski J.: *Materials Science-Poland* **21**, 215 (2003)
9. Augustyniak-Jabłokow M.A., Borshch S.A., Daniel C., Hartl H., Yablokov Y.V.: *New Journal of Chemistry* **29**, 1064 (2005)
10. Augustyniak-Jabłokow M.A., Daniel C., Hartl H., Spandl J., Yablokov Y.V.: *Inorg. Chem.* **47**, 322 (2008)
11. Yablokov M.Y., Augustyniak-Jabłokow M.A., Kempinski W., Stankowski J., Yablokov Y.V.: *Phys. Stat. Solidi B* **243**, R66 (2006)
12. Augustyniak-Jabłokow M.A., Yablokov Y.V., Andrzejewski B., Kempinski W., Łoś S.; Tadyszak K., Yablokov M.Y., Zhikharev V.A.: *Physics and Chemistry of Minerals* **37**, 237 (2010)
13. Augustyniak-Jabłokow M.A., Yablokov Y.V., Andrzejewski B., Tadyszak K., Yablokov M.Y., Zhikharev V.A., to be published.
14. Augustyniak-Jabłokow M.A., Tadyszak K., Maćkowiak M., Yablokov Y.V.: *Phys. Stat. Solidi – Rapid Research Letters* **5**, 271 (2011)

EPR of Clusters Containing Dysprosium Ions

V. K. Voronkova¹, A. A. Sukhanov¹, A. Baniodeh², and A. K. Powell²

¹ Zavoisky Physical-Technical Institute, Russian Academy of Sciences, Kazan 420029, Russian Federation

² Karlsruhe Institute of Technology, University of Karlsruhe, Karlsruhe D-76131, Germany

EPR studies of paramagnetic clusters at the Zavoisky Physical-Technical Institute is a story of success and it is associated with Prof. Yuriy Yablokov. Yu. V. Yablokov was one of the first to study the exchange interactions and the structure of copper dimers by EPR. The EPR investigations of magnetic and spin properties of various dimers and triads of transition metal ions contributed to the study of the exchange interactions between the 3d-ions. The first investigations of the spin-spin interaction between transition metal and rare-earth ions by EPR method were also performed at here under the guidance of Yu. V. Yablokov.

Recently clusters built up of transition metal and rare-earth ions have attracted much attention in the field of molecular magnetism. Of particular interest are clusters containing dysprosium ions as perspective candidates for the design of single-molecule magnets (SMMs). The SMM behavior of these clusters is connected with the strong magnetic anisotropy which is a feature of dysprosium ions in the low-symmetry environment. The design of new SMMs on the basis of clusters with dysprosium ions requires the understanding of the correlation between the relaxation rate of the magnetization and anisotropy of the local magnetic properties of Dy³⁺ ion. Here, we report the results of the EPR investigation of a family of compounds with different substituted benzoate ligands [Fe₂Dy₂(OH)₂(teaH)₂(R-C₆H₄COO)₆] built up of Fe₂Dy₂ clusters and showed SMM behavior [1–3].

This research is supported in part by the Russian Foundation for Basic Research (project no. 13-02-01157).

1. Mereacre V., Baniodeh A., Anson C.E., Powell A.K.: *J. Am. Chem. Soc.* **133**, 15335 (2011)
2. Baniodeh A., Lan Y., Novitchi Gh. *et al.*: *Dalton Trans.* DOI:10.1039/C3DT00105A (2013)
3. Baniodeh A., Mereacre V., Lan Y., Wolny J.A., Anson Ch.E., Schünemann V., Powell A.K.: *Lanthanide Anisotropy* (2013), in print.

SECTION 2

CHEMICAL AND BIOLOGICAL SYSTEMS

EPR of Switchable Magneto-Active Materials with Nitroxides

**E. G. Bagryanskaya^{1,2}, M. V. Fedin², S. L. Veber², I. Yu. Drozdyuk²,
E. V. Tretyakov², V. I. Ovcharenko², A. M. Sheveleva²,
D. I. Kolokolov³, and A. G. Stepanov³**

¹N. N. Vorozhtsov Novosibirsk Institute of Organic Chemistry SB RAS, Novosibirsk,
Russian Federation, egbagryanskaya@tomo.nsc.ru

²International Tomography Center SB RAS, Novosibirsk, Russian Federation,
elena@tomo.nsc.ru

³Institute of Catalysis SB RAS, Novosibirsk, Russian Federation

Switchable magneto-active materials attract significant attention due to both fundamental interest and potential applications in spintronics. Among other techniques, EPR plays important role in studying spin states of these compounds and their dynamics under external stimuli. In this report we focus on two types of switchable compounds containing nitroxides. The first one, copper-nitroxide based molecular magnets $\text{Cu}(\text{hfac})_2\text{L}^{\text{R}}$, represents an interesting type of thermo- and photo-switchable materials which exhibit reversible magneto-structural rearrangements with significant changes of the unit cell volume (and therefore are often called “breathing crystals”). The unusual type of magnetic switching between weakly- and strongly exchange-coupled states occurs in spin triads nitroxide-copper(II)-nitroxide. We overview experimental approaches developed for these systems, discuss general trends and focus on the characteristics of light-induced spin state switching and relaxation using CW X/Q-band and time-resolved EPR [1]. Since light-induced phenomena in “breathing crystals” are promising for spintronics, our recent efforts have been focused on optimization of their optical and relaxation properties by chemical modification of nitroxide ligands. In particular, complexes with *tert*-butylpyrazolyl nitroxides show superior optical properties and slower relaxation rates, allowing photoswitching at up to ~65 K. Another interesting direction on the way to applications is the study of light-induced phenomena in thin polymer films and layers based on “breathing crystals”, where the high sensitivity of EPR compared to SQUID-magnetometry is crucial. We discuss recent results and future research in this field [2].

The second type of “breathing” structures addressed in this work refers to the metal-organic framework (MOF) compound MIL-53(Al), which undergoes reversible temperature-induced structural transition between large-pore and narrow-pore crystalline states with a significant hysteresis. We report CW and pulse X/Q-band EPR study of MIL-53(Al) with adsorbed guest molecules of stable nitroxide (TEMPO). We have found that the mobility of nitroxides in nanochannels of MIL-53(Al) strongly depends on both temperature and crystalline state of the MOF. In addition, guest-host interactions of TEMPO with OH groups of the framework have been investigated. The “breathing” mode of MIL-53(Al) is suppressed at high concentrations of guest molecules,

therefore application of many analytical methods in this mode is impossible. High sensitivity of EPR in conjunction with low concentrations of spin probes makes it an indispensable tool to study guest-host interactions in MIL-53(Al) and other structurally flexible MOFs [3]. This work was supported by RFBR (11-03-00158, 12-03-33010, 12-03-31329) and Russian Ministry for Education and Science (8436, 8456).

1. Ovcharenko V., Bagryanskaya E.: “Breathing Crystals from Copper Nitroxyl Complexes”, Chapt. 9 in book “Spin-Crossover Materials – Properties and Applications” (Halcrow M.A., ed.), p. 239–280. Chichester, UK, John Wiley & Sons, 2013.
2. Fedin M.V., Maryunina K.Yu., Sagdeev R.Z., Ovcharenko V.I., Bagryanskaya E.G.: *Inorg. Chem.* **51**, 709 (2012)
3. Veber S., Fedin M., Maryunina K.Yu., Boldyrev K., Sheglov M., Kubarev V., Shevchenko O., Vinokurov N., Kilipanov G., Sagdeev R., Ovcharenko V., Bagryanskaya E.: *J. Phys. Chem. A.* **117**, 1483 (2013)

Structural Studies of Biological Membranes Using ESEEM Spectroscopy of Spin Labels and Deuterium Substitution

S. A. Dzuba

Voevodsky Institute of Chemical Kinetics and Combustion SB RAS, Novosibirsk State University,
Novosibirsk, Russian Federation, dzuba@kinetics.nsc.ru

Electron Spin Echo Envelope Modulation (ESEEM) spectroscopy in conjunction with biochemical techniques of site-directed spin labeling and deuterium substitution in molecules or parts of molecules can be used to gain insights into supramolecular structure of biological membranes. The presentation covers the applications of this approach to study penetration of water and cryogenic agents into the hydrophobic part of model phospholipid membranes, to determine the localization and orientation of peptide antibiotics in membranes and conformations of membrane proteins.

Short Nitroxide Biradicals: Comparison of EPR Data with Quantum-Chemical Calculations

**A. I. Kokorin¹, E. N. Golubeva², B. Y. Mladenova-Kattnig³,
and G. Grampp³**

¹ N. N. Semenov Institute of Chemical Physics RAS, Moscow 119991, Russian Federation, kokorin@chph.ras.ru

² Department of Chemistry, M. V. Lomonosov Moscow State University, Moscow 119992, Russian Federation, legol@mail.ru

³ Institute of Physical and Theoretical Chemistry, Graz University of Technology, Graz, Austria, grampp@tugraz.at

Nitroxide biradicals (NB) attract attention of researchers because of their unique abilities for investigating the mechanism and features of the intramolecular electron spin exchange (IESE) [1]. Properties of NB dissolved in different molecular solvents and in various ionic liquids (ILs) were discussed in detail in [2, 3]. Recently, unrestricted density-functional-theory calculations of the geometry and electronic structure of biradical $O=S(OR_6)_2$ were carried out using the ORCA program package [4]. Quantum-chemical calculations allowed explain some unusual peculiarities of IESE in short-chain NB dissolved in ionic liquids (ILs) [4]. In this work we compare the results of EPR investigation of several short nitroxide biradicals with quantum-chemical calculations.

Two 1-alkyl-3-methylimidazolium ILs (omimBF₄ and bmimPF₆) were used for comparison with usual molecular solvents. Here o means octyl, and b – bu-

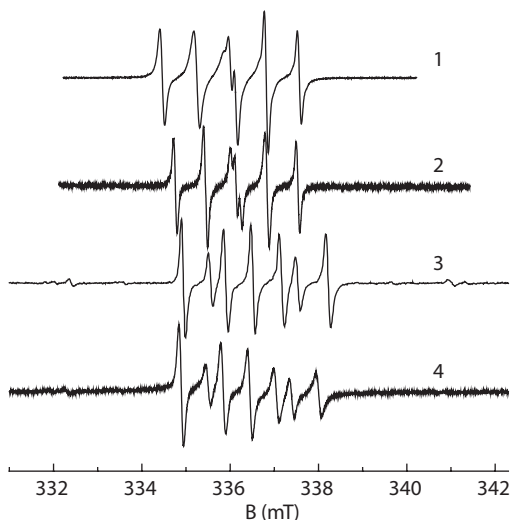


Fig. 1. EPR spectra of biradical **I** in bmimPF₆ at 383 (1) and in dioxane at 374 K (2), and **II** in ethanol at 341 (3) and in omimBF₄ at 370 K (4). Measured values of $|J|$ are equal to: 186 ± 8 G in bmimPF₆, 215 ± 10 G in dioxane, 38 ± 3 G in ethanol, 33 ± 2 G in omimBF₄.

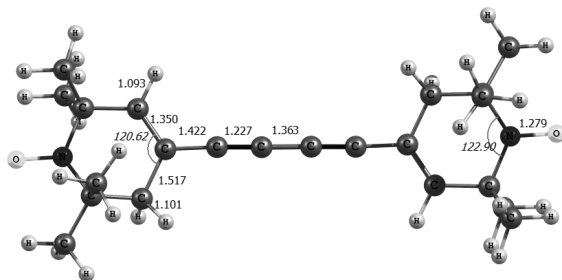


Fig. 2. Calculated geometry (B3LYP/cc-pVdz) of the biradical **I** is in a good agreement with its X-ray structure [5].

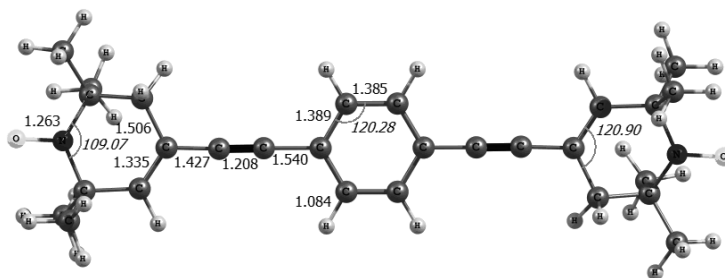


Fig. 3. Calculated geometry (B3LYP/cc-pVdz) of biradical **II**.

tyl groups. Two NB: $R_6-C\equiv C-C\equiv C-R_6$, **I**, and $R_6-C\equiv C-p-C_6H_4-C\equiv C-R_6$, **II**, were studied. R_6 is 1-oxyl-2,2,6,6-tetramethyl-3,4-ene-piperidine ring. Typical EPR spectra of **I** and **II** are given in Fig. 1.

Geometry optimization and D-tensor calculations of biradicals **I** and **II** were carried out on the DFT/UB3LYP/cc-pVdz and DFT/ROPBE/N07D levels of theory. Probable differences in biradicals behavior are discussed. These calculated geometries are shown in Fig. 2 and 3.

Regularities and peculiarities of the intramolecular spin exchange of both NB dissolved in various solvents, and the effect of ILs nature on the IESE will be discussed in the paper.

The work was supported by Russian Foundation for Basic Research (grant 12-03-00623-a).

1. Nitroxides: Theory, Experiment, Applications (Kokorin A.I., ed.). Rijeka, InTech, 2012.
2. Kokorin A.I.: *Appl. Magn. Reson.* **26**, 253 (2004)
3. Kokorin A.I., Tran V.A., Vorobieva G.A.: *Appl. Magn. Reson.* **37**, 473 (2010)
4. Kokorin A., Mladenova B., Golubeva E., Grampp G.: *Appl. Magn. Reson.* **41**, 353 (2011)
5. Shibaeva R.P., Rozenberg L.P.: *Zh. Strukt. Khimii* **16**, 258 (1975) (in Russian)

Spin Relaxation and Magnetic Interactions in Light-Induced Spin-Correlated Radical Pairs in P3HT:PC60BM Composite

L. V. Kulik¹, M. N. Uvarov¹, A. A. Popov^{1,2}, and E. A. Lukina^{1,2}

¹ Institute of Chemical Kinetics and Combustion, Siberian Branch of Russian Academy of Sciences, Novosibirsk 630090, Russian Federation, chemphy@kinetics.nsc.ru

² Novosibirsk State University, Novosibirsk 630090, Russian Federation

The composite of [6,6]-Phenyl C₆₁ butyric acid methyl ester (PCBM) and poly(3-hexylthiophene) (P3TH) is a perspective material for active layer of organic solar cells. Upon light absorption the charge transfer occurs in this material with quantum yield close to unity. Short-living spin-correlated radical pairs PCBM⁻/P3HT⁺ are formed [1], which can be further separated to free charge carriers.

In this work the spin dynamics of photogenerated radicals PCBM⁻ and P3HT⁺ was studied by Electron Spin Echo (ESE) in order to clarify the mechanism of light-induced charge separation in P3HT:PCBM composite. The radicals were generated either by continuous visible light illumination or by laser flashes with 532 nm wavelength. The echo-detected (ED) EPR spectrum of PCBM⁻/P3HT⁺ strongly depends on delay after laser flash (*DAF*). At short *DAF* values (*DAF* < 30 μs) both microsecond-living spin-correlated radical pairs PCBM⁻/P3HT⁺ and free long-living non-coupled radicals PCBM⁻ and P3HT⁺ contribute to ED EPR spectrum [2].

The transversal relaxation times T_2 were determined from ESE decays in two-pulse sequence $\pi/2-\tau-\pi$ -ESE at temperature 80 K. For non-coupled radicals PCBM⁻ and P3HT⁺ in thermal equilibrium generated by continuous light $T_{2,c} = 2.0 \pm 0.1$ μs and $T_{2,h} = 1.6 \pm 0.1$ μs were obtained, respectively. T_2 of laser-generated spin-correlated radical pair PCBM⁻/P3HT⁺ measured at small *DAF* (about 100 ns) was about twice shorter.

The model of instantaneous diffusion in ESE explains the effect of transversal relaxation time decrease for spin-correlated radical pairs PCBM⁻/P3HT⁺. It assumes that microwave pulses affect both electron spins in the pair simultaneously. From the obtained transversal relaxation rate difference the average strength of magnetic interaction in spin-correlated radical pairs PCBM⁻/P3HT⁺ about 1 MHz was estimated. Presumably, the major contribution to this interaction is given by dipolar interaction between PCBM⁻ and P3HT⁺ radicals. Its strength corresponds to average interspin distance of about 4 nm.

For small *DAF* values net emissive polarization (CIDEP) is observed in ED EPR spectra of PCBM⁻/P3HT⁺ pair. It is probably generated by singlet-triplet mixing during the light-induced charge separation and formation of this pair [3].

The work was supported by RFBR grant №12-03-00238-a and by program of Presidium of RAS № 23/24.48 “Nanodynamics of disordered media”.

1. Behrends J., Sperlich A., Schnegg A., Biskup T., Teutloff C., Lips K., Dyakonov V., Bittl R.: Phys. Rev. B **85**, 125206 (2012)
2. Uvarov M.N., Kulik L.V.: Appl. Magn. Res. **44**, 97–106 (2013)
3. Salikhov K.M., Schlupmann J., Plato M., Möbius K.: Chem. Phys. **215**, 23–35 (1997)

SECTION 3

CHEMICAL AND BIOLOGICAL SYSTEMS.
ELECTRON SPIN BASED METHODS FOR
ELECTRONIC AND SPATIAL STRUCTURE
DETERMINATION

EPR Study on Mechanism of Catalyzed Reactions from Arylboronic Acids to Phenols

H. Yang, Y. Li, M. Jiang, and H. Fu

Department of Chemistry, Tsinghua University, Beijing 100084, P. R. China,
hxxly@mail.tsinghua.edu.cn

Phenols were used as fundamental intermediates and synthetic building blocks for the construction of basic molecules such as pharmaceuticals, polymers and materials. Due to the importance of phenols derivatives, much attention had been focused on their synthesis. Arylboronic acids could be converted to phenols by a variety of ways [1–3]. It was reported that the mechanism of those reactions was based on oxidation of the arylboronic acids. However, the details of the process, such as what it happened for the oxygen, and whether there were radicals in the reactions, are not clear. In order to clarify the mechanism of those reactions and develop the new methods with more advantage in organic synthesis, EPR (Electron Paramagnetic Resonance) was used to monitor and explore the mechanism of those reactions.

We had developed a general copper-catalyzed transformation of arylboronic acids to phenols in water firstly [1]. The EPR experiments provided the evidence that coordination of oxygen with copper and boron was observed, and Cu(I), Cu(II) and Cu(III) were determined. The results showed that the catalytic cycle underwent transform of the three copper salts. Obviously, the environmentally benign transition metal-free approaches are preferred in organic synthesis. Inspired by this reaction mechanism, we developed a new catalytic system without metal to replace the copper salts catalytic system. As we known, 2,2,6,6-tetramethyl-1-piperidinyloxy (TEMPO) was a stable radical. TEMPO was used to replace the copper salts according this mechanism. Good yields were obtained at 80 °C from arylboronic acids to phenols with 5% TEMPO as catalyst in presence of KOH in water and methanol with 3:1 (v:v) under O₂ atmosphere. EPR results showed that $\cdot\text{O}_2^-$ radical was observed when KOH was added to the system above trapped by DMPO (Dimethyl Pyridine N-oxide). Encouraged by this reaction, recently we used hydrogen peroxide and carbonate salts as a high oxidant system to catalysis arylboronic acids to phenols with excellent yield (more than 90%) at room temperature. EPR results showed that hydrogen peroxide and bicarbonate salts to produce peroxymonocarbonate ($\cdot\text{HCO}_4^-$) radical which was a stronger oxidant than TEMPO.

We can conclude that mechanism of the reaction from arylboronic acids to phenols might be processed coordination of oxygen to boron, then production of aryl radical and hydroxyl radicals from the results by EPR. And a series of radical catalyzed reactions from arylboronic acids to phenols were developed according the reaction mechanism proposed above. All synthesis results also

give a clear and direct evidence to clarify the reaction mechanism and provide a base to predict the new organic synthesis methods in the future.

The financial support of the National Natural Science Foundation of China (Grant No. 21105054) is gratefully acknowledged.

1. Yang H., Li Y., Jiang M., Wang J., Fu H.: *Chem. Eur. J.* **17**, 5652 (2011)
2. Zou Y., Chen J., Liu X., Liu X., Lu L., Davis R., Jørgensen K.A., Xiao W.: *Angew. Chem. Int. Ed.* **51**, 784 (2012)
3. Simon J., Salzbrunn S., Olah G.A.: *J. Org. Chem.* **66**, 622 (2001)

Continuous-Wave and Time-Resolved Electron Paramagnetic Resonance Study of Dimerized Aza-Crown Copper Porphyrins

**Yu. E. Kandrashkin¹, V. S. Iyudin¹, V. K. Voronkova¹,
E. A. Mikhailitsyna², and V. S. Tyurin²**

¹ Zavoisky Physical-Technical Institute, Russian Academy of Sciences, Kazan 420029, Russian Federation, spinalgebra@gmail.com

² Frumkin Institute of Physical Chemistry and Electrochemistry RAS, Moscow 119071, Russian Federation

Porphyrins and their derivatives have a unique ability to bind a wide variety of metals and paramagnetic ligands and to provide a wide range of redox photophysics and photochemistry. Special attention is attracted by the property of self-organization of the porphyrins and metalloporphyrins, which leads to the formation of supramolecules and nanoscale porphyrin assemblies [1]. Here we present the EPR evidence of the dimerization of the compound based on 5-(40-(aza-15-crown-5)-phenyl) copper porphyrin (CuP) [2, 3].

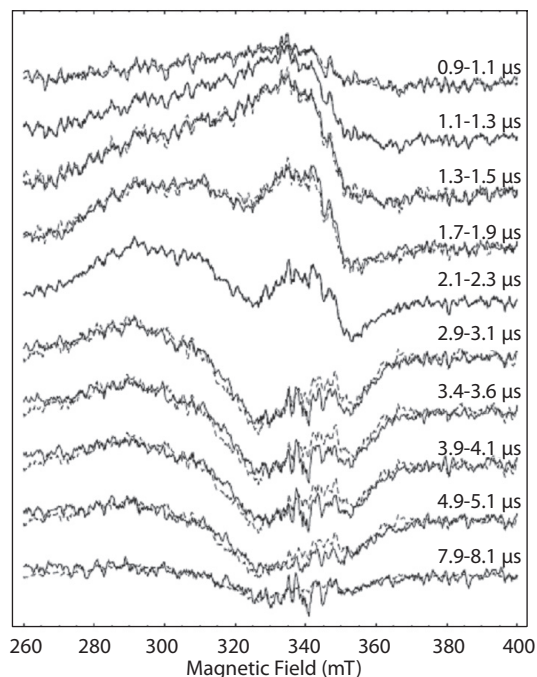


Fig. 1. TR EPR spectra of the dimerized CuP. The spectra (solid curves) are derived by integrating the dataset in the selected time windows given above the relevant curves. The dashed curves represent the results of the fitting of the experimental spectra with the sum of two spectra obtained by integration in the time windows 1.1–1.3 and 2.1–2.3 μs .

Continuous-wave (CW) EPR spectroscopy is used to study the ground states of the CuP monomer and the supramolecular complex that appear upon addition of the K(SCN) salt to a solution of the CuP monomer. The magnetic resonance parameters of the CuP monomer, and the exchange interaction parameter, $J = 0.25 \text{ cm}^{-1}$, and the Cu-Cu distance of the CuP dimer, $R = 0.5 \text{ nm}$, have been determined by comparing the experimental CW EPR spectra with the results of the numerical calculations.

Time resolved (TR) EPR investigations of the photoexcited CuP demonstrate the crucial changes of the spectral and kinetic properties of the molecules after the dimerization. The shape of the spectrum of CuP monomer under the light excitation corresponding to the CW EPR spectrum as well as the monoexponential decay indicates that the spin-polarized signal originates from the ground state of the porphyrin. The TR EPR spectrum of the photoexcited CuP dimer has essentially more complicated behavior (see Fig. 1). The overall lifetime of the signal of the dimerized complexes is about three times larger than that of monomers ($\sim 10 \mu\text{s}$. vs. $\sim 3 \mu\text{s}$). The results of the TR EPR study of the supramolecules have been rationalized by the assumption that spin-polarized excited states contribute to the observed signal. The simulations are in agreement with the suggestion that the observed excited state of the supramolecule is formed by the interaction of the photoexcited porphyrin in the quartet state and the nearby non-excited porphyrin in the ground state.

The research was supported in part by the Russian Foundation for Basic Research (project nos. 12-03-97078).

1. Mamardashvili G.M., Mamardashvili N.Zh., Koifman O.I.: *Usp. Khimii* **77**(1), 60–74 (2008)
2. Mikhailitsyna E.A., Tyurin V.S., Zamyatskov I.A., Khrustalev V., Beletskaya I.: *Dalton Trans.* DOI:10.1039/c2dt30123g (2012)
3. Kandrashkin Yu.E., Iyudin V.S., Voronkova V.K., Mikhailitsyna E.A., Tyurin V.S.: *Appl. Magn. Reson.* DOI 10.1007/s00723-013-0461-y (2013)

The Molten Globule State of Maltose Binding Protein: DEER Measurements at pH 3

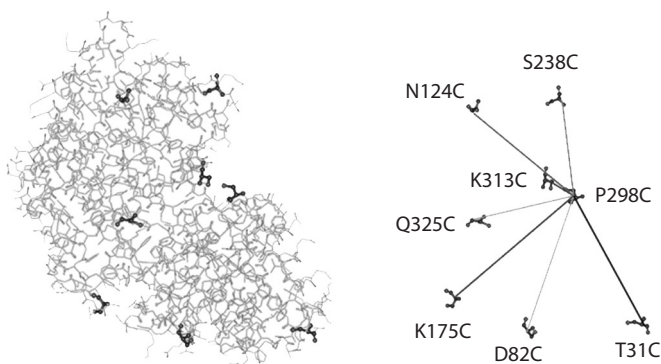
M. Chakour¹, J. Reichenwallner², B. Selmke¹, C. Chen¹, S. Theison¹,
R. Chakraborty³, S. Indu³, R. Varadarajan³,
D. Hinderberger², and W. E. Trommer¹

¹ Department of Chemistry, TU Kaiserslautern, Kaiserslautern D-67653, Germany,
trommer@chemie.uni-kl.de, chakour@chemie.uni-kl.de, sandratheison@gmx.de

² Max Planck Institute for Polymer Research, Mainz D-55128, Germany,
hinderberger@mpip-mainz.mpg.de, reichenw@mpip-mainz.mpg.de

³ Molecular Biophysics Unit, Indian Institute of Science, Bangalore 560004, India,
varadar@gmail.com, indugopalan@gmail.com, rusha1989@gmail.com

Maltose-binding protein (MBP) is in a molten globule state at pH 3 as characterized by ANS binding [1]. DEER measurements of seven spin-labeled double mutants as shown in Figures in the native state at pH 7 had shown excellent agreement with X-ray data [2]. At pH 3 corresponding DEER measurements of all the mutants yield a broad distribution of distances. This was to be expected if there is no defined tertiary structure and the individual helices pointing into all possible directions. However, as MBP still binds maltose as molten globule although more weakly, the native structure must be retained at or near the active site. This is now being investigated with a new set of mutants.



1. Prajapati et al.: *Biochem.* **46**, 10339–10352 (2007)
2. Reichenwallner *et al.*: *Appl. Magn. Reson.* (2013), in press.

Investigation of C₆₀ Derivatives with Two and Four Nitroxide Groups by Time-Resolved and Pulse EPR Spectroscopy

**R. B. Zaripov¹, A. E. Mambetov¹, V. K. Voronkova¹, K. M. Salikhov¹,
V. P. Gubskaya², and I. A. Nuretdinov²**

¹ Zavoisky Physical-Technical Institute, Russian Academy of Sciences, Kazan 420029,
Russian Federation

² Arbuzov Institute of Organic and Physical Chemistry of RAS, Kazan, Russian Federation

In the last decade synthesis of hybrid nanostructures has attracted a lot of attention. One of the type of nanomaterials is nonocarbon structures, in particular, built up of fullerene derivatives. Fullerene derivatives find a new fields of the application due to their high reactivity, unique photoinduced properties. Their interesting chemical and physical properties give opportunity to synthesis of new perspectives molecules such as biologically active water-soluble compounds which can be used as efficient compounds in a treatment of serious diseases [1]. To optimize a strategy of the synthesis of these new compounds and to elucidate their application potentials one needs to study comprehensively the physical properties of these substances. The electron paramagnetic resonance spectroscopy allows us to obtain the information about the magnetic properties of molecules, the electron spin density distribution, the Heisenberg exchange interaction, the molecular structure and dynamics, and so on.

In this work methano[60]fullerenes with two (**1**) and four (**2**) covalently linked nitroxide radicals were studied by the pulse and time-resolved EPR. Toluene solutions of **1** and **2** with concentration of 10^{-3} M were investigated in the X- and Q- bands at different temperatures. Photoexcitation of fullerenes was performed by YAG:Nd laser at 532 nm. Using the nutation spectroscopy it was defined that the EPR spectrum of photoexcited compound **1** is described by the spin state with S equals to 2. The spin states with $S = 2, 1, 0$ are expected due to the exchange intraction between excited triplet state of C₆₀ derivative and two radicals. The manifestation of this interaction is not found in the spectra of time-resolved and spin-echo detected EPR of compound **2** before and after laser excitation. Apparently this happens due to the strong dipolar interaction between radical centers.

The work was supported in part by Russian Foundation for Basic Research (grant 12-03-97078).

1. Gubskaya V. *et al.*: Org. Biomol. Chem. **5**, 976 (2007)

SECTION 4

THEORY OF MAGNETIC RESONANCE,
MODERN METHODS OF MAGNETIC RESONANCE

Molecular Dynamics and Electron Spin Relaxation

M. Brustolon and A. Barbon

Dipartimento di Scienze Chimiche, Università di Padova
marinarosa.brustolon@unipd.it

The electron spin relaxation behaviour of paramagnetic species has recently attracted a renewed interest since the knowledge of relaxation rates in electron spin systems is essential in some advanced applications such as DNP, *in vivo* EPR, pulse EPR experiments, and spintronics applications. In this communication we report some examples of studies, in the framework of the EPR group activity in Padova in the last decade, on longitudinal and transverse spin relaxation in solids and in liquid solutions of radicals and triplet states, with a particular emphasis on the correlation between spin relaxation and molecular dynamics. We report examples of intramolecular and intermolecular motions studied by various EPR methods, in supramolecular solids [1, 2] in glassy matrix [3] and in solution [4, 5]. We will show recent results based on new experimental and computational approaches leading to an interesting comparison between relaxation behaviors of different spin probes, nitroxides vs nitronyl nitroxides.

1. Brustolon M., Barbon A., Bortolus M., Maniero A.L., Sozzani P., Comotti A., Simonutti R.: *JACS* **126**, 15512 (2004)
2. Barbon A., Bortolus M., Maniero A.L., Brustolon M.: *PCCP* **7**, 2894 (2005)
3. Collauto A., Mannini M., Sorace L., Barbon A., Brustolon M., Gatteschi D.: *J. Mater. Chem.* **22**, 22272 (2012)
4. Collauto A., Barbon A., Brustolon M.: *J. Magn. Reson.* **223**, 180 (2012)
5. Collauto A., Barbon A., Zerbetto M., Brustolon M.: *Mol. Phys.* DOI:10.1080/00268976.2013.798695 (2013)

PELDOR Theory Revisited

K. M. Salikhov

Zavoisky Physical-Technical Institute, Russian Academy of Sciences, Kazan 420029,
Russian Federation

Nowadays the pulse electron-electron double paramagnetic resonance (PELDOR) experiments are widely used for determining the distance between spin labels and/or a number of dipolar coupled spins, e.g., in oligomers of singly labelled proteins. In these experiments one detects the manifestation of the spin-spin dipole-dipole interaction. The dipole-dipole interaction leads to the oscillations of the observed EPR signals, while the frequency of the oscillations equals the magnitude of the dipole-dipole interaction in the frequency units.

The first theoretical description of the 3-pulse PELDOR experiment was presented in [1]. A model system of the randomly distributed AB pairs of paramagnetic particles was considered. It was assumed that the EPR spectra of these particles do not overlap and in the course of the PELDOR experiment the A and B particles can be selectively excited by the MW pulses. The spin echo is formed by the MW excitation of A particles at $t = 0$ and $t = \tau$. The additional (pump) pulse excites B particles of the AB pairs at $t = T$. In this case the amplitude of the spin echo exhibits the modulation described at any fixed interval τ as

$$V(T) = V_0(\tau)(1 - p_B + p_B \cos(DT)), \quad (1)$$

where $V_0(\tau)$ is the primary spin echo signal amplitude without the pump pulse, p_B is the probability of the inversion of the B particle spins by the MW pump pulse at $t = T$, D is the parameter of the dipole-dipole interaction (see Eq. (2))

$$H_{d-d} = \nabla D_{AB} S_{Az} S_{Bz},$$

$$D_{AB} = (g_A g_B \beta^2 (1 - 3 \cos^2 \theta) / r_{AB}^3) / \nabla \equiv D_{0AB} (1 - 3 \cos^2 \theta). \quad (2)$$

Here r_{AB} is the distance between A and B particle spins, θ is the angle between the vector \mathbf{r}_{AB} and the direction of the external magnetic field. It was supposed that the distance between the partner in a pair is larger than 1 nm so that the contribution of the short-range exchange interaction between spin labels can be ignored.

Equation (1) describes the well-known mechanism of the so-called instantaneous spectral diffusion induced by the “instant” modulation of the dipole-dipole spin-spin interaction when the MW pulse inverts the partner spin projection. This effect of the instantaneous spectral diffusion makes it possible to detect the manifestation of the spin-spin interaction between the spin labels in the pulse EPR experiments. As a result, the information about the spatial distribution of the paramagnetic particles is obtained. For example, to characterize complex

molecular structures, the PELDOR experiments are used, when several spin labels are introduced. Let us assume there are groups of N spin labels. The common paradigm is to present the observable as a product of two terms

$$V(\tau, T) = V(\tau)V(T), \quad (3)$$

where $V(T)$ describes the contribution to the signal of the spin labels which are pumped by the MW pulse at the moment $t = T$. $V(T)$ contains the contributions $V_{\text{intra}}(T)$ and $V_{\text{inter}}(T)$ of the spin-spin interaction inside the groups of spin labels and between these groups, respectively,

$$V(T) = V_{\text{intra}}(T)V_{\text{inter}}(T). \quad (4)$$

Ignoring any correlations of the positions of the spin labels in the groups, $V_{\text{intra}}(T)$ is usually presented as [2]

$$V_{\text{intra}}(T) = (1 - p_B + p_B \langle \cos(DT) \rangle)^{N-1} \approx 1 - (N - 1)p_B(1 - \langle \cos(DT) \rangle). \quad (5)$$

Here $\langle \dots \rangle$ means averaging over orientations of the \mathbf{r}_{AB} vector and distances between spin labels in these groups. Equation (5) is used for determining the distribution of the inter pair distances in the group of N spin labels.

It is expected that with increasing T the contribution of the interaction inside groups $V_{\text{intra}}(T)$ tends to

$$V_{\text{intra}}(T) \Rightarrow (1 - p_B)^{N-1} \cong 1 - (N - 1)p_B. \quad (6)$$

This asymptotic value of the PELDOR signal does not depend on the distances between the spin labels in the groups, and it depends only on the number N of the spin labels in the group.

Equations (1)–(6) are widely used for the interpretation of the PELDOR data in the cases when the spin labels in the pairs or the groups are nitroxide free radicals. Moreover, typically all spin labels are the same nitroxides. Equation (1) was derived for the situation where partner spin labels in a pair are paramagnetic particles with the EPR spectra which do not overlap, so that A and B paramagnetic particles can be selectively excited by MW pulses. Therefore Eq. (1) is not applicable to the systems where both spin labels in pairs are the same nitroxides or nitroxides with close magnetic resonance parameters, so their EPR spectra overlap substantially. As concerns the common paradigm of treating the groups of spin labels (see Eqs. (4)–(6)), they contain several strict assumptions which might highly restrict their application to real systems.

How to treat PELDOR data in the case when both paramagnetic particles in the pairs are paramagnetic particles with the EPR spectra which overlap essentially will be discussed in this report. It is mainly focused on the nitroxide free radicals. Equation (1) has been generalized to describe the contribution of the intra pair interaction to the PELDOR signal when the EPR spectra of the partner spin labels in the pair overlap (or even coincide). A consistent approach

when treating PELDOR data for the groups of more than two spin labels has been presented.

The basic idea of treating the manifestation of the spin-spin interaction in the PELDOR experiments in the general case when the EPR spectra of the spin labels in the pair or groups overlap (or even coincide) was already presented at the Ringberg conference [3].

1. Milov A.D., Salikhov K.M., Schirov M.D.: *Fiz. Tverd. Tela* **23**, 975–982 (1981); *Sov. Phys. Solid State* **23**, 565 (1981)
2. Milov A.D., Maryasov A.G., Tsvetkov Yu.D.: *Appl. Magn. Reson.* **15**, 107 (1998)
3. Salikhov K.M.: Some observations concerning PELDOR methodology. Invited talk at “Int. Symposium on Integrating Advanced Spectroscopy Tools for Structure and Dynamics of Biological Macromolecular Complexes *in vitro* and *in vivo*.” Ringberg, Kreuth, Germany, 12.12.2012–15.12.2012.

Bruker BioSpin: Latest Developments in EPR Instrumentation

D. A. Kuznetsov

Bruker Ltd., Division of Bruker BioSpin, Moscow 119017, Russian Federation,
denis.kuznetsov@bruker.ru

Vector Models in Echo Detected EPR, ESEEM, and PELDOR of Anisotropic Paramagnetic Centers

A. G. Maryasov¹, M. K. Bowman², and Yu. D. Tsvetkov¹

¹ Institute of Chemical Kinetics & Combustion SB RAS, Novosibirsk 630090, Russian Federation, maryasov@kinetics.nsc.ru

² Department of Chemistry, University of Alabama, Tuscaloosa 35487, USA, mkbowman@as.ua.edu

Electron paramagnetic resonance allows the study of structures containing paramagnetic centers (PCs). Visualizing of the process of signal formation in magnetic resonance experiments provides a better understanding of how to optimize measurements of different signal types. The Bloch-type equations are the most effective visualization means which provides an intuitively clear picture of the evolution of the measured quantity as a 3D effective magnetic moment precession under the influence of some effective magnetic field (EMF). The other types of vector models involve construction of effective magnetic field vectors using vectors of the expectation values of the PC spin vector (effective spin vectors, ESVs) when the PC is in one of its eigenstates.

Here we consider both types of models. Bloch equations for PCs with spin of 1/2 having significant g -tensor anisotropy ($\delta g \sim g$) are obtained and are applied to echo-detected EPR spectra. Effective hyperfine and local dipole fields are constructed using ESVs. Several samples of Pake patterns for isotropic PC with $S = 1/2$ interacting with anisotropic PC with $S = 1/2$ or 1 are calculated. The spin dynamics of an electron spin coupled to nuclei or to a non-resonant PC's (B-type spin) is described using EMFs. Both pulse electron-electron double resonance (PELLDOR) signal and electron spin echo envelope modulation (ESEEM) signal may be presented by means of precessing spin vectors of B-type electron spin or nuclei spins, respectively. The precession frequencies of the auxiliary vectors are defined by the EMF vectors. The spectral analysis of the signals provides a key to structural information.

This work was supported by the National Institutes of Health through R01GM069104 and R01HL095820 and by grant no. 5.6.1 of the Divisional project of the Russian Academy of Sciences 5.6.

Magnetic Resonance of Nd^{3+} Nanostructures in Perovskite Type Crystals

M. L. Falin^{1,2}, V. A. Latypov¹, and M. M. Zaripov¹

¹ Zavoisky Physical-Technical Institute, Russian Academy of Sciences, Kazan 420029, Russian Federation

² Kazan (Volga Region) Federal University, Kazan 420008, Russian Federation

Double fluoride crystals with perovskite structure ABF_3 ($A = \text{K}^+$, $B = \text{Mg}^{2+}$, Zn^{2+}) are very interesting because they are convenient model systems for studying the magneto-optical properties of impurity dopant ions. In principle, in these matrices it is possible to substitute two various cations being inequivalent positions. This enables one to carry out investigations of impurity dopant ions in sixfold or uncommon twelfold coordinations. The physical properties of rare-earth ions in these compounds are not sufficiently studied. The introduction of three-charge rare-earth ions is hampered because of heterovalent substitution and the essential difference in the ionic radii of rare-earth ions and lattice cations. Previously the study of Nd^{3+} in KMgF_3 and KZnF_3 was carried out [1]. This report is concerned with the further investigation of impurity paramagnetic centers formed by Nd^{3+} ion in ABF_3 single crystals.

The crystals were grown using the Bridgman-Stockbarger method. EPR was carried out using an X-band spectrometer ERS-231 at $T = 4$ K.

The new paramagnetic center Nd^{3+} of rhombic symmetry, which as proposed is formed by self-organized nanocrystals in ABF_3 crystals, was detected by EPR. The parameters of the corresponding spin Hamiltonians were determined. Structural models of the observed complexes were proposed. The analysis of the obtained results was carried out.

This work was supported by the grant NSh-5602-2012.2 and the Russian Foundation for Basic Research (grant 13-02-97031r_Volga region_a).

1. Abdulsabirov R.Yu., Falin M.L., Fazlizhanov I.I., Kazakov B.N., Korableva S.L., Ibragimov I.R., Safiullin G.M., Yakovleva Zh.S.: Appl. Magn. Reson. **5**, 377 (1993)

Combined Magneto-Electric Spin Resonance of Impurity Ho Ions in Synthetic Forsterite

**V. F. Tarasov¹, N. K. Solovarov¹, A. A. Sukhanov¹, R. B. Zaripov¹,
and E. V. Zharikov^{2,3}**

¹ Zavoiisky Physical-Technical Institute, Russian Academy of Sciences, Kazan 420029,
Russian Federation, tarasov@kfti.kc.ru

² Prokhorov General Physics Institute, Moscow 119991, Russian Federation

³ Mendeleev University of Chemical Technology of Russia, Moscow 125047, Russian Federation

Usually magnetic radiospectroscopy deals with resonance transitions excited by the magnetic component of the microwave field. Specially designed resonators are used to simplify a treatment of experimental results and samples are placed into the region with the maximal homogeneity of the microwave magnetic field and the minimal value of the electric component of the microwave field. In the case of dielectric resonators used in ELEXYS E580 EPR spectrometers (Bruker) and open resonators at submillimeter frequencies, the sample is simultaneously affected by magnetic and electric components of the microwave field. It was found in the EPR study of the impurity Ho³⁺ ions in synthetic forsterite that the EPR signals are the contour of the absorption line instead of the conventional derivative of the absorption contour. Conditions of appearance and characteristics and of the anomalous lines are studied.

This observation was explained by the combined excitation of the spin and orbital subsystems of the Ho³⁺ electron system by the magnetic and electric components of the microwave field, respectively. The absorption lines observed when the spin and orbital subsystems are characterized by different inertia relative to the change of the magnetic field during the magnetic field modulation. As a result, the phase shift between the internal oscillations of the orbital and spin subsystem oscillates with the frequency of magnetic field modulation and the sign of the phase shift between subsystems varies twice during the modulation period.

The work was supported by the Russian Foundation for Basic Research (grant 12-02-00535).

Manipulating Spin Hyper-Polarization by means of Adiabatic Switching of a Spin-Locking RF-Field

A. S. Kiryutin^{1,2}, K. L. Ivanov^{1,2}, A. V. Yurkovskaya^{1,2},
H.-M. Vieth³, and N. N. Lukzen^{1,2}

¹ International Tomography Center SB RAS, Novosibirsk 630090, Russian Federation,
ivanov@tomo.nsc.ru

² Novosibirsk State University, Novosibirsk 630090, Russian Federation

³ Freie Universität Berlin, Berlin D-14195, Germany

A new method has been proposed allowing one to convert initial multiplet spin order into polarization of almost any desired kind. It is based on hyper-polarizing a system of scalar coupled spins in the presence of a strong RF-field, which is subsequently slowly (adiabatically) reduced to zero. The technique can be useful for manipulating hyper-polarization, in particular, in cases where multiplet spin order gives the main contribution to hyper-polarization. The method allows one not only reversing the sign of the multiplet polarization but also converting it into net hyper-polarization without any loss of the spin order. In contrast to multiplet spin order the contributions coming from net polarization do not disappear in the NMR spectrum in the presence of line broadening. Therefore net hyper-polarized signals can be used in NMR spectroscopy and imaging in combination with standard pulse sequences. For instance, our technique can be applied to the case of PHIP, which gives very strong hyper-polarization resulting in NMR enhancements of up to 10.000; in contrast, the original polarization is purely of the multiplet kind. For the two-spin system we were able to show theoretically and experimentally that PHIP can be fully converted into net spin order: for instance, by properly setting the RF-field frequency one can convert the initial state population pattern into one where only the $\alpha\alpha$ and $\beta\beta$ spin states are populated; therefore both spins will get net polarized. The method can also be extended to higher-spin systems, which initially carry only multiplet polarization, thus allowing one to create net hyper-polarization.

Financial support by the Russian Foundation for Basic Research (projects No. 12-03-31042, 12-03-33082, 12-03-31775, 13-03-00437), the Alexander von Humboldt Foundation and the program of Russian Government to support research conducted by the leading scientists (grant №11.G34.31.0045) is gratefully acknowledged.

Distance and Orientation Measurements with DEER/PELDOR at 95 and 263 GHz

I. Tkach and M. Bennati

Research Group EPR Spectroscopy, Max Planck Institute for Biophysical Chemistry,
Göttingen 37077, Germany, Igor.Tkach@mpibpc.mpg.de

PELDOR spectroscopy is a well-known technique to measure inter-spin distances in a nanometer range. Besides this, if applied at high fields/frequencies (95 and 263 GHz), the method exhibits an enhanced orientation selectivity. Thus, it can be used to provide information on the relative orientation of spin-labels in a pair, assuming those are rigidly oriented in a studied bio-macromolecule.

However, general applicability of the method is hampered by two major difficulties:

First, at high fields, PELDOR performance is aggravated by a narrow bandwidth of a single mode resonator. This prompted us to develop a dual-mode resonator that allows performing dual-frequency experiments with a variable separation of pump and detection frequencies up to 800 MHz [1–3]. The design of the resonator will be presented and discussed.

Second, the inherent symmetry of the magnetic interactions complicates the analysis of the orientation selective PELDOR data. We attempt to refine the experimental data and its analysis by implementing the dual-mode approach and by increasing the frequency of the measurements. Our recent results on two representative biological systems, i.e. an RNA and an α -helical peptide, permit to explore the feasibility of the method [2]. We show how its performance can be improved by enhancing resolution toward orientation selectivity and by setting proper constraints for the orientation analysis.

1. Tkach I., Sicoli G., Höbartner C., Bennati M.: *JMR* **209**, 341–346 (2011)
2. Tkach I., Pornsuwan S., Höbartner C., Wachowius F., Sigurdsson S.Th., Baranova T.Y., Diederichsen U., Sicoli G., Bennati M.: *Phys.Chem.Chem.Phys.* **15**, 3433–3437 (2013)
3. Kaminker I., Tkach I., Manukovsky N., Huber Th., Yagi H., Otting G., Bennati M., Goldfarb D.: *JMR* **227**, 66–71 (2013)

SECTION 5

STRONGLY CORRELATED ELECTRON SYSTEMS

Magnetic Order and Excitations in Iridium Oxides

G. Khaliullin

Max Planck Institute for Solid State Research, Stuttgart D-70569,
Germany

In 5d transition metal compounds such as iridium oxides, large spin-orbit coupling entangles the spin and orbital subspaces and may lead to unusual interactions and ground states. In this talk, after some basic introduction to the iridates, the following topics will be addressed: (i) magnetic ordering and excitations in single layer Sr_2IrO_4 [1–3] and bilayer $\text{Sr}_3\text{Ir}_2\text{O}_7$ [4, 5] iridium perovskites; (ii) exchange interactions in a hexagonal lattice iridates, Kitaev-Heisenberg model, its phase diagram including spin-liquid states [1, 6]; (iii) origin of the zigzag magnetic order and spin waves in Na_2IrO_3 [7].

1. Jackeli G., Khaliullin G.: Phys. Rev. Lett. **102**, 017205 (2009)
2. Kim J. *et al.*: Phys. Rev. Lett. **108**, 177003 (2012)
3. Kim B.H., Khaliullin G., Min B.I.: Phys. Rev. Lett. **109**, 167205 (2012)
4. Kim J. *et al.*: Phys. Rev. Lett. **109**, 037204 (2012)
5. Kim J. *et al.*: Phys. Rev. Lett. **109**, 157402 (2012)
6. Chaloupka J., Jackeli G., Khaliullin G.: Phys. Rev. Lett. **105**, 027204 (2010)
7. Chaloupka J., Jackeli G., Khaliullin G.: Phys. Rev. Lett. **110**, 097204 (2013)

NMR and High-Field ESR Study of the Low-Dimensional Quantum Magnet $\text{BaAg}_2\text{Cu}[\text{VO}_4]_2$

**E. L. Vavilova¹, V. Kataev^{1,2}, M. Schäpers², Y. Krupskaya²,
A. U. B. Wolter-Giraud², H.-J. Grafe², A. Möller³, and B. Büchner²**

¹ Zavoisky Physical-Technical Institute, Russian Academy of Sciences, Kazan 420029, Russian Federation, jenia.vavilova@gmail.com

² Leibniz Institute for Solid State and Materials Research IFW-Dresden, Dresden 01069, Germany

³ Texas Center for Superconductivity, and Department of Chemistry, University of Houston, Houston, Texas 77204-5003, United States

$\text{BaAg}_2\text{Cu}[\text{VO}_4]_2$ is a novel transition-metal (TM) oxide compound that belongs to a new material class of low-dimensional quantum magnets. Depending on the type of the TM ion, either frustrated triangular 2D spin lattices or a network of 1D spin chains can be realized in this material [1]. The physics of $\text{BaAg}_2\text{Cu}[\text{VO}_4]_2$ is supposed to be determined by a superposition of ferromagnetic and antiferromagnetic uniform spin-1/2 chains with nearest neighbor exchange couplings of $J_{\text{FM}} = -19$ K and $J_{\text{AFM}} = 9.5$ K [2]. It puts forward the $\text{BaAg}_2\text{Cu}[\text{VO}_4]_2$ as a new model system for studies of low-dimensional Heisenberg quantum magnetism.

Here we report the results of the NMR and high-field ESR study of the local magnetic properties of $\text{BaAg}_2\text{Cu}[\text{VO}_4]_2$. A comparative analysis of the Cu(II) ESR and ^{51}V NMR spectra enables to identify non-equivalent V sites which suggests a non-equivalency of the VO_4 structural fragments mediating the superexchange between the Cu ions in the chains. We have analyzed the frequency-, magnetic field and temperature dependence of the Cu(II) ESR signals and the temperature dependence of the ^{51}V Knight shifts and the T_1 relaxation rates. The distribution of local magnetic fields arising due to the onset of the spin correlations in the chains at low temperatures was determined. Our results support the scenario of the tunable ferro- and antiferromagnetic coupling in the Cu spin-1/2 chains driven by the specific tilting of the VO_4 exchange mediators.

1. Amuneke N.E. *et al.*: Inorg. Chem. **50**, 2207 (2011)
2. Tsirlin A.A. *et al.*: Phys. Rev. B **85**, 014401 (2012)

NMR Evidence for a Strong in Plane Electronic Anisotropy of Cobalt Ions in Sodium Cobaltates $\text{Na}_{2/3}\text{CoO}_2$

I. R. Mukhamedshin^{1,2} and H. Alloul²

¹ Institute of Physics, Kazan Federal University, Kazan 420008, Russian Federation, Irek.Mukhamedshin@kpfu.ru

² Laboratoire de Physique des Solides, Université Paris-Sud, Orsay 91405, France

The cobaltates Na_xCoO_2 are layered oxide materials somewhat similar to the cuprates in as much as the charge doping of the CoO_2 layers is controlled on a large range by variation of the Na content. One significant difference with the cuprates is that the Co of the CoO_2 plane are ordered on a triangular lattice and not on a square lattice as for the CuO_2 plane of the cuprates. A rich variety of physical properties ranging from ordered magnetic states, large thermoelectric effect, high Curie-Weiss magnetism and metal insulator transition, superconductivity *etc* have then been observed in the cobaltates. NMR experiments and structural investigations in the cobaltates have given evidence that for $x > 0.5$ a large interplay occurs between atomic arrangements and electronic properties, as the Na atoms are found to be ordered [1]. In this talk we report a complete set of ^{59}Co NMR data taken on the $x = 2/3$ phase of sodium cobaltates Na_xCoO_2 , for which we have formerly established the in plane Na ordering and its 3D stacking [2]. Also we report a method of analysis of NMR spectra which allowed us to resolve the parameters of the Zeeman and quadrupolar Hamiltonians for all four cobalt sites in the unit cell and report the temperature dependencies of the NMR shift data for these sites. The moderately complicated atomic structure resumes then in a very simple electronic structure in which the electrons delocalize on the kagomé sublattice of the triangular lattice of Co sites. We evidence that they display a strong in plane electronic anisotropy initially unexpected but which accords perfectly with an orbital ordering along the kagomé sublattice organization [3].

This work was partially supported by the Ministry of Education and Science of the Russian Federation (Budget Theme No. 12-24).

1. Alloul H., Mukhamedshin I.R., Collin G., Blanchard N.: EPL **82**, 17002 (2008)
2. Platova T.A., Mukhamedshin I.R. *et al.*: Phys. Rev. B **80**, 224106 (2009)
3. Mukhamedshin I.R., Alloul H.: Phys. Rev. B **84**, 155112 (2011)

EPR Study of Magnetic Anomalies in the $\text{La}_{2-x}\text{Sr}_x\text{CuO}_4$ Single Crystals above the Critical Temperature

**V. O. Sakhin¹, Yu. I. Talanov², L. F. Salakhutdinov², T. Adachi³,
T. Noji³, and Y. Koike³**

¹ Institute of Physics, Kazan (Volga region) Federal University, Kazan 420015,
Russian Federation, sakhin.vasily@gmail.com

² Zavoisky Physical-Technical Institute, Russian Academy of Sciences, Kazan 420029,
Russian Federation

³ Department of Applied Physics, Tohoku University, Sendai, Japan

The magnetic state of the high- T_c superconductor $\text{La}_{2-x}\text{Sr}_x\text{CuO}_4$ (LSCO) was studied in the temperature range close to the superconducting transition temperature T_c . The LSCO crystals were investigated with the different strontium doping concentrations. The crystal with the Sr concentration of $x = 0.16$ is optimally doped and undergoes a superconducting transition at $T_c = 39.4$ K. T_c of the underdoped crystal ($x = 0.07$) is 18 K, and the third sample has the Sr concentration near to the “1/8” anomaly doping level ($x = 0.116$, $T_c = 27$ K).

To obtain the information about distribution of magnetic field on the sample surface the electron paramagnetic resonance (EPR) method in combination with the surface paramagnetic probe was used. A thin layer of diphenyl-picrylhydrazyl (DPPH) was used as a probe. It was deposited onto the crystal surface by the vacuum evaporation technique. The layer thickness was of about 100 nm. DPPH was used as a probe because of the very small width of its resonance signal (~ 1.5 G). In order to increase the resolution of the method: one can observe the field variation of about 0.1 G over the applied field level of about 3300 Oe.

The obtained temperature dependences of the EPR signal parameters (broadening and shift) in the temperature range from 10 to 300 K were obtained. The magnitude and variation of the magnetic fields generated by the sample above and below T_c were estimated. Below T_c the EPR signal strongly broadens and shifts due to the vortex lattice formation in all samples. Above T_c the broadening is weak, within the experimental error. The signal shift is noticeable in the temperature range from T_c to $T_c + 20$ K. On the basis of these results it was concluded that above T_c the LSCO crystals exhibit appreciable magnetization. Moreover, the field generated by the sample is uniformly distributed over its surface, or its variations in the magnitude and the space are so small that they do not cause the noticeable broadening of the EPR signal. It is probably due to the stripe structure.

SECTION 6

OTHER APPLICATIONS OF MAGNETIC RESONANCE

NQR Cross Relaxation of N-14 Nuclei in Low Magnetic Field

**G. V. Mozzhukhin^{1,2}, B. Z. Rameev^{1,3}, G. S. Kupriyanova⁴,
P. Aksu¹, and B. Aktaş¹**

¹ Gebze Institute of Technology, Gebze-Kocaeli 41400, Turkey

² Kazan State Power Engineering University, Kazan 420066, Russian Federation

³ Zavoisky Physical-Technical Institute, Russian Academy of Sciences, Kazan 420029,
Russian Federation

⁴ Baltic Federal State University, Kaliningrad 320014, Russian Federation

The prototypes of NQR devices for luggage scanners and landmine detectors have been designed. However, there are still some issues preventing a wide practical application of this technology for explosive detection. A very long spin-lattice relaxation time T_1 of some explosives (pentaerythritol tetranitrate PETN ($C_5H_8N_5O_{12}$), ammonium nitrate NH_4NO_3 (AN) and trinitrotoluene (TNT, $C_7H_5N_3O_6$)) prevents a fast accumulation of quadrupole signal in ^{14}N NQR detection. We studied an influence of small magnetic field to NQR signal in AN and TNT.

In our work we study in details those double-resonance protocols, which theoretically do not provide the largest gain, but are more feasible to apply in practice. In our scheme, we apply pulses of small magnetic field including the match the proton resonance frequency ν_L to the lowest quadrupole resonance frequency ν_0 . We detect the spin-echo NQR signal on the ν_+ and ν_- transition. The action of magnetic field sequence applied at the beginning and after the end of multipulse NQR sequence. It has been revealed that this technique provides at least four-fold shortening of the effective spin-lattice relaxation time and therefore can be applied in the detection of explosive materials.

The T_1 and T_2 Relaxation Times Distribution for the ^{35}Cl and ^{14}N NQR in Microcomposites and in Porous Materials

N. Ya. Sinyavsky¹, G. S. Kupriyanova², and F. N. Dolinenkov²

¹ Physics Department, Baltic State Academy, Kaliningrad 236029, Russian Federation, n_sinyavsky@mail.ru

² Physical-Technical Institute, Immanuel Kant Baltic Federal University, Kaliningrad 236041, Russian Federation, galkupr@yandex.ru

The purpose of this work was the experimental study of the distribution of relaxation times T_1 and T_2 for the ^{35}Cl and ^{14}N NQR in potassium chlorate (PCl) and hexamine (HMT) in composite and porous materials. To inverse Laplace transform was used RILT program (Regularized Inverse Laplace Transform) of I.-G. Marino [1], which is an emulation of CONTIN program of S. Provencher and uses a regularization method of least squares.

As basis of microcomposite material we used: epoxy resin, silica gel, machine oil, a saturated aqueous solution of PCl (or HMT), a mixture for grout (fugue). As porous media used: foam rubber, paper, millet, activated charcoal. These materials are impregnated with a saturated aqueous solution of PCl (or HMT) and dried before the measurements.

Studies have shown that the spin-lattice relaxation times have a unimodal distribution, and the spin-spin relaxation times – bimodal distributions for all the samples. The spin-lattice relaxation time in the epoxy resin is maximal, due, apparently, mechanical stresses generated at low temperature and reduced the mobility of PCl lattice. Differences in T_1 relaxation times in PCl, crystallized out from solution in the pores due likely different crystallite sizes.

The model with the spin diffusion [2] explains the shortening of the fall signal with decreasing grain size, but not confirmed by the experimental distribution of relaxation times obtained by means of the inverse Laplace transform.

The obtained results are of considerable interest to determine the role of impurities, dislocations, lattice defects, of the temperature dependence of NQR parameters and requires further research of microcomposites and porous media using NQR relaxometry.

1. Marino I.-G.: <http://www.mathworks.com/matlabcentral/fileexchange/6523-rilt/content/rilt.m>
2. Rabbani S.R., Edmonds D.T.: Phys. Rev. **50**(9), 6184 (1994)

Characterization of Porous and Nanostructured Solid-Phase Systems by EPR of pH-sensitive Probes and Labels

E. G. Kovaleva¹ and L. S. Molochnikov²

¹ Institute of Chemical Engineering, Ural Federal University, Yekaterinburg 620002, Russian Federation, e.g.kovaleva@ustu.ru

² Ural State Forest Engineering University, Yekaterinburg 620100, Russian Federation, lsmolochnikov@gmail.com

Spin-probes and labels are usually used to get some information about the molecules to which they are bound (the rate of macromolecule motion etc.), the amount of thermal motion in a membrane in which they have been inserted and the polarity of its environments. Determination of local pH, other acid-base and electro surface characteristics in pores of inorganic and organic materials is of a great practical interest, since the catalytic and adsorption properties of solid-phase objects are effected by both chemical nature of solutions and specific conditions inside of pores and on the surface of these materials. pH-sensitive nitroxide radicals (NR) which are sensitive to changes of medium acidity due to participation in reactions of proton exchange, may be used as pH probes and labels for measuring local pH and for studying of pH-dependent processes in different objects including porous and nano-structured systems.

This report is aimed to review the application of pH-sensitive NR as probes and labels in variety of solid-phase systems from organic porous objects with uncontrolled pore size (ion-exchange resins and films) to inorganic materials with pore size determined by their structure (from microporous molecular materials to finely dispersed nanostructured oxides and related systems).

We developed a new method for the determination of medium acidity in pores of solids (pH_{intr}) by means of pH-sensitive NR as spin probes and EPR method [1]. Initially, this method was used us to measure pH_{intr} in micropores of various cross-linked organic polyelectrolytes (ion-exchange resins and films). We found that pH_{intr} inside organic sorbents differ from the pH of external solutions by 0.8–2.1 units. The method developed allowed us to study the processes of sorption and hydrolysis on different types of sorbents (weak cation and anion-exchange resins, functionalized and nonfunctionalized polymeric films, inorganic porous oxides) and the catalytic properties of Cu^{2+} -containing carboxyl cation exchangers to determine ionization constants of functional groups, and to give a critical estimation to the regularities previously found for the behavior of adsorbents in aqueous media.

For MMS, we developed a technique for direct measurement of the near-surface (Stern) potential and the potential in the center of MMS channels; negative and positive values of Stern potential for the positively and negatively charged surface of MMS channels were found, Stern layer thickness (0.28 nm) were determined; pH inside channels (pH_{intr}) were found to be less than those of external solution; a technique for determining pH_{intr} on depending on channels size

was developed [2]. An effect of aluminum and boron incorporation on the sieve surface electric charge, potential and acid-base properties of MMS was found. For nanostructured SiO_2 , a pH-sensitive nitroxide has been attached to a sample surface through the chain of aminopropyltriethoxysilane $(\text{EtO})_3\text{Si}(\text{CH}_2)_3\text{NH}_2$. The values of surface electrical potential (SEP) were calculated from the shifts in titration curves of NR located nearby nano-oxide surface. The SEP of SiO_2 particles was found to be -90 mV [3]. The obtained value correlates well with those for silica-supported mesoporous molecular sieves (MMS) being equal to -109 mV. For Cu^{2+} -containing composite materials based on SiO_2 , TiO_2 and cellulose powder (CMs), the influence of pH_{intr} and the charged state of the CM surface on complexation with Cu^{2+} ions and the catalytic activity of the obtained samples in model oxidative dehydrogenation of trimethylhydroquinone with air oxygen was analyzed using pH-sensitive NR with pK_a values 5.14 and 3.04 [4]. For pure and Co^{2+} -containing hybrid organo-inorganic materials based on the chitosan- SiO_2 , chitosan- Al_2O_3 , and chitosan-cellulose systems (GMs), the surface structure and processes that occur during their formation and the GMs catalytic properties in the oxidation reactions of alkenes were investigated using the above-mentioned stable pH-sensitive NR [4].

The studies presented in this report were financially supported by the Ministry of the Education of the Russian Federation (2007–2011, Theme 01.2.007-06425).

1. Molochnikov L., Kovalyova E., Grigor'ev I. *et al.* : J. Phys. Chem. B **108**, 1302 (2004)
2. Golovkina E., Kovaleva E., Molochnikov L. *et al.*: Rus. J. Sorp. & Chrom. Processes **8**, 971 (2008)
3. Kovalyova E., Petkevich T., Medyantseva E., Molochnikov L. *et al.*: Russ. J. Sorp. & Chrom. Processes **6**, 991 (2006)
4. Kovaleva E.G., Molochnikov L.S.: Nitroxides: Theory, Experiment and Applications (Kokorin A.I., ed.), pp. 211–246. Croatia, InTech Publisher, 2012.

Application of Spin-Probe Method To Study the Effect of Antioxidants on Biological Membranes *in vitro*

**E. L. Maltseva, V. V. Belov, T. E. Chasovskaya,
and N. P. Palmina**

N. M. Emanuel Institute of Biochemical Physics of Russian Academy of Sciences,
Moscow 199334, Russian Federation, email@sky.chph.ras.ru

The method of spin-probe is useful to study the biological and artificial membranes [1]. In the present work we studied the effect of two antioxidants: natural alfa-tocopherol (TL) and synthetic – potassium salt of β -(4-hydroxy-3,5-ditert-butylphenyl) propionic acid – phenoan potassium salt (PP) in a wide range of concentration (10^{-3} – 10^{-20} M) on the plasmatic (PM) and endoplasmic reticulum membranes (ERM), isolated from liver cells of mice. The different concentrations of TL and PP were prepared by successive dilutions. The lipid structure studied by use two spin-probes: 5- and 16-doxylstearic acids (5- and 16-DSA) localized in different regions of lipid bilayer [2] computerized radio-spectrometer Bruker-EMX. A microviscosity value of the hydrophobic lipid regions estimated by rotation correlation time (τ_c) of 16-DSA and rigidity of surface membrane lipids by order parameter (S) of 5-DSA calculated from EPR-spectra obtained. The nonlinear and polymodal “dose-effect” dependencies of τ_c and S for both antioxidants have been found. It was observed three “waves” of microviscosity increase: at high concentration 10^{-4} M TL and in the range of 10^{-4} – 10^{-8} M TL, explained by its incorporation into the lipids, 10^{-10} – 10^{-16} M TL related with formation of the micro-domains and rafts, and range of 10^{-17} – 10^{-20} M TL (ultra-low dilutions – ULD), which can be related with properties of solution and structure of water.

It was shown an increase of parameter S in the range of concentration 10^{-10} – 10^{-18} M TL, which is correlated with activity of membrane-bound enzyme-

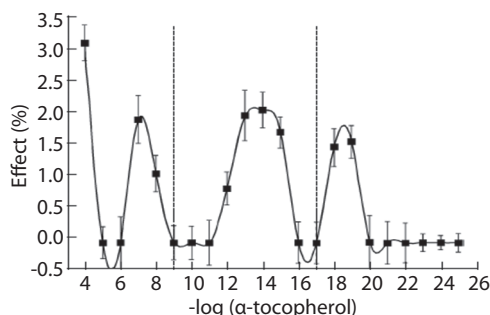


Fig. 1. The effect (expressed in %) of TL in a wide range of concentrations on the microviscosity of hydrophobic regions of lipids (τ_c of 16-DSA) of PM. $T = 2930$ K.

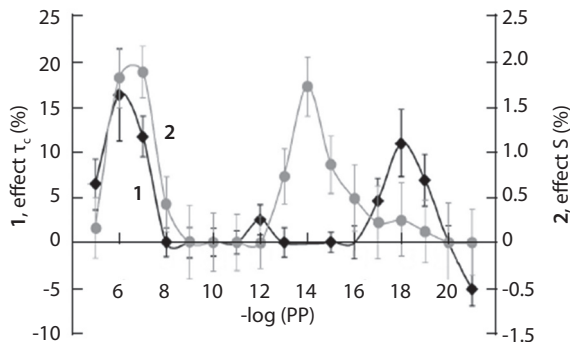


Fig. 2. The effect (%) of PP in a wide range of concentrations on the microviscosity of deep-lying lipids regions (curve 1) and rigidity of surface lipids (curve 2) of PM. $T = 2930$ K.

protein kinase C. A study of thermo-induced structural transitions showed an appearance of additional transitions in membrane lipids at the range of physiological temperature (307–314 °K) in concentration of 10^{-4} – 10^{-20} M TL.

It was observed a polymodal dependences of changes in lipid microviscosity (τ_c of 16-DSA) and rigidity of surface lipids (S of 5-DSA) of PM and ERM on the concentration of PP. The maxima of increase of microviscosity observed at concentrations 10^{-6} M and 10^{-18} M, rigidity – at 10^{-6} M and 10^{-14} M PP.

It was shown a similarity between changes of τ_c of 16-DSA and protein kinase C activity upon the effect of PP on plasmatic membranes. In this case the thermo-induced transitions in the hydrophobic lipid regions of PM appeared at physiological temperature at 10^{-18} M PP – concentration at which microviscosity value increased.

It was concluded that polymodal effect of antioxidants in a wide range of concentrations on structural parameters of biological membranes is typical to “dose-effect” of the substances effective at ULD [3] and is important to understand the role of this substances not only as inhibitors of lipid peroxidation, but modulators of lipid membrane structure.

1. Kuznetsov A.N.: Method of Spin Probe, pp. 177–182. Moscow, Nauka, 1976.
2. Berliner L.J.: Spin Labeling, pp. 570–605. NY, San Francisco, Academic Press, 1979.
3. Burlakova E.B., Konradov A.A., Maltseva E.L.: J. Adv. Chem. Phys. **2**, 140 (2003)

Hyperfine Structure of EPR Spectra of Eu^{2+} in SrMoO_4 . The Determination of $\text{Sign } b_2^0$ and P_2^0 at all Temperatures

A. D. Gorlov

Ural Federal University, INS, Ekaterinburg 620083, Russian Federation,
Anatoliy.Gorlov@usu.ru

The EPR specters and hyperfine structure (HFS) of signals of the odd isotopes Eu^{2+} in SrMoO_4 single crystals have been investigated at different temperatures. The observation HFS of forbidden (with the nuclear spin flip) transitions (FT)

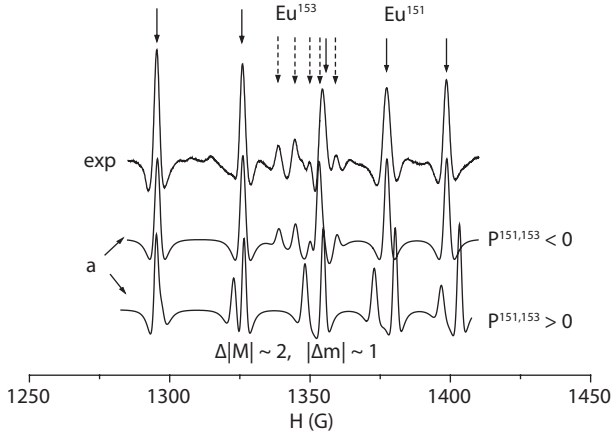


Fig. 1. Observed (exp) and simulated (a) HFS of the EPR signals of $\text{SrMoO}_4:\text{Eu}^{2+}$ ($\theta = 0, A_x < 0$), at $T = 100$ K (second derivation).

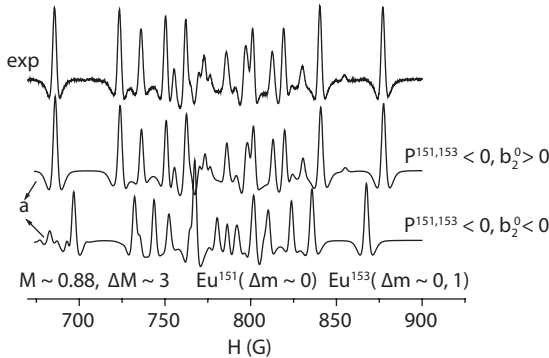


Fig. 2. The experimental and simulated (a) HFS of the EPR signals of $\text{SrMoO}_4:\text{Eu}^{2+}$ ($A_x < 0, \theta = 90, \varphi = 0$) at $T = 100$ K (second derivation).

has made it possible to determine quadrupole interaction P_2^0 associated with the gradient of the electric field of ligands at the impurity. The simulation of HFS of EPR transitions (as in [1]) allows to determine the magnitudes of splitting and observed asymmetry in a hyperfine structure (at various orientations of the magnetic field). It is shown that HFS FT asymmetry depends on mutual signs of parameters of initial splitting b_2^0 and P_2^0 (see Fig. 1). The signs of the HFS constants $A_{x,z}$ were chosen negative in accordance with the literature data. The signs P_2^0 and b_2^0 were chosen in accordance with Fig. 1, 2.

The studying of the specters at various temperatures have demonstrated that $|b_2^0|$ is decreasing with temperature increase while $|P_2^0|$ – const. For example $b_2^0 = 813.8(7)$ MHz, $P_2^0 = -10.7(5)$ MHz at 100 K and $b_2^0 = 795.8(10)$ MHz, $P_2^0 = -10.8(6)$ MHz at 390 K ($|A_{x,z}|$ is decreasing with temperature increase). This dependence of $|P_2^0(T)|$ is differ from the similar dependence for the Gd^{3+} odd isotopes in $PbMoO_4$, YVO_4 [1], $SrMoO_4$.

1. Gorlov A.D.: Phys. Solid State **55**, no. 5, 960 (2013)

Electron Spin Density Distribution in Cu(II)-(bis)Oxamato Complexes: an ESR Study

**A. Aliabadi¹, A. Petr¹, M. A. Abdulmalic², T. Ruffer², V. Kataev¹,
and B. Büchner^{1,3}**

¹ Leibniz Institute for Solid State and Materials Research IFW Dresden, Dresden D-01171, Germany, a.aliabadi@ifw-dresden.de, A.Petr@ifw-dresden.de, V.Kataev@ifw-dresden.de

² Fakultät für Naturwissenschaften, Technische Universität Chemnitz, Chemnitz D-09107, Germany, "mohammad-a.abdulmalic"@s2008.tu-chemnitz.de, tobias.rueffer@chemie.tu-chemnitz.de

³ Institut für Festkörperphysik, Technische Universität Dresden, Dresden D-01062, Germany, B.Buechner@ifw-dresden.de

Cu(II)-(bis) oxamato complexes containing three [1] and four nitrogen ligands have been investigated using ESR spectroscopy at 10 GHz. The ESR spectra were modeled in order to determine the g -factor and the hyperfine (HF) coupling parameters. The isotropic g -factor and HF coupling constants for Cu and N have been obtained from the ESR measurements on liquid solutions at room temperature. From the ESR measurements on the powder sample we were able to extract the g -tensor and the Cu HF coupling tensor. In addition, the angular dependence of the ESR spectra was studied by rotation of a single crystal in two perpendicular planes. These results were used to refine the g -tensor and Cu HF coupling tensor and determine the N HF coupling tensor.

Two models introduced by Maki and McGarvey [2] and Morton and Preston [3] were used to calculate the spin density from experimentally obtained HF coupling constants of the Cu(II) ion and N-donor atoms. The results do not reveal a substantial change of the spin density on the Cu(II) ion the studied molecules compared to a previous study of Cu(II)-(bis) oxamato complex containing two nitrogen ligands [4]. However, the smaller spin density on the N-donor atoms has been obtained. This might be suggestive of the redistribution of the total spin density between the donor atoms towards the third and fourth N-donor atoms with no additional "leakage" from the central metal ion.

1. Abdulmalic M.A., Aliabadi A., Petr A., Krupskaya Y., Kataev V., Büchner B., Hahn T., Kortus J., Rueffer T.: Dalton Trans. **41**, 14657 (2012)
2. Maki A.H., McGarvey B.R.: Chem. Phys. **29**, 31 (1958)
3. Morton J.R., Preston K.F.: Magn. Reson. **30**, 577 (1978)
4. Bräuer B., Ruffer T., Kirmse R., Griebel J., Weigend F., Salvan G.: Polyhedron. **26**, 1773 (2007)

EPR-Based Evaluation of the Oxidative Status Using Cyclic Dinitrones as Spin Probe Precursors

T. V. Kobzeva and G. G. Dultseva

Institute of Chemical Kinetics and Combustion, SB RAS, Novosibirsk 630090,
Russian Federation, Kobzeva@mail.ru

The accumulation of peroxy radicals in chemical or biological systems may be uncontrollable until a definite critical concentration is achieved, allowing direct identification. However, even low concentrations of various organic peroxy radicals may switch on undesirable processes, so it may be necessary to evaluate the oxidative status of a reaction mixture or a biological system. Very helpful compounds for these purposes are some organic compounds that may act as precursors of paramagnetic species formed in the interaction with peroxy radicals. In case if the resulting organic radical is a long-lived one, this technique in combination with EPR examination of the formed species allows one to accumulate, detect and identify the overall oxidative status of the system due to the presence of peroxy radicals.

Spin trapping technique is often insufficiently sensitive to accumulate peroxy spin adducts due to the low trapping rate constants. A promising organic compound for evaluation of the oxidative status is a cyclic dinitrone compound with isolated double bonds, namely dihydropyrazine-1,4-dioxide (DPDO). The compound is known as a spin trap [1] but its use is limited to oxygen-free systems because of the triplet signal that arises in the presence of paramagnetic oxygenated species. This triplet was expected to be uncontrollable but our studies showed that the sensitivity of its intensity to the presence of peroxy radicals provides an excellent opportunity to assess the oxidative status, or the presence of reactive oxidizers. This is important in biological systems where the presence of peroxy species brings about cell wall damage and may mean inflammation or stressed immune response. We used DPDO to measure the oxidative activity of the species that were formed *in vitro* during the oxidation of a series of biologically active species including vitamins, widely used antioxidants including flavonoid compounds. EPR-based measurement of the oxidative status was supplemented by the detailed analysis of the reaction mixtures by means of high-performance liquid chromatography to estimate rate constants of oxidation and reduction processes in the systems.

1. Dultseva G.G. *et al.* : J. Phys. Chem. **100**, 17523 (1996)

EPR Study of the Impurity Defects in Diamonds Grown in Carbonate Medium

**A. Y. Komarovskikh, V. A. Nadolinny, Y. N. Pal'yanov,
and I. N. Kupriyanov**

Nikolaev Institute of Inorganic Chemistry, Novosibirsk 630090, Russian Federation,
komarr@ngs.ru

Oxygen-containing defects in diamonds were always of great interest. OK1 and N3 centers were supposed to contain oxygen atoms in their local structures [1, 2]. However, recent investigations of the luminescence spectra and EPR spectra of these centers have shown that these defects contain titanium atoms instead of oxygen [3].

To study oxygen incorporation into the diamond structure, crystals were grown in a carbonate medium. The diamond crystals were grown using press-less high-pressure split sphere (BARS) without catalysts (Co, Fe and Ni) on the seeds and without them.

IR absorption spectra of the grown crystals contain intense band system 1332, 1046, 950 cm^{-1} , caused by N^+ at substitutional sites. The EPR spectra of these crystals are the result of superposition of the EPR spectrum of substitutional nitrogen atoms and three new anisotropic EPR spectra. Study of the angular dependence of one of them (OX1) has shown that the spectrum is caused by the defect with an electron spin $S = 1/2$ and anisotropic g -factor with principal values: $g_{xx} = g_{yy} = 2.0032$, $g_{zz} = 2.0038$. Principal directions of the g -tensor are the next: g_{xx} is tilted at 44° from [100], g_{yy} is directed along the [0-11], g_{zz} is tilted at 44° from [011]. Background study has revealed the hyperfine structure of the one ^{13}C relating to the spectrum of OX1 (in the samples with natural abundance of 1.1%): $A(^{13}\text{C})_{xx} = 326$ Gs, $A(^{13}\text{C})_{yy} = 260$ Gs, $A(^{13}\text{C})_{zz} = 210$ Gs. The analysis of ^{13}C HFS has shown that unpaired electron is localized mostly at one of the carbon atoms. The second paramagnetic center (OX2) is characterized by the spin Hamiltonian parameters: spin $S = 1/2$ and anisotropic g -factor: $g_{xx} = 2.0098$, $g_{yy} = 1.9991$, $g_{zz} = 2.0113$. Principal directions of the g -tensor are the next: g_{xx} is tilted at 9° from [100], g_{yy} is tilted at 9° from [011], g_{zz} is directed along the [0-11]. The third paramagnetic center (OX3) is characterized by the spin Hamiltonian parameters: spin $S = 1/2$ and anisotropic g -factor: $g_{xx} = 2.0064$, $g_{yy} = 2.0008$, $g_{zz} = 2.0052$. Principal directions of the g -tensor are the next: g_{xx} is tilted at 15° from [100], g_{yy} is tilted at 15° from [011], g_{zz} is directed along the [0-11].

The unusual high g -factor anisotropy of the observed centers in the absence of transition metal ions in the diamonds, grown in oxygen-containing medium, suggests the presence of oxygen atoms in the structure of the studied centers. In accordance with this assumption, structural models of OX1, OX2 and OX3 centers have been proposed based on the symmetry properties of these centers and their electronic state data. OX1 center assumed to have the structure of

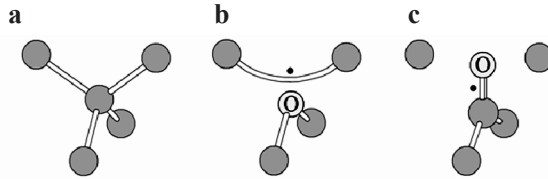


Fig. 1. Proposed models of the new oxygen centers in synthetic diamond. **a** Diamond crystal structure. **b** OX1 center assumed to have the structure of negatively charged substitutional oxygen atom. **c** OX2 center assumed to have the structure of negatively charged $\langle 100 \rangle$ -split interstitial with impurity oxygen atom.

negatively charged substitutional oxygen atom, OX2 center assumed to have the structure of negatively charged $\langle 100 \rangle$ split interstitial (Fig. 1), OX3 center assumed to have the following structure: oxygen atom and vacancy occupy adjacent carbon positions. Another possible structure for this center is di- $\langle 100 \rangle$ -split interstitial configuration containing an impurity oxygen atom.

Nitrogen is an electron donor for the studied impurity centers, its state N^+ is observed in the IR absorption spectra (band system 1332, 1046, 950 cm^{-1}).

1. Newton M.E., Baker J.M.: *J. Phys.: Condens. Matter.* **1**, 10549 (1989)
2. Van Wyk J.A., Loubser G.H.N., Newton M.E., Baker J.M.: *J. Phys.: Condens. Matter.* **4**, 2651 (1992)
3. Nadolinny V.A., Yuryeva O.P., Shatsky V.S., Stepanov A.S., Golushko V.V., Rakhmanova M.I., Kupriyanov I.N., Kalinin A.A., Palyanov Yu.N., Zedgenizov D.: *Appl. Magn. Reson.* **36**, 97 (2009)

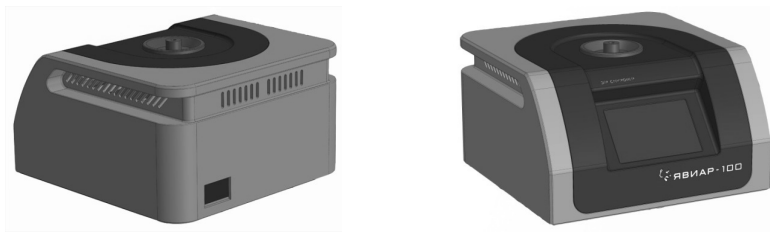
New Compact Coherent Heterodyne EPR-Spectrometer

A. N. Tcherepanov¹ and A. N. Tararkov²

¹ Ural Federal University, Yekaterinburg 620002, Russian Federation, tchustu@mail.ru

² Spectr Ltd, Yekaterinburg 620002, Russian Federation, spectrum.ekb@gmail.com

In the report new compact coherent heterodyne EPR-spectrometer is presented. Operating principle of the device is based on coherent heterodyne method of registration signals. This method guarantees registration of the widest and the narrowest spectral lines ESR. Intellectual property protection of the basic technical solution is realized by SU-patent and now patent application for compact coherent heterodyne EPR-spectrometer is filed [1].



New compact coherent heterodyne EPR-spectrometer has the next unique technical features:

- Availability of two modes: with modulation and without modulation magnetic field.
- Possibility of registration paramagnetic centers with long time relaxation.
- Wide range of modulation frequency magnetic field from 0 to 12 kHz.
- Wide range of microwave power 80 dB.
- Self-tuning of frequency microwave generator is realized without modulation and as a result registration line doesn't expand.
- Measuring resonator has own adjustment.

Basic features:

- weight, kg 15;
- size, mm 300×265×170;
- X-band;
- power consumption, W 60.

1. Rokeakh A.I., Sherstkov Ju.A.: Coherent Heterodyne Spectrometer of Electronic Paramagnetic Resonance, SU-patent № 1739751, 1995.

SECTION 7

SPIN-BASED INFORMATION PROCESSING

Recent Trends in Open Shell Chemistry: Can Chemistry Contribute to Electron Spin Science/Spin Technology of QC/QIP?

T. Takui

Department of Chemistry and Molecular Materials Science, Graduate School of Science,
Osaka City University, Osaka 558-8585, Japan

The field of quantum computing/quantum information processing (QC/QIP) has been emerging a new phase since 2012 Nobel Prize for Physics was awarded to two pioneers who first manipulate, independently, a single atom/ion and photon with its quantum nature maintained. These spin manipulation techniques are essential to implement QC/QIP technology. In recent development of QC/QIP, all the relevant physical qubit systems are facing two problems; the scalability of qubits and their decoherence. The latter is intrinsic to their quantum nature. Among many candidates for physically realisable qubits, molecular spin qubits are the latest arrival [1], but have their own right [2, 3]. We introduce the latest achievements based on molecular spin qubits in ensemble and discuss their advantages and disadvantages in terms of spin technology [4]. Attempts to apply molecular spins to the implementation of QC/QIP have been underlain by enormous efforts by organic chemist to synthesise stable molecular spins which fulfil the requirements of qubits for QC gate operations. In terms of the gate operations, we utilise weakly exchange-coupled multi-partite electron spin systems because of the limitations of current pulse microwave technology. In order to implement practical QC/QIP systems, a large number of quantum memory elements are required as well. We illustrate that open shell chemistry plays an important role to afford the memory elements for the architecture of practically scalable qubits.

1. Rahimi R., Sat K., Takui T. *et al.*: *Int. J. Quantum Inf.* **3**, 197–204 (2005); Sato K., Takui T. *et al.*: *Physica E* **40**, 363–366 (2007); Sato K., Morita Y., Takui T. *et al.*: *J. Mater. Chem.* **19**, 3739–3754 (2009)
2. Special issue, Molecular Spintronics and Quantum Computing, *J. Mater. Chem.* **19**, 1670–1766 (2009)
3. Troiani F., Bellini V., Candini A., Lorusso G., Affronte M.: *Nanotechnology* **21**, 274009 (2010)
4. Nakazawa S., Nishida S., Morita Y., Takui T. *et al.*: *Angew. Chem. Int. Ed.* **51**, 9860–9864 (2012)

Light-induced Generation and Coherent Manipulation of Entangled Quantum States in Molecular Crystals

**G. Kothe¹, T. Yago¹, M. Lukaschek¹, J.-U. Weidner¹,
G. Link¹, and T.-S. Lin²**

¹ Department of Physical Chemistry, University of Freiburg, Freiburg 79104, Germany,
gerd.kothe@physchem.uni-freiburg.de

² Department of Chemistry, Washington University, St. Louis, MO 63130, USA

Huge nuclear spin polarization has been observed in organic triplet states at level anti-crossing (LAC) conditions [1–3]. So far, however, the quantum mechanical mechanism responsible for the nuclear hyperpolarization was not identified. Here, we explore this mechanism using pulsed low-field magnetic resonance in combination with pulsed laser excitation. The model system for our studies is triplet pentacene embedded in a host single crystal. On the basis of an analytical theory, developed for LAC conditions, the results can be summarized as follows. First, a laser pulse generates the triplet state and initiates the formation of multipartite entanglement between the electron spin and 14 hyperfine coupled proton spins. This gives rise to huge oscillatory electron and nuclear spin polarization. Then, by the action of a resonant high-power microwave pulse, the electron spin is disentangled from the nuclear spins. As a result, the longitudinal nuclear magnetization evolves separately under the nuclear spin Hamiltonian. Due to robust entanglement among the 14 proton spins, one observes quantum oscillations [4] at the nuclear Larmor frequency.

Thus, at triplet LAC conditions, a multitude of entangled nuclear spin states is created simply by light excitation. In case of perfect crystal alignment, we expect ultra-long spin coherence times in the order of seconds. Using advanced pulse NMR techniques, the entangled spin states can be addressed and coherently controlled in the time domain. Because of the huge polarization of the nuclear spins, these quantum systems are capable of room temperature operation. This makes them promising candidates for various applications in quantum information processing.

1. Veeman W.S., van der Poel A.L.J., van der Waals J.H.: *Mol. Phys.* **29**, 225 (1975)
2. Atsarkin V.A., Morshnev S.K.: *Sov. Phys. JETP* **44**, 795 (1976)
3. Stehlik D., Rösch P., Lau P., Zimmermann H., Hausser K.H.: *Chem. Phys.* **21**, 301 (1977)
4. Kothe G., Yago T., Weidner J.-U., Link G., Lukaschek M., Lin T.-S.: *J. Phys. Chem. B* **114**, 14755 (2010)

Electron Spin Echo Memory Realized in a Native Atomic Frequency Combs Structure at Room Temperature

K. I. Gerasimov^{1,2}, S. A. Moiseev^{1,2}, V. I. Morosov³, and R. B. Zaripov¹

¹ Zavoisky Physical-Technical Institute, Russian Academy of Sciences, Kazan 420029, Russian Federation, gerasimov@kfti.knc.ru, samoi@yandex.ru

² Institute of Informatics of Tatarstan Academy of Sciences, Kazan 420111, Russian Federation,

³ A. E. Arbutov Institute of Organic and Physical Chemistry, Kazan 420088, Russian Federation

Realization of quantum memory (QM) in microwave spectral range seems to be one of the key tools for the construction of multi-qubit hybrid superconducting quantum computer [1] as well for the microwave-optical interface in optical quantum communications [2]. Using of photon/spin echo approach [3, 4] promises practically important advantages in quantum storage of multi-qubit states. Here, it is worth noting a successful realization of such QM in optical region for storage up to 1000 temporal light field modes [5] and record quantum efficiency [6]. In this letter we have demonstrated a spin echo QM protocol for the first time in microwave spectral range.

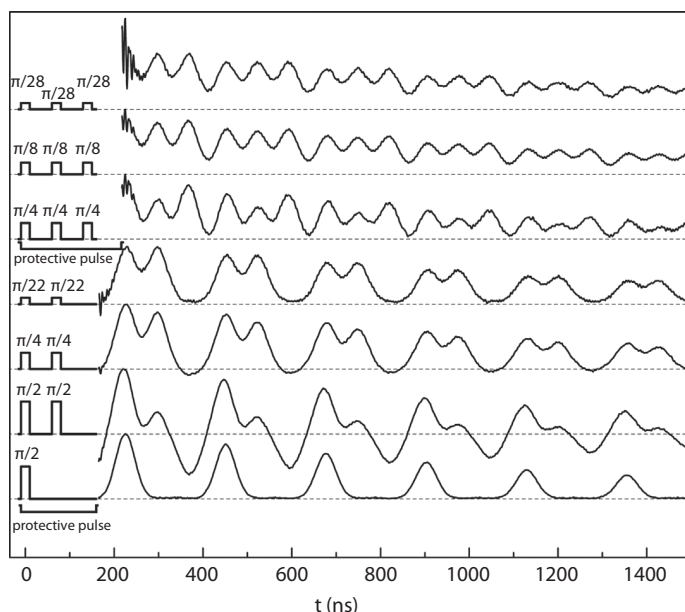


Fig. 1. Periodical echo signals from the input pulse with one, two and three temporal modes with various pulse areas. Temporal width of the pulses was 20 ns. Time delays between the nearest temporal modes was 70 ns. Series of the temporal modes and additional protective pulse (black bold lines) are shown schematically in the form of rectangular pulses. Temperature $T = 300$ K, external magnetic field $H = 3456.80$ G (for central EPR line in a CW EPR spectrum at frequency of 9.658 GHz).

We have realized storage of electromagnetic pulses in AFC-protocol of electron spin echo QM based on native periodic atomic (electron) frequency combs of narrow resonant EPR lines. The electron spin system is realized in tetracyanoethylene anion radical (TCNE⁻) in toluene at room temperature. Similarly to [7] the nine strong resonant lines exhibit intensity ratios close to 1:4:10:16:19:16:10:4:1 expected for four equivalents N¹⁴ ($I = 1$) nuclei. Spectral interval between the EPR lines of HF N¹⁴ was $a^N = 1.590 \pm 0.005$ G ($D_{\text{HF}} = 4.443 \pm 0.014$ MHz, $g = 1.996$) and half-width of EPR lines $\sim 0.20 \pm 0.02$ G ($\gamma = 0.56 \pm 0.06$ MHz). These lines have been characterized by quite high finesse $F_{\text{AFC}} = \Delta_{\text{HF}}/\gamma \approx 8$ and rephasing time $\tau = 1/\Delta_{\text{HF}} = 225.1 \pm 0.7$ ns.

Robust storage of signal field with up to three temporal modes has been realized (Fig. 1) on conventional Eleksys E-580 X-band pulse EPR spectrometer with a Bruker Flexline dielectric cavity ER4118X-MD5W1. First “echo” signal arisen at moment $\approx \tau$, the other next signals excited periodically one by one with time interval τ . The echo signal temporal behavior from one exciting pulse is described by smooth Gaussian shape. As seen in Fig. 1, perfect storage of the input temporal mode intensities has been observed for relatively small pulse areas less than $\pi/8$.

We have also realized a controlled retrieval of the stored input pulses for pre-determinant moments of time by using an appropriate sequence of rephasing π -pulses. The obtained experimental data show new possible class of electron spin systems with native AFC-structure for realization of QM in microwave spectral range at room temperature.

1. Wesenberg J.H. *et al.*: Phys. Rev. Lett. **103**, 070502 (2009); Wu H. *et al.*: Phys. Rev. Lett. **105**, 140503 (2010)
2. Togan E. *et al.*: Nature (London) **466**, 730 (2010); Greve K.D. *et al.*: Nature (London) **491**, 421 (2012); Probst S. *et al.*: Phys. Rev. Lett. **110**, 157001 (2013)
3. Tittel W. *et al.*: Laser and Phot. Rev. **4**, 244 (2010)
4. Moiseev S.A., Andrianov S.N.: J. Phys. B: At. Mol. & Opt. Phys. **45**, 124017 (2012)
5. Bonarota M., Le Gouet J.-L., Chaneliere T.: New J. Phys. **13**, 013013 (2011)
6. Usmani I. *et al.*: Nat. Commun. **1**, 1 (2010)
7. Phillips W.D., Rowell J.C., Weissman S.I.: J. Chem. Phys. **33**, 626 (1960)

Point Defects in Silicon Carbide as a Perspective Basis for Quantum Electronics Operating at Room Temperature

**V. A. Soltamov¹, A. A. Soltamova¹, P. G. Baranov¹, F. Fuchs²,
G. V. Astakhov², and V. Dyakonov²**

¹Ioffe Physical-Technical Institute, St. Petersburg 194021, Russian Federation,
victor_soltamov@mail.ru

²Experimental Physics VI, Julius-Maximilian University of Wuerzburg, Wuerzburg 97074, Germany

In recent decade a special attention has been paid for nitrogen-vacancy (NV) center in diamond because of its' unique quantum properties. Particular, owing to its unique optical excitation cycle that leads to the optical alignment of triplet sublevels of the defect ground state, the NV center can be easily initialized, manipulated, and readout by means of optically detected magnetic resonance (ODMR) at room temperature. Such feature gives rise for application of the NV defects in quantum magnetometry with optical pumping, quantum information processing and bioimaging [1].

The diamond NV defect is in many ways the ideal object but it is currently quite difficult to fabricate devices from diamond. It remains difficult to gate these defects electrically. That is why a search for systems possessing unique quantum properties of the NV defect in diamond that can extend the functionality of such systems seems to be a very promising objective.

A search to find defects with even more potential has now been launched. Silicon Carbide (SiC) was suggested to be able to open up a whole new world of scientific applications [2, 3].

The main result is that the optically induced alignment (polarization) of the ground-state spin sublevels of the Si vacancy related defects in two most common hexagonal SiC polytypes (4H- and 6H-SiC) was observed for the first time at room temperature [4]. In distinction from the known NV defect in diamond [1] and recently observed defects in SiC [5], two opposite schemes for the optical spin alignment of the defects in 4H- and 6H-SiC were realized at room temperature upon illumination with unpolarized light. The alignment schemes vary depending on the defect type, temperature, SiC polytype, and crystalline position.

As far as SiC is a well-developed semiconductor material we fabricate the p/n junction based on 6H-SiC polytype and achieve the electrically driven luminescence of the and Si vacancy related defects. Such result potentially means that spin sublevels of the defects can be aligned not only optically but also electrically [6].

So that, SiC with developed device technologies is a very attractive material for practical applications. These altogether make the Si-vacancy related defects in SiC very favorable candidate for spintronics, quantum optics, quantum information processing, magnetometry, biolabelling.

The financial support of the Ministry of Education and Science, Russia under agreements №8017, №8568, grants of RAS, RFBR and grant of the President 14.122.13.6053-MK, Russia is gratefully acknowledged.

1. Jelezko F., Wrachtrup J.: *Phys. Status Solidi A* **203**, 3207 (2006)
2. Baranov P.G. *et al.*: *Phys. Rev. B* **83**, 125203 (2011)
3. Weber J.R., Koehl W.F. *et al.*: *Proc. Natl. Acad. Sci.* **107**, 8513 (2010)
4. Soltamov V.A., Soltamova A.A. *et al.*: *Phys. Rev. Lett.* **108**, 226402 (2012)
5. Falk A.L. *et al.*: *Nat. Commun.* 4:1819 doi: 10.1038/ncomms2854 (2013)
6. FuchsF., Soltamov V.A. *et al.*: *Sci. Rep.* **3**, 1637 (2013)

SECTION 8

LOW-DIMENSIONAL SYSTEMS AND NANO-SYSTEMS

High Field NMR Studies of Magnetic Field Driven Quantum Criticality in $S = 1/2$ Antiferromagnetic Spin Chains

H.-H. Klauss

Institute for Solid State Physics, TU Dresden, Dresden D-01062, Germany

The one dimensional $S = 1/2$ antiferromagnetic Heisenberg chain with nearest neighbor interactions ($S = 1/2$ AFHC) is a model systems to study quantum many body physics. The ground state is determined by quantum fluctuations and it is very sensitive to small perturbations. For example, an alternating exchange interaction strength or strong spin phonon coupling leads to a spin excitation gap. Using an applied external magnetic field as the control parameter a quantum critical point (QCP) at $g \mu_B B_c = 2 J$ marks the transition between a Luttinger liquid and an ferromagnetically polarized state. This transition is accompanied by a collapse of the continuous two-spinon excitation spectrum into a one magnon dispersion.

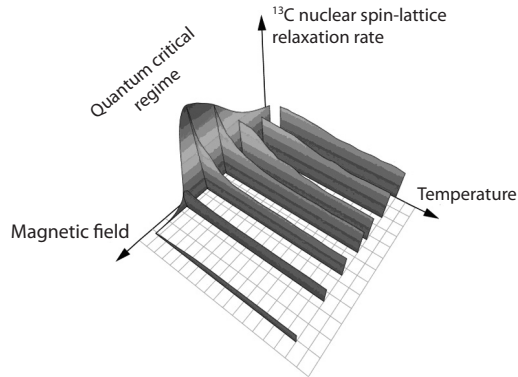


Fig. 1. ^{13}C -spin-lattice relaxation rate in copper pyrazine dinitrate as a function of the external magnetic field and temperature [H. Kühne *et al.*: PSS B 247, 671 (2010)].

Copper pyrazine dinitrate (CuPzN) is known as one of the best realizations of the $S = 1/2$ AFHC with a small coupling constant $J/k_B = 10.7$ K [1]. Here, the quantum critical point is at $B_c = 14.6$ T. We present a comprehensive ^{13}C -NMR study of CuPzN up to $B = 30$ T. A comparison of our experimental findings with both numerical (quantum Monte Carlo) and analytical (conformal field theory) approaches is made and yields a very good agreement. In particular, a well-defined maximum of the spin-lattice relaxation rate $1/T_1(B;T)$ below B_c is revealed as the signature of essential spin-spin interactions in the Luttinger liquid phase [2, 3].

1. Hammar P.R. *et al.*: PRB 59, 1008 (1999)
2. Kühne H. *et al.*: PRB 80, 045110 (2009)
3. Kühne H. *et al.*: PRB 83, 100407 (2011)

Size-Dependent Lattice Distortions in Nanocrystalline Ceria Doped with Gd³⁺ and Y³⁺: an EPR study

**R. M. Rakhmatullin¹, L. K. Aminov¹, I. N. Kurkin¹, R. Böttcher²,
A. Pöpl², and S. Sen³**

¹MRS Laboratory, Kazan State University, Kazan 420008, Russian Federation,
rrakhmat@kpfu.ru

²Faculty of Physics and Earth Sciences, University of Leipzig, Leipzig D-04103, Germany

³Department of Chemical Engineering and Materials Science, University of California at Davis,
California 95616, USA

Ceria (CeO₂) is an important material for many technological applications such as solid oxide fuel cells (SOFC), solar cells, three way catalysts, etc. [1–3]. These applications are based on the oxygen storage capacity (OSC) of ceria – the ability to store oxygen under oxidizing conditions and to release it under reducing conditions. In pure ceria this process is associated with the change in the oxidation state of cerium between Ce³⁺ and Ce⁴⁺ and formation of oxygen vacancies in the lattice structure by loss of oxygen and/or its electrons [1]. Doping with trivalent rare earth ions introduce additional oxygen vacancies in ceria and increases OSC of ceria. In recent years many efforts focus on the study of nanocrystalline ceria that have the promise to display OSC significantly higher and more stable than that characteristic of their micro-crystalline counterparts. This feature was supposed to be related to the increased surface contribution though unambiguous and clear understanding of their local structure remains lacking to date.

In this work the size-dependent changes in EPR spectra of Gd³⁺ ions in nanocrystalline ceria (with grain sizes of 10 and 600 nm) doped with yttrium (0.5, 1 at.%) have been investigated. The observed spectra were fitted by the superposition of contributions having cubic and trigonal symmetry. The spectra of the bulk sample (600 nm grain size) with the minimal concentration of yttrium (0.5 at%) is about of cubic symmetry; the trigonal contribution becomes notable at 1 at% of yttrium concentration.

The spectra of the samples with fine grains (10 nm) reveal two types of trigonal centers, which contributions to the spectra differ for different concentration of yttrium. These two types of centers are referred to interior and surface parts of the crystallites. Our findings point out clearly at the local distortions in the lattice structure when the size of grains decreases down to nanometer scales.

For samples with 10 nm grains the contribution of the broad line with *g*-values close to that of superoxide radicals was found.

This work was partially supported by DFG (Project PO 426/10-1).

1. Trovarelli A. (ed.): Catalysis by Ceria and Related Materials. London, Imperial College Press, 2002.
2. Murray E.P., Tsai T., Barnett S.A.: Nature **400**, 649–651 (1999)
3. Corma A., Atienzar P., Garcia H., Chane-Ching J.Y.: Nature materials **3**, 394–397 (2004)

Electronic and Magnetic Properties of Three Dimensional Disordered Network of Nanographites: ESR and Magnetic Susceptibility Data

A. M. Ziatdinov and N. S. Saenko

Institute of Chemistry, Far Eastern Branch of the RAS, Vladivostok 690022, Russian Federation,
ziatdinov@ich.dvo.ru

According to the calculations [1], the magnetic properties of nanographene and stack of nanographenes (nanographite) may differ significantly from the magnetic properties of bulk graphite due to the presence of edge π -electron states, which are localized near the peripheral regions of zigzag form and are spin-polarized. In this work, the results of investigation by the EPR and magnetic susceptibility methods of electronic and magnetic properties of nanographites – the structural blocks of activated carbon fibers (ACFs) are presented.

With the set of complementary physical methods has been found that studied PAN-based ACFs consist of three-dimensional disordered network of nanographite domains, divided from each other by two types of micropores. Each nanographite consists of 2–4 nanographene layers. The mean in-plane size of nanographite is ≈ 2 nm.

The ESR and magnetic susceptibility data show that there are two types of spin carriers in ACFs: conduction electrons and localized centers, which characterizes with the same values of g -factor and lineshape asymmetry parameter A/B . The slow temperature dependence of ESR signal linewidth for localized spins also in non-evacuated sample indicates that they are in inner layers of nanographites. Furthermore, the Curie-Weiss type temperature dependence of ACFs magnetic susceptibility gives evidence that the localized spins form small clusters. Basing on this data, it was shown that the density of states near the Fermi level of nanographites is several orders higher than same value of the bulk graphite. According to the data of calculations [1], this result indicates the existence of edge π -electronic states of nanographites. At the reversible adsorption of oxygen, the number of current carriers near the Fermi level of nanographite slightly changes, without changing of their g -factor value. The anomalous increase of spin relaxation rate of current carriers in ACFs after abrupt oxygen puffing and following slow decrease to the value of initial non-evacuated sample were found and origin of this phenomenon discussed.

1. Fujita M. *et al.*: J. Phys. Soc. Jpn. **65**, 1920 (1996)

Spin-Crossover Like Transitions in Quasi 1D Compounds of Cu(II) Based Exchange Clusters

V. A. Morozov

International Tomography Center, Novosibirsk 630090, Russian Federation,
moroz@tomo.nsc.ru

Thermal spin-crossover like phenomena of paramagnetic “breathing” crystals (polymer-chain heterospin complexes of $\text{Cu}(\text{hfac})_2$ with nitronyl nitroxide radicals [1]) display a great variety and are sometimes rather unusual. Both ESR spectra governed by averaged exchange integral J_{av} of the clusters and the effective magnetic moment μ_{eff} of these complexes can very sharply change in a narrow temperature range that is typical for solid state phase transitions. The cooperative phenomena may occur both in chains of two- and three-spin exchange Cu(II) clusters with different motifs of polymer chains. The quasi one-dimensional molecular structure of the complexes is essential [2] for the cooperative spin-crossover like phenomena to take place.

In the report we provide our theoretical approach to describe the spin structural transitions in chains of three-spin exchange clusters and discuss possible scenarios of cooperative spin-crossover in these molecular systems containing the Jahn-Teller paramagnetic centre Cu(II) of two types. The major part of “breathing” crystals compounds are just of this kind. The approach developed is a generalization of two-spin exchange cluster theory suggested earlier [3]. The basic integral equation to be solved is found of type:

$$\int \sqrt{Z_{1S}(x)} \left(\int \exp(-\alpha(x+v)^2) Z_{2S}(v) \exp(-\alpha(y+v)^2) dv \right) \times \sqrt{Z_{1S}(y)} \varphi_1(y) dy = \exp(-F/T) \varphi_1(x) ,$$

where Z_{1S} , Z_{2S} stand for partition functions of adjacent Cu(II) paramagnetic centres of the chain and F is free energy per the chain unit cell.

Different versions of thermal spin structural transitions involving both step-wise and smooth change of μ_{eff} are described and explained in terms of distribution functions $f(x) = \varphi_1(x)^2$ corresponding to the exchange cluster deformations. The results obtained are applied to well reproduce the available experimental data [1, 4] on the effective magnetic moment μ_{eff} versus temperature thus giving information on the temperature change of averaged exchange integral J_{av} in these compounds. Cooperative spin transition of a new type with upward jump of positive exchange integral with decreasing temperature is predicted.

The work was supported by the Ministry of Education and Science of Russian Federation (project 8436).

1. Ovcharenko V.I., Romanenko G.V., Maryunina K.Yu., Bogomyakov A.S., Gorelik E.V.: *Inorg. Chem.* **47**, 9537 (2008)
2. Tretyakov E.V., Fokin S.V., Romanenko G.V., Ikorskii V.N., Vasilevsky S.F., Ovcharenko V.I.: *Inorg. Chem.* **45**, 3671 (2006)
3. Morozov V.A., Lukzen N.N., Ovcharenko V.I.: *Phys.Chem.Chem.Phys.* **12**, 13667 (2010)
4. Ovcharenko V.I., Fokin S.V., Romanenko G.V., Ikorskii V.N., Tretyakov E.V., Vasilevsky S.F., Sagdeev R.Z.: *Mol. Phys.* **100**, 1107 (2002)

Spin Dynamics in a New Quasi 1D Sodium Cobalt Tellurate

**E. A. Zvereva¹, M. I. Stratan¹, T. M. Vasilchikova¹, A. N. Vasiliev¹,
V. B. Nalbandyan², I. L. Shukaev², M. A. Evstigneeva², and B. Büchner³**

¹ Physics Faculty, Moscow State University, Moscow 119991, Russian Federation
zvereva@mig.phys.msu.ru

² Chemistry Faculty, Southern Federal University, Rostov-on-Don 344090, Russian Federation

³ Leibniz Institute for Solid State and Materials Research IFW Dresden, D-01069 Germany

Static and dynamic magnetic properties of a new quasi one-dimensional compound $\text{Na}_{3.9}\text{Co}_{1.05}\text{TeO}_6$ were investigated by means of magnetization and ESR techniques. A new complex oxide was prepared by conventional solid-state reactions and represents a novel monoclinic superlattice type derived from $\alpha\text{-NaFeO}_2$. A structure of $\text{Na}_{3.9}\text{Co}_{1.05}\text{TeO}_6$ contains essentially ordered mixed-cations magnetic layers alternating with nonmagnetic alkali layers (Fig. 1). All cations and anions are in distorted octahedral coordination. Within magnetically-active layers the edge-sharing octahedra of magnetic ions (Co^{2+}) form the zig-zag one-dimensional (1D) chains, providing lower-dimensional conditions for the magnetic interactions. Nevertheless, the compound was found to order antiferromagnetically at low temperatures with $T_N \sim 3$ K. The magnetization isotherms do not display a hysteresis and saturation in magnetic fields up to 5 T, but indicate a presence of competing antiferro- and ferromagnetic interactions and reveal a sharp spin-flop type transition at $T < 3$ K in applied field of ~ 0.18 T.

The ESR spectra show complex behavior with at least three different dynamic regimes over the temperature range investigated. In the paramagnetic phase (80–300 K) we observed a superposition of two Lorentzian-shaped absorption lines probably corresponding to two different magnetic subsystems in the compound (Fig. 2). The temperature dependence of their parameters is rather complicated revealing a presence of two anomalies (possible crossover transitions) at about 220 K and 110 K respectively. At lower temperatures, in the pre-ordering phase 20–70 K, the resonance signal weakens progressively and merges into one

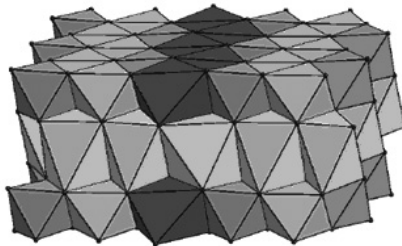


Fig. 1. Polyhedral model of the crystal structure of $\text{Na}_{3.9}\text{Co}_{1.05}\text{TeO}_6$: TeO_6 octahedra are shown in gray, CoO_6 octahedra are in dark gray, NaO_6 octahedra are in light gray, respectively, oxygen ions are small spheres.

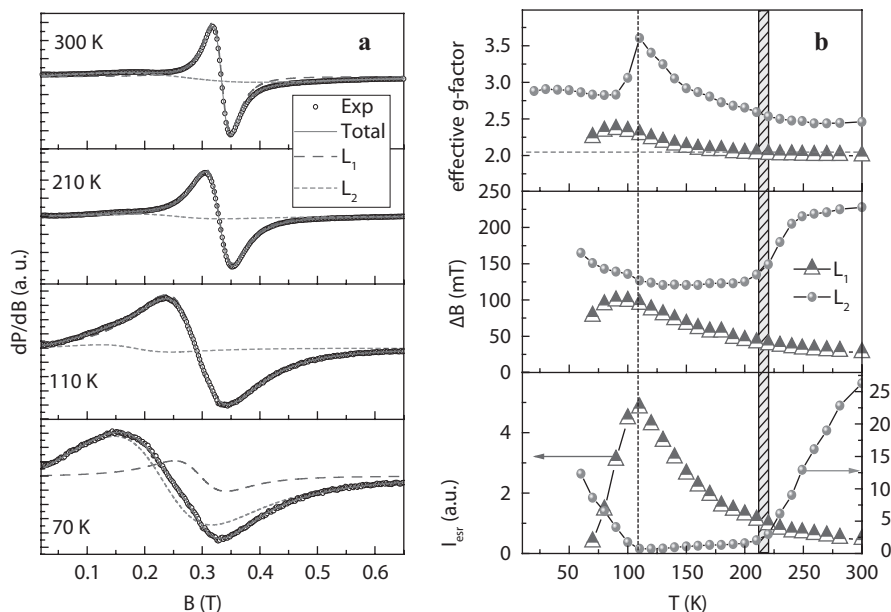


Fig. 2. Representative ESR spectra at elevated temperature (a) and temperature dependence of the effective g-factor, the linewidth and integral ESR intensity (b) for powder sample $\text{Na}_{3.9}\text{Co}_{1.05}\text{TeO}_6$.

line, which, in its turn, becomes markedly anisotropic. Eventually, at helium temperature, a strong broad line shifted to lower fields is observed, indicating approaching the long-range ordering transition and concomitant opening of the energy gap for resonance excitation.

The financial support of the Foundation for Basic Research (grants 11-03-01101, 13-02-00374) is gratefully acknowledged.

A Multi-Frequency EPR and ENDOR study of NO_3^{2-} Defect in Nanosized Hydroxyapatite

**T. B. Biktagirov¹, M. R. Gafurov¹, G. V. Mamin¹, S. B. Orlinskii¹,
A. A. Rodionov¹, B. V. Yavkin¹, E. S. Klimashina², and V. I. Putlayev²**

¹ Institute of Physics, Kazan Federal University, Kazan 420008, Russian Federation,
tbiktagirov@gmail.com

² Department of Chemistry, Moscow State University, Moscow 119992, Russian Federation

Nanosized synthetic hydroxyapatite $\text{Ca}_{10}(\text{PO}_4)_6(\text{OH})_2$ (nano-HAP) is considered to be a promising candidate for use as bio-material. Due to its chemical composition mirroring that of bone mineral and teeth enamel it is extensively employed for the hard tissues implantation [1].

It is known that the lattice of hydroxyapatite is highly labile for the different types of ionic substitutions. These impurities can affect physicochemical properties of nano-HAP and its biocompatibility. Previously we have shown the abilities of high-frequency electron paramagnetic resonance (EPR) spectroscopy for studying paramagnetic impurities both in the synthetic HAP and mineralized biological tissue [2, 3].

In the present work the combination of X- (10 GHz) and W-band (94 GHz) EPR and electron-nuclear double resonance (ENDOR) pulsed techniques has been employed to investigate the distribution of nitrate and carbonate impurities in the lattice of nano-HAP produced via wet synthesis process.

We have observed the EPR signal of radiation induced paramagnetic center which is supposed to be a stable NO_3^{2-} radical allocated in the nano-HAP structure and produced from NO_3^- anionic impurity. X- and W-band field-swept spin-echo spectra and their simulations are presented at Fig. 1. The spectra could be quite well described by the spin-Hamiltonian of the axial symmetry.

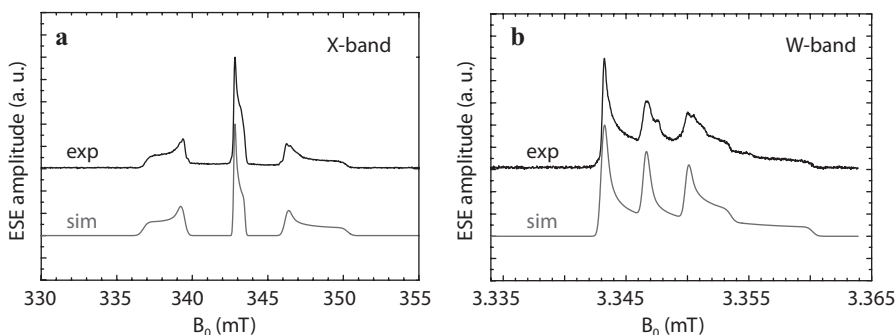


Fig. 1. Field swept echo detected EPR spectra (exp) of nano-HAP: (a) X-band (9.6 GHz), $T = 300$ K; (b) W-band (94.1 GHz), $T = 50$ K and their corresponding simulations (sim).

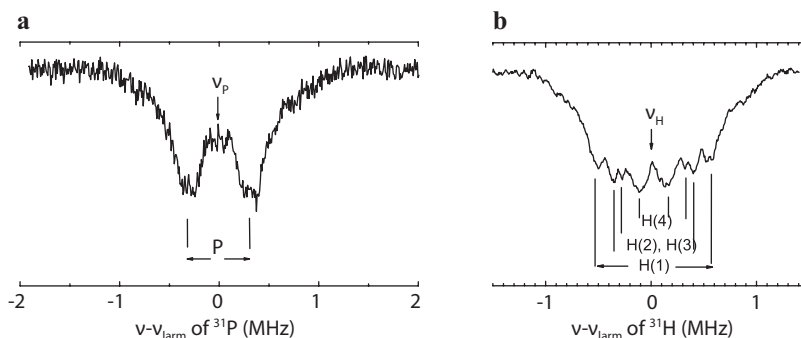


Fig. 2. ENDOR spectra of nano-HAP in the vicinity of (a) phosphorous and (b) hydrogen Larmor frequencies. W-band, $T = 50$ K.

To specify the position of the NO_3^{2-} radical ENDOR experiments were carried out. Figure 2 shows the Mims-ENDOR spectra in the vicinity of phosphorous and hydrogen Larmor frequencies at 50 K in W-band.

From ENDOR results it is suggested that NO_3^{2-} radical is most probably embedded into the OH channels of the hydroxyapatite lattice. It is supposed that the nitrate anions incorporate in the structure of nano-HAP during the synthesis process from the reagents (by-products). We propose that determination of the localization of impurity may be important for revealing the dynamics of nano-HAP growth.

1. Lafon J.P., Champion E., Bernache-Assollant D.: *Eur. Cer. Soc.* **28**, 139 (2008)
2. Abdul'yanov V.A., Galiullina L.F., Galyavich A.S., Izotov V.G., Mamin G.V., Orlinskii S.B., Rodionov A.A., Salakhov M.Kh., Silkin N.I., Sitdikova L.M., Khairullin R.N., Chelyshev Yu.A.: *JETP Lett.* **88**, 69 (2008)
3. Gafurov M.R., Yavkin B.V., Biktagirov T.B., Mamin G.V., Orlinskii S.B., Izotov V.V., Salakhov M.Kh., Klimashina E.S., Putlayev V.I., Abdul'yanov V.A., Ignatjev I.M., Khairullin R.N., Zamochkin A.V., Chelyshev Yu.A.: *Magn. Reson. Solids* **15**, 13102 (2013)

Uncovering Heterogeneous Metal-Ion Coordination in Aggregating Peptides

S. Saxena

¹ Department of Chemistry, University of Pittsburgh, Pittsburgh, PA, 15260, USA,
sksaxena@pitt.edu

Despite significant progress there is still uncertainty about the molecular basis for the onset of Alzheimer's disease. The misfolding of amyloid- β peptide ($A\beta$), wherein a soluble peptide aggregates to form plaques is central to this process. *In vitro* results indicate that metal ions like Zn^{2+} and Cu^{2+} affect the rate of formation of fibrils. The talk will focus on the use of pulsed ESR to understand the microscopic interactions of the metal ions with the peptide. The peptide exhibits a highly heterogeneous coordination environment which changes as a function of pH as well as metal ion concentrations. At the same time the aggregated morphology of amyloid- β depends on the concentration of metal ions. Taken together, the data suggests that microscopic metal- $A\beta$ interaction play a major role in dictating the aggregated state of $A\beta$. The high concentrations of metal ions in plaques found in the brains of Alzheimer's patients suggest that the *in vitro* results may have real significance *in vivo*.

POSTERS

Quantum Chemistry Calculations of EPR Parameters of a Reduced $[4\text{Fe}4\text{S}]^+$ Cluster: Hyperfine Constants of Hydrogen Atoms

L. I. Savostina¹, W. Lubitz², and M. van Gastel²

¹ ZPhTI, Kazan 420029, Russian Federation, savostina@mail.knc.ru

² MPI CEC, Mülheim (Ruhr) 45470, Germany, maurice.van-gastel@cec.mpg.de

The study of iron-sulfur proteins involved in electron transport in a number of metabolic reactions is important for the field of modern biophysics. In nature, they serve as a biological “capacitor” that can accept and donate electrons, depending on the oxidation of the iron atoms (+1, +2, +3). Compounds with a $[4\text{Fe}4\text{S}]^+$ cluster in the doublet ground state $S = 1/2$ have been found in some metalloproteins: nitrogenase III, aconitase and $[\text{NiFe}]$ hydrogenase.

Quantum chemical calculations were performed with ORCA [1] with several functional (BP86, B3LYP, PBE) and basis sets (SVP, TZVP) on the computer

Table 1. The values of the coefficients $\langle S_{iz} \rangle$ calculated by different methods ($K_i = \langle S_{iz} \rangle / \langle S_i \rangle$).

	Scheme “2-2”	$\langle S_{iz} \rangle$ Scheme “3-1”	Our calc.
0Fe ($\text{Fe}^{2+}\text{-Fe}^{2+}$)	-0.66	-0.55	-0.63
1Fe ($\text{Fe}^{3+}\text{-Fe}^{2+}$)	1.02	1.17	1.12
2Fe ($\text{Fe}^{3+}\text{-Fe}^{2+}$)	0.81	0.45	0.67
3Fe ($\text{Fe}^{2+}\text{-Fe}^{2+}$)	-0.66	-0.55	-0.66

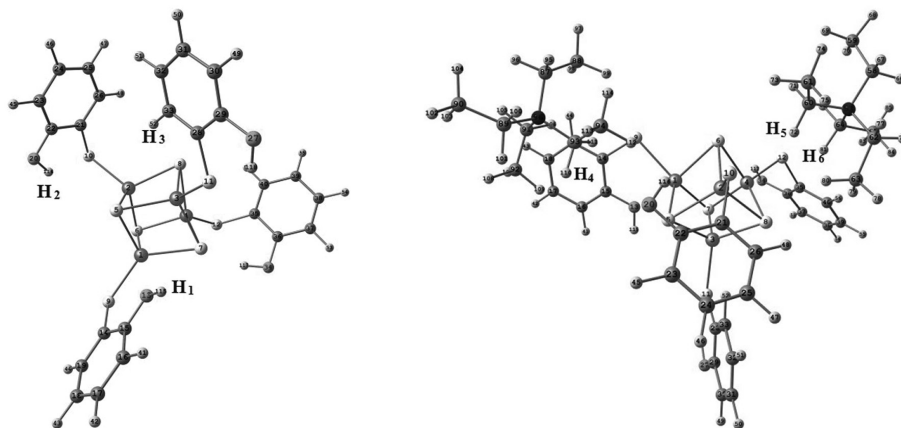


Fig. 1. Structure of interest and positions of selected hydrogen atoms.

Table 2. The values of the HFC constants (MHz) of hydrogen atoms calculated by different methods.

	Exp [4]		Scheme "2-2" [2]		Scheme "3-1" [2]		[3]	
H ₁	-0.64	1.94	1.33	-1.57	1.11	-1.31	0.95	-1.55
		5.82		-4.86		-4.05		-5.07
		-7.76		6.43		5.36		6.62
H ₂	-0.18	-2.97	0.26	-1.87	0.30	-2.15	0.16	-1.78
		-5.31		-3.47		-3.99		-3.35
		8.28		5.34		6.13		5.14
H ₃	-0.07	-2.29	-0.66	-2.08	-0.37	-1.16	-0.72	-2.06
		-5.97		-4.84		-2.69		-4.84
		8.26		6.92		3.85		6.90
H ₄	-0.06	-0.84	-0.04	-0.62	-0.04	-0.51	0.01	-0.59
		-3.34		-1.82		-1.51		-1.79
		4.18		2.43		2.03		2.38
H ₅	0	-4.31	0.04	-1.87	0.04	-2.14	0.09	-1.77
		-6.47		-3.63		-4.17		-3.53
		10.79		5.50		6.31		5.30
H ₆	0	-0.52	0.05	-0.43	0.04	-0.36	0.04	-0.46
		-7.11		-2.71		-2.26		-2.74
		7.64		-3.14		2.62		3.20

cluster of the Max Plank Institute for Chemical Energy Conversion (Mülheim (Ruhr) Germany).

Calculations of EPR parameters (e.g. HFC constants) of compounds containing iron atoms are not a trivial task, especially for $[4\text{Fe}4\text{S}]^+$ clusters in the ground state $S = 1/2$. Calculations are performed with the broken symmetry method and the calculation of spin projection coefficient K_i giving the projection of the local site spin S_i onto the total spin S_t of the system ($S_t = 1/2$). We calculated these coefficients K_i by three methods developed by the group of Noodleman [2] (scheme "2-2" and "3-1") and the group of Neese [3]. It was shown that coefficients K_i calculated in different ways are similar to each other (see Table 1).

From these approaches calculated HFC constants were obtained in satisfactory agreement with experimental data [4] for the hydrogen atoms H₁, H₂ and H₃. For the other three hydrogen atoms (H₄, H₅ and H₆) an underestimation of the HFC constants is observed (see Fig. 1 and Table 2).

1. Neese F.: *Comp. Mol. Science* **2**, 73 (2012)
2. Noodleman L.: *Inorg. Chem.* **30**, 246 (1991)
3. Pantazis D.A. *et al.*: *Chem. Eur. J.* **15**, 5108 (2009)
4. Pape L.L. *et al.*: *J. Am. Chem. Soc.* **119**, 9771 (1997)

The Transformation of the Copper Centres in $\text{Pb}_5\text{Ge}_3\text{O}_{11}$ Crystals at Annealing in Halogen Atmosphere

V. A. Vazhenin, M. Yu. Artyomov, A. P. Potapov, and A. V. Fokin

Institute of Physics and Applied Mathematics, Ural Federal University, Ekaterinburg 620000, Russian Federation, vladimir.vazhenin@usu.ru

By the EPR method we detected that annealing of the lead germanate crystals (undoped, doped with iron (0.2 mol.%) or gadolinium (0.1 mol.%) in the chlorine- or bromine-containing atmosphere (800 K) results to strong growth of concentration of doubly-charged copper centres (Fig. 1). The copper contains in samples as uncontrolled impurity. The annealing in atmosphere containing fluorine doesn't give such effect. The centres of doubly-charged copper were investigated by authors in [1–3].

The presence of halogens in the crystals detected due to appearance of the dimer centres spectra ($\text{Fe}^{3+}\text{-Cl}^-$, $\text{Fe}^{3+}\text{-Br}^-$, $\text{Gd}^{3+}\text{-Cl}^-$, $\text{Gd}^{3+}\text{-Br}^-$), anions of which are situated in interstitial channels of the structure and paramagnetic ions located in trigonal lead positions [4, 5].

We suppose that most of copper enters in original crystals of lead germanate in non-magnetic state (for example as Cu^+) and oxidize to Cu^{2+} at annealing in the chlorine- or bromine-containing atmosphere. We observed two types (a and b) of Cu^{2+} triclinic centres with similar spin Hamiltonian parameters and

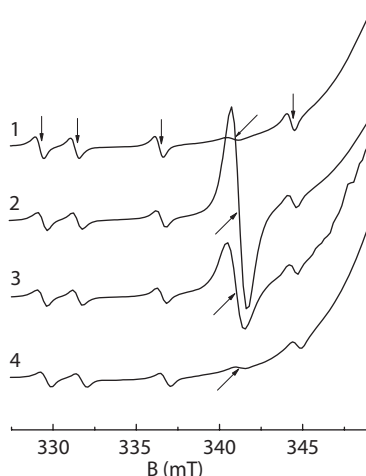


Fig. 1. Part of the EPR spectrum (derivative of the absorption signals) of single crystal $\text{Pb}_5\text{Ge}_3\text{O}_{11}:\text{0.2\% Fe}$ on low field slope of intense line $1/2 \leftrightarrow -1/2$ of the Fe^{3+} centre with signals of Mn^{2+} centre (indicated by vertical arrows) and Cu^{2+} centre (indicated by inclined arrows) at $B \parallel C_3$ (B – magnetic field induction) at room temperature: 1, original sample; 2, after annealing with ZnCl_2 ; 3, after annealing with CsBr ; 4, after annealing with PTFE (Teflon).

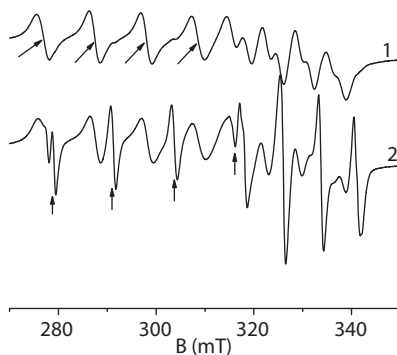


Fig. 2. Part of EPR spectrum $\text{Pb}_5\text{Ge}_3\text{O}_{11}:\text{0.3\% Cu}$ at 300 K at $B\parallel Z\perp C_3$ (Z – principal axis of one of three Cu^{2+} b-centres). Inclined arrows indicate a-centre hyperfine quartet signals and vertical arrows indicate ^{63}Cu isotope b-centre. 1, original sample, 2, annealed in chlorine-containing atmosphere.

close orientation of the principal magnetic axes. The a-centre shows transitions between three equivalent triclinic configurations and as result of it above 350 K single trigonal spectrum is observed.

The annealing at presence of chlorine or fluorine (but not bromine) of the crystals doped with copper (0.06–0.3 mol.%) leads to strong growth of b-centre spectrum intensity (Fig. 2).

The subsequent annealing of the samples in air returns spectra to original state. The spin Hamiltonian parameters of b-centres have been determined. The transformation mechanisms of copper centres are discussed.

1. Vazhenin V.A., Gorlov A.D., Krotkii A.I., Potapov A.P., Starichenko K.M.: *Fiz. Tverd. Tela* **31**, 187 (1989)
2. Trubitsyn M.P., Waplak S., Ermakov A.S.: *Fiz. Tverd. Tela* **42**, 1303 (2000)
3. Vazhenin V.A., Potapov A.P., Guseva V.B., Gorlov A.D.: *Physics of the Solid State* **49**, 660 (2007)
4. Vazhenin V.A., Starichenko K.M., Gur'ev A.V., Levin L.I., Musalimov F.M.: *Fiz. Tverd. Tela* **29**, 409 (1987)
5. Vazhenin V.A., Potapov A.P., Fokin A.V., Artyomov M.Yu.: *Physics of the Solid State* **54**, 2450 (2012)

Magnetic Features of Spin-Crossover Dendrimeric Iron(III) Complex

N. E. Domracheva¹, A. V. Pyataev², V. E. Vorobeva¹, and E. M. Zueva³

¹ Zavoisky Physical-Technical Institute, Russian Academy of Sciences, Kazan 420029, Russian Federation, domracheva@mail.knc.ru, vvalerika@gmail.com

² Kazan Federal University, Kazan 420008, Russian Federation, 151eu@mail.ru

³ Kazan State Technological Institute, Kazan 420015, Russian Federation, zueva_ekaterina@mail.ru

The unusual magnetic behavior of the first dendrimeric iron(III) complex [1] shown in Fig. 1 has been investigated by EPR and Mössbauer spectroscopy. EPR display that complex consists of the three types of magnetically active iron centers: one $S = 1/2$ low-spin (LS) and two $S = 5/2$ high-spin (HS) centers with strong low-symmetry and weak distorted octahedral crystal fields.

Analysis of the magnetic behavior reflected by I versus T (where I is the EPR lines integrated intensity of the whole spectrum) demonstrates that dendrimeric Fe(III) complex has sufficiently different behavior in three temperature intervals. The first (4.2–50 K) interval corresponds to the intermolecular exchange interactions between LS-LS, LS-HS and HS-HS centers coupled antiferromagnetically by means of water molecule and Cl counterion. The appearance of the presumable magnetoelectric effect is registered in the second (50–200 K) temperature interval, whereas a spin transition process between LS and HS centers occurs in the third (200–330 K) one. The Mössbauer spectroscopy data completely confirm the EPR results. DFT calculations demonstrate the coordination sphere structure of the compound.

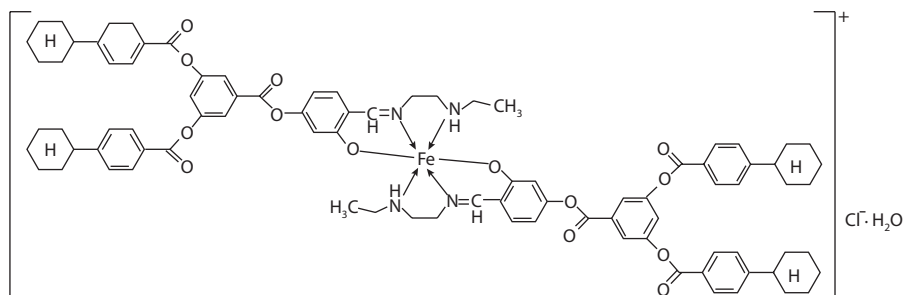


Fig. 1. Schematic model of the compound.

The simultaneous coexistence of the magnetic ordering, presumable magnetoelectric effect and spin crossover in one and the same material has been revealed for the first time.

The work was supported by RAS Presidium program No. 24 and in part by the Foundation for Basic Research (project 11-03-01028).

Suspended Long-Lived NMR Echo in Solids

A. N. Turanov¹ and **A. K. Khitrin²**

¹ Zavoisky Physical-Technical Institute, Russian Academy of Sciences, Kazan 420029, Russian Federation, sasha_turanov@rambler.ru

² Kent State University, Kent 44242, OH, USA

We report an observation of extremely long-lived spin states in systems of dipolar-coupled nuclear spins in solids. The “suspended echo” experiment uses a simple stimulated echo pulse sequence and creates non-equilibrium states which live many orders of magnitude longer than the characteristic time of spin-spin dynamics T_2 . Large amounts of information can be en-coded in such long-lived states, stored in a form of multi-spin correlations, and subsequently retrieved by an application of a single “reading” pulse.

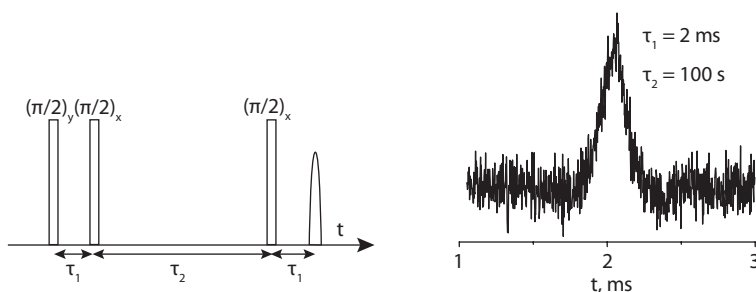


Fig. 1. Pulse sequence and suspended echo in naphthalene.

The authors acknowledge a financial support from NSF CHE-1048645 (AK) and the Ful-bright Foundation (AT).

EPR Study of Non-Resonance Microwave Absorption of $\text{Cu}(\text{aetkpz})_2\text{Br}_2$

A. S. Berezin, V. A. Nadolinny, L. G. Lavrenova, and E. V. Lider

Nikolaev Institute of Inorganic Chemistry, Novosibirsk 630090, Russian Federation,
berezin-1991@ngs.ru

The study of substances capable of effectively absorbing SHF radiation is highly relevant, due to its use as radio absorbing coating, as switches and filters in the microwave technique [1]. Furthermore, such materials may be used to create a new generation of memory elements based on the magnetic interactions.

The main goal of this paper is an investigation of microwave nonresonant absorption in the powdered sample $\text{Cu}(\text{aetkpz})_2\text{Br}_2$. Experiments were carried out on EPR spectrometer Varian E-109 in X and Q frequency range at the temperature range 77–400 K.

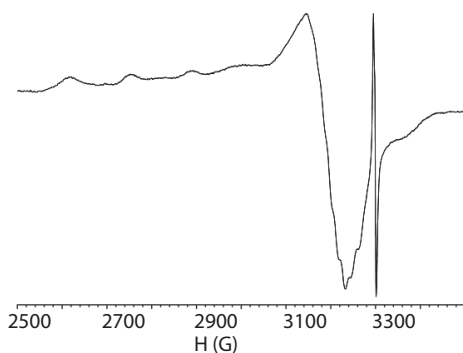


Fig. 1. The EPR spectrum of the $\text{Cu}(\text{aetkpz})_2\text{Br}_2$ frozen solution in ethanol at $T = 77$ K.

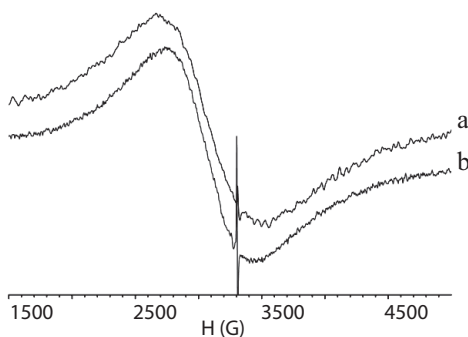


Fig. 2. EPR spectra at $T = 300$ K (a) and frozen at $T = 77$ K (b) powder of the $\text{Cu}(\text{aetkpz})_2\text{Br}_2$.

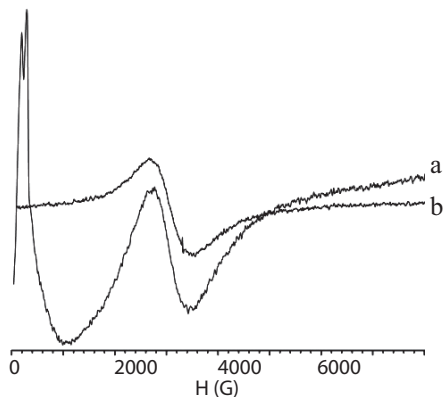


Fig. 3. EPR spectra of the original sample at $T = 300$ K (a) and the sample seasoned at $T = 300$ K (after $T = 77$ K) (b).

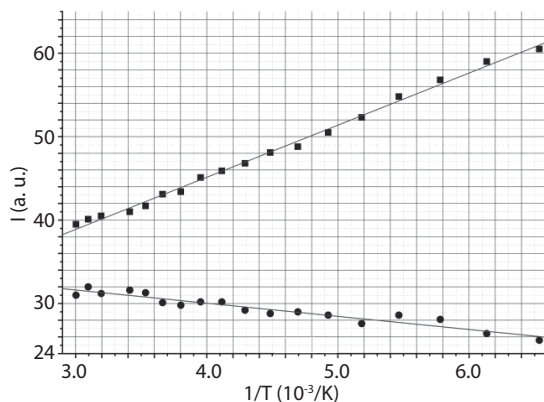


Fig. 4. The temperature dependence of the EPR line intensity from initial powder sample (■) and non-resonant absorption (●)

The frozen solution of $\text{Cu}(\text{aetkpz})_2\text{Br}_2$ in ethanol has the EPR spectrum shown in Fig. 1. The spectrum has axial symmetry with the g -factor $g = 2.067$ and $g_{\parallel} = 2.343$, and is described by the spin Hamiltonian with HFS parameters from one nitrogen atom ($A(\text{N}) = 16$ G), two equivalent bromine atoms ($A(\text{Br}) = 16$ G) and one copper atom ($A(\text{Cu})_{zz} = 135$ G).

The EPR spectrum of the initial powder sample presents a single line with the $g = 2.155$ and the half-width of the line $\Delta H = 830$ G (Fig. 2a).

By lowering the temperature of the sample to $T = 77$ K, the line half-width is reduced to $\Delta H = 720$ G (Fig. 2b). Upon subsequent heating the sample to

$T = 300$ K in the EPR spectrum the line of non-resonant microwave absorption in low magnetic fields appear (Fig. 3b) without changing the line half-width of the copper ions ($\Delta H = 720$ G).

We assume that the oxygen present in the air is penetrated and incorporated into the lattice of sample, coordinating the copper ions. This leads to the structure disordering and formation of the ferromagnetic and antiferromagnetic regions, as confirmed by the temperature dependence of the line intensities (Fig. 4). The temperature dependence of EPR spectrum of initial powder sample obeys the Curie-Weiss law. While, the nonresonant absorption line has a different behavior.

The obtained temperature dependence of EPR spectrum in zero magnetic fields is conformed to literature data about “spin glasses” [2, 3]. This lets us suppose that powder sample is transformed in “spin glass” at the temperature treatment.

The financial support of the project (№66) of the RAS Presidium Programme (№24) is gratefully acknowledged.

1. Sidorenko E.N. *et al.*: *Fazovyie perekhody, uporyadochennyie sostoyaniya i novyye materialy* **1** (2007)
2. Petrakovskiy G.A.: *SOZH* **7**, no. 9, 83 (2001)
3. Dotsenko V.S.: *UFN* **163**, no. 6, 1 (1993)

Investigation of Healthy and Infected (Brucellosis, Mastitis) Blood and Milk Samples: an ESR Spin Labeling Study

**U. Sayin^{1,2}, L. Palali¹, Z. Sayin³, R. Tapramaz⁴, E. Ergun¹,
G. Bakkal¹, and A. Ozmen^{1,2}**

¹ Physics Dep., Science Faculty, Selcuk Univ., Konya, Turkey, uakpinar@selcuk.edu.tr

² Advance Technology Research and Application Center, Selcuk Univ., Konya, Turkey

³ Microbiology Dep., Veterinary Faculty, Selcuk Univ., Konya, Turkey, zsayin@selcuk.edu.tr

⁴ Physics Dep., Science Faculty, Ondokuz Mayıs Univ., Konya, Turkey, receipt@omu.edu.tr

Spin labeling is a technique for investigating the structure and local dynamics of molecules using electron spin resonance [1]. Spin labels are a unique molecular reporter, in that they are paramagnetic (contain an unpaired electron). Spin labels were first synthesized in the laboratory of H. M. McConnell in 1965 [2]. Since then, a variety of nitroxide spin labels have enjoyed widespread use for the study of macromolecular structure and dynamics because of their stability and simple EPR signal.

In this study, lyophilized powders and not lyophilized liquid states of Mastitis infected and healthy milk samples and also Brucellosised and healthy blood serum samples were examined using TEMPO stable nitroxide radical between the temperature range of 123–243 K with ESR spin labeling technique with JEOL JESFA-300 spectrometer. In the studied examples, rotation correlation times, τ , of TEMPO spin labels at different temperatures, perpendicular and parallel components of spectroscopic splitting factor, g_{\perp} , g_{\parallel} , line width of mid-peak, ΔH_0 , perpendicular and parallel components of hyperfine coupling constant, A_{\perp} , A_{\parallel} were calculated. By comparing ESR parameters measured from spectra and infected blood and milk samples, it was determined that TEMPO spin label is exhibited a different behavior for “Brucellosis” infected samples, but did not show any difference “Mastitis” disease. Also it was understood that there was no need to lyophilize the milk samples for ESR spin labeling studies.

This work was financially supported by the BAP, Selcuk University in Turkey.

1. Berliner L.J.: Spin Labeling I: Theory and Applications. New York, Academic Press, 1976.
2. Stone T.J., Buckman T., Nordio P.L., McConnell H.M.: Spin-Labeled Biomolecules, Proc. Natl. Acad. Sci. USA **54**, no. 4, 1010–1017 (1965)

Magnetic Properties of Gamma Irradiated 2,3-Butanedione Monoxime: an Experimental and Theoretical ESR Study

L. Ates^{1,2}, H. U. Taşdemir³, U. Sayin^{1,2}, E. Türkkan³, and A. Ozmen^{1,2}

¹ Physics Dep., Science Faculty, Selcuk Univ., Konya, Turkey, leventates@selcuk.edu.tr

² Advance Technology Research and Application Center, Selcuk Univ., Konya, Turkey

³ Physics Edu. Dep., A.K. Education Faculty, Nec. Erb. Univ., Konya, Turkey

An oxime is one in a class of chemical compounds with the general formula, $R^1R^2C = NOH$ where R^1 is an organic side chain and R^2 is either hydrogen, forming an aldoxime, or another organic group, forming a ketoxime [1]. 2,3-Butanedione monoxime (BDM) is the well-characterized, low-affinity, non-competitive inhibitor of skeletal muscle myosin-II. It has been widely used at millimolar concentrations in cell biological experiments with the assumption that it is an ATPase inhibitor of the myosin superfamily.

Magnetic properties of gamma irradiated BDM powder have been investigated at 123 K and room temperature between microwave power of 0.1 mW and 100 mW by Electron Spin Resonance (ESR) with JEOL JESFA-300 spectrometer. Considering the ESR spectra and molecular structure of BDM, we identified iminoxy radical formed in irradiated BDM powder. To theoretically determine the types of radicals, the most stable structure of BDM was obtained by molecular mechanic and B3LYP/6-31G+(d,p) calculations. EPR parameters were calculated for theoretically modeled radical and found to be in strong agreement with experimental values of iminoxy radical. Also the values were confirmed with the simulation of the spectra. The experimental and theoretical ESR parameters of the radical were determined to be: $a(N)_{av} = 30.13$ G, $(g)_{av} = 2.0048$ and $a(N)_{av} = 30.05$ G, $(g)_{av} = 2.0045$, respectively.

This work was financially supported by the BAP, Selcuk University in Turkey.

1. Chakravorty A.: *Coord. Chem. Rev.* **13**, 1–46 (1974)
2. Ostap E.M.: *J. Muscle Res. Cell. Motil.* **23**, 4, 305–308 (2002)

Research of Two-Circuit System of Surface Type of the Receiving Sensor of MRI-Tomography

A. A. Bayazitov and Ya. V. Fattakhov

Zavoisky Physical-Technical Institute, Russian Academy of Sciences, Kazan 420029,
Russian Federation, bajazitv.alf@rambler.ru

In the nuclear magnetic resonance modern medical equipment of high resolution different types and configurations of receiving sensors are used. Among them – multiple loop systems of sensors (connected), capable to work both jointly, and independent from each other. The images of objects received at present with use of these receiving sensors can be considered as very successful.

The purpose of this work is to conduct the research and upgrade of the sensor of surface type. This allows to choice the construction of the receiving sensor with the best sensitivity and a signal-to-noise ratio.

Researches were conducted for sensors taking into account magnetic field strength of 0.06 T. The sensor is a part of the “TMR-0.06-KFTI” MRI system (Operating frequency is $f = 2.5$ MHz).

The research of the sensor “Spine” of surface type was conducted. The different experiments were carried, the received results are analyzed. These results will help to develop the new “Kidney” sensor. Results received during research can be applied to other types of MRI systems with corrections of operating frequency. The receiving system must to correspond to the following requirements: 1) the B_1 field created by the sensor, shall be directed perpendicularly to the main B_0 field of transferring system; 2) quality factor of system shall be an order 200–300, the higher is the quality factor of a circuit, the higher is the amplitude of a signal.

Superparamagnetic Behavior in LaSrMnZnO Systems

R. M. Eremina, K. R. Sharipov, and L. V. Mingalieva

Zavoisky Physical-Technical Institute, Russian Academy of Sciences, Kazan 420029,
Russian Federation, REremina@yandex.ru

The transport and magnetic properties of manganites of various compositions are explained assuming the existence of ferromagnetically correlated regions in the paramagnetic phase. We assume that ferromagnetically correlated regions in the paramagnetic phase should have a similar effect on the paramagnetic resonance spectrum like superparamagnetic particles. We investigated the zinc-doped lanthanum-strontium manganites. Ions Zn^{2+} , with electronic configuration $3d^{10}$, do not participate in the exchange interaction, resulting in an increasing tendency to charge localization and reduced mobility of the carriers. ESR spectrum of $La_{0.905}Sr_{0.095}Mn_{0.925}Zn_{0.075}O_3$ contains a single line at $g \approx 1.978 \pm 0.005$ at temperature range $175 \text{ K} \leq T \leq 340 \text{ K}$. The temperature dependencies of the ESR spectra of these compounds were presented in Fig. 1. The analysis of the temperature dependence of the ESR spectra, based on theory of Raikher and

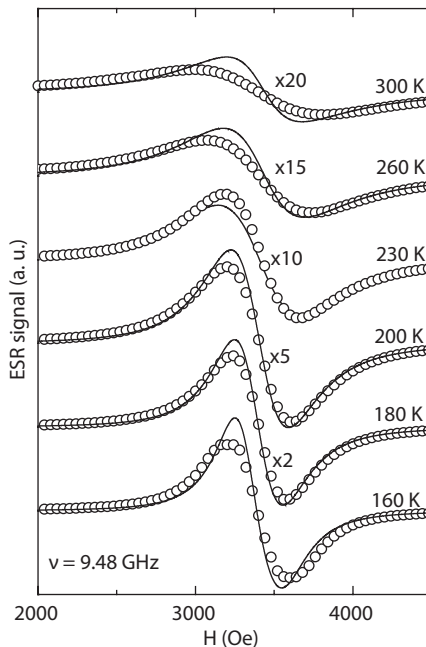


Fig. 1. Temperature dependence of the ESR spectra of $La_{0.905}Sr_{0.095}Mn_{0.925}Zn_{0.075}O_3$.

Stepanov (line in Fig. 1) [1] for superparamagnetic particles, allowed to estimate size of ferromagnetically correlated regions and the magnitude of the magnetic anisotropy, where magnetic moment of the ferromagnetic correlated region $M = 400 \pm 10 \mu_B$; anisotropy energy $W_a = 3.5 \pm 0.5$ K; the dissipation coefficient $\alpha = 0.055 \pm 0.014$; ordering temperature $T^* = 138$ K, for $x = 0.075$.

1. Raikher Yu.L., Stepanov V.I.: Journal of Magnetism and Magnetic Materials **316**, 417 (2007)

Density Functional Computations of the EPR, NMR Spectra and Spatial Molecular Structure of Ortho-Nitrophenol

S. Gündoğdu¹, H. U. Taşdemir², E. Türkkan², and Ö. Dereli²

¹ Physics Department, Necmettin Erbakan Univ. Institute of Educational Sciences, Konya 42090, Turkey

² Physics Department, Necmettin Erbakan University, Konya 42090, Turkey, eturkkan@konya.edu.tr

The density functional computations were studied to examine the suggested type of model anion radicals M1, M2, M3, and M4 that have been formed upon electrolytically reduction in dimethyl formamide solution of ortho-nitrophenol. M1 and M2 type models were modelled by gas phase monomer and dimer form of ortho-nitrophenol respectively. M3 and M4 type models were modelled by solution phase monomer and dimer form of ortho-nitrophenol respectively.

The spatial molecular structure, EPR parameters and NMR parameters of ortho-nitrophenol have been investigated with combined experimental and theoretical study. The first step, the possible conformations of the ortho-nitrophenol were obtained using the PM3 method. The most stable conformer of the title compound was obtained from the result of geometry optimizations (B3LYP/6-311++G(d,p) level) of these possible conformers. The second step, M1, M2, M3, and M4 type model anion radicals have been modelled by B3LYP method using 6-311++G(d,p), 6-31+G(d,p), 6-311++G(d,p), and 6-31+G(d,p) as basis sets respectively. Subsequently, hyperfine coupling constants, atomic spin density, and NMR chemical shift parameters calculations of these models were performed using the same level of geometry optimization calculations. Theoretically the calculated values were compared with the experimental values. Calculated isotropic hyperfine coupling constant values and chemical shift values of dimer model M4 were in good agreement with experimental values. However, the agreement was rather poor in the case of the M1 and M2 models. According to the findings from the present study, spatial molecular structure of ortho-nitrophenol was predicted by using density functional computations.

This work was financially supported by the BAP of Konya Necmettin Erbakan University (Project number 121210003).

Electron Magnetic Resonance Technique in the Study of Macromolecule Adsorption on Magnetic Nanoparticle Surface on Dispersion

**A. V. Bychkova, O. N. Sorokina, A. V. Shapiro, M. Rosenfeld,
A. L. Kovarski, and V. Berendyaev**

Federal State Budgetary Institution of Science
Emanuel Institute of Biochemical Physics of Russian Academy of Sciences,
Moscow 119334, Russian Federation, anna.v.bychkova@gmail.com

Spin label technique allows studying adsorption of macromolecules on magnetic nanoparticles (MNPs) in dispersion without separation processes of solution components [1]. Influence of local fields of MNPs on spectra of radicals in solution depends on the distance between MNPs and radicals [2]. If this distance is lower than 40 nm for magnetite nanoparticles with the average size of 17 nm ESR spectra lines of the radicals broaden strongly and their amplitude decreases to zero [3]. The decreasing of the observed spectrum amplitude is proportional to the part of radicals which are located inside the layer of 40 nm around MNP. The same happens with spin labels covalently bound to protein macromolecules (Fig. 1). An intensity of spin label spectra decreases as a result of adsorption of macromolecules on MNPs (Fig. 2). Adsorption of bovine serum albumin (BSA), thrombin, fibrinogen (FG) and polyethyleneimine on magnetite MNPs was studied [4–6]. We have shown that spin label technique can be used for the study of adsorption value, adsorption kinetics, calculation of average number of molecules in adsorption layer and adsorption layer thickness, concurrent adsorption of macromolecules. The method of ferromagnetic resonance (FMR) can also be used to study adsorption layer formation. Due to linear aggregate formation in magnetic field of spectrometer resonance conditions for MNPs in dispersion change. FMR spectrum shifts. The shift parameter is proportional to a local field created by MNPs. The local field is inversely proportional to a cubic distance between MNPs in linear aggregates [7]. Coating formation and the thickness of adsorption layer influence on the distance between MNPs and decrease dipole interactions. As a result the centre of FMR spectrum moves to higher fields. This phenomenon was observed in the systems containing MNPs and albumin after FG addition [6]. The similar centre positions of FMR spectra of MNPs without coating (3254 G) and MNPs in BSA coating (3253 G) point to a very thin coating and low adsorption of BSA (Fig. 3). According to FMR centre position (3449 G) the thrombin coating on MNPs is thicker than BSA coating (the spectrum of MNPs with thick coating becomes similar to FMR spectra of isolated MNPs). This result correlates with the data obtained by ESR spectroscopy and dynamic light scattering.

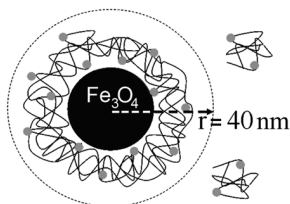


Fig. 1. MNP and spin-labelled macromolecules in dispersion.

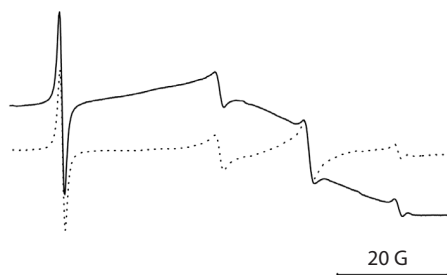


Fig. 2. ESR spectra of spin labels on BSA macromolecules (1 mg/ml) before (dotted line) and 75 min after (solid line) MNPs addition to protein solution at 25 °C. Fe_3O_4 concentration – 4 mg/ml. External standard is Mn^{2+} .

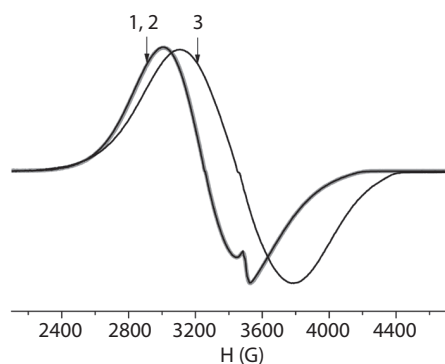


Fig. 3. FMR spectra of MNPs (1), MNPs in the mixture with BSA (1 mg/ml) after incubation time of 120 min (2) and MNPs in the mixture with thrombin (1 mg/ml) after incubation time of 120 min (3).

The reported study was supported by RFBR, research projects No. 12-03-00564a and 12-03-31452mol_a.

1. Bychkova A.V., Sorokina O.N., Shapiro A.B., Tikhonov A.P., Kovarski A.L.: *Open Colloid Sci. J.* **2**, 15 (2009)
2. Noginova N., Chen F., Weaver T., Giannelis E.P., Bourlinos A.B., Atsarkin V.A.: *J. Phys.: Cond. Matter.* **19**, 246208 (2007)
3. Sorokina O.N., Kovarski A.L., Bychkova A.V. in: *Progress in Nanoparticles Research*, pp. 91–102. New York, Nova Science Publishers, 2008.
4. Bychkova A.V., Sorokina O.N., Kovarskii A.L., Shapiro A.B., Leonova V.B., Rosenfeld M.A.: *Biophysics (Russ. J.)* **55**(4), 544 (2010)
5. Bychkova A.V., Sorokina O.N., Kovarski A.L., Shapiro A.B., Rosenfeld M.A.: *Nanosci. Nanotechnol. Lett.* **3**, 591 (2011)
6. Bychkova A.V., Rosenfeld M.A., Leonova V.B., Lomakin S.M., Sorokina O.N., Kovarski A.L.: *Russ. Colloid J.* **75**, 7 (2013)
7. Dolotov S.V., Roldughin V.I.: *Russ. Colloid J.* **69**, 9 (2007)

The Edge Magnetism of Monolayer Graphene and Nanographite

M. A. Augustyniak-Jablokow, M. Maćkowiak,
R. Strzelczyk, and K. Tadyszak

Institute of Molecular Physics, Polish Academy of Sciences, Poznan 60-179, Poland

The zig-zag edges of graphene layers are specific defects as the broken σ bonds, named also the dandling bonds should be magnetic and the exchange interactions between unpaired spins localized on them should be of ferromagnetic character. Theoretically it is predicted, that spins on one edge should interact ferromagnetically. Two edges on the same graphene sheet should be antiferromagnetically coupled [1], except the very broad graphene sheets. The antiferromagnetic character is predicted also for the interlayer coupling.

Despite several reports [2–5] claiming observation of ferromagnetic interactions in graphene and graphite, there are no reliable evidence that these ferromagnetic properties are due entirely to carbon. Opposite there are papers showing presence of ferromagnetic contaminations in graphite [6], or demonstrating that the magnetic effects observed by magnetometry for the intentionally introduced dopant are the same as those reported for graphite and graphene [7].

Here we present our EPR study showing presence of the FMR signal in graphene and multilayer graphene platelets obtained by graphite cavitation in 1-propanol.

The nanographite sample was prepared by deposition of the nanographite dispersion on amorphous SiO_2 followed by 3 hours of drying in vacuum combined with 30 minutes annealing at ~ 360 °C. After this the tube was sealed and the spectrum registered. The broad signals, which cannot be associated with

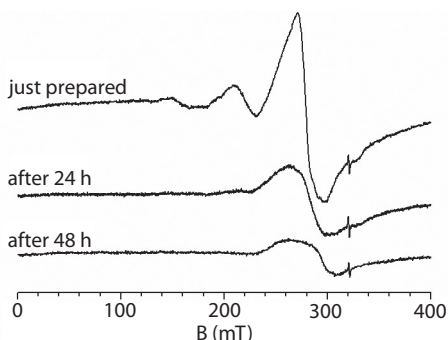


Fig. 1. The time evolution of the EPR signals observed for the multilayer graphene platelets prepared from the graphite flakes. The narrow signal with $g \sim 2.0023$ originates from conduction electrons.

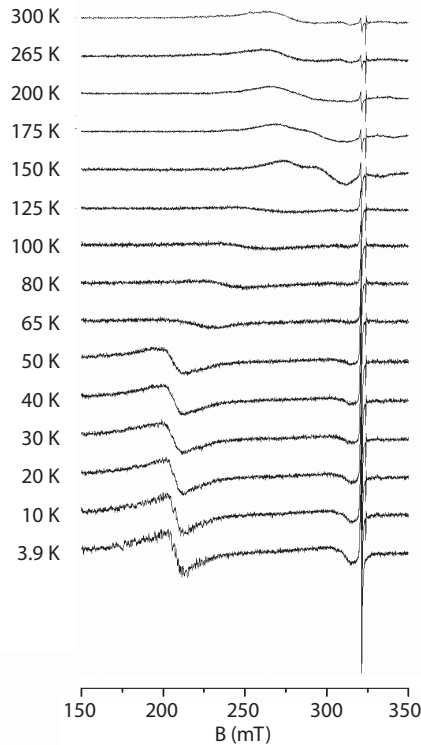


Fig. 2. The temperature evolution of the spectra observed for the monolayer graphene. The narrow line, which intensity increases with temperature originates from conducting electrons coupled to some localized centers. The weak narrow signal on its right is due to standard fixed on the resonator wall. The broad lines are the FMR signals from the edge states.

conduction electrons or structural defects in graphite, are observed. The narrow and weak signal at $g \sim 2.0023$ originates from conduction electrons.

The time evolution of the signals shown in Fig. 1 indicates, that these signals are not associated with ferromagnetic contaminations.

In the Fig. 2 we show the temperature evolution of the EPR spectra observed for the monolayer graphene. The observed picture is consistent with the theoretical prediction of the edge magnetism in graphene [8].

1. Lee H., Son Y.-W., Park N., Han S., Yu J.: *Phys. Rev. B* **72**, 174431 (2005)
2. Kopelevich Y., Esquinazi P., Torres J.H.S., Moehlecke S.: *J. Low Tem. Phys.* **119**, 699 (2000)
3. Esquinazi P., Setzer A., Höhne R., Semmelhack C., Kopelevich Y., Spemann D., Butz T., Kohlstrunk B., Lösche M.: *Phys. Rev. B* **66**, 024429 (2002)
4. Wang Y., Huang Y., Song Y., Zhang X., Ma Y., Liang J., Chen Y.: *Nano Lett.* **9**, 220 (2009)
5. Cervenka J., Katsnelson M.I., Flipse C.F.J.: *Nature Physics* **5**, 840 (2009)
6. Sepioni M., Nair R.R., Tsai I-Ling, Geim A.K., Grigorieva I.V.: *EPL* **97**, 47001 (2012)
7. Venkatesan M., Dunne P., Chen Y.H., Zhang H.Z., Coey J.M.D.: *Carbon* **56**, 279 (2013)
8. Yazyev O.V., Katsnelson M.I.: *Phys. Rev. Lett.* **100**, 047209 (2008)

Detection of Explosive Precursors Using Low-Field Magnetic Resonance Imaging and Spectroscopy

N. A. Krylatykh, Ya. V. Fattakhov, A. R. Fakhrutdinov, V. N. Anashkin, V. A. Shagalov, I. A. Nurmamyatov, and R. Sh. Khabipov

Zavoisky Physical-Technical Institute, Russian Academy of Sciences, Kazan 420029,
Russian Federation, natalya.p4lka@gmail.com

The problem of security in crowded places is a topical problem to date. The main issue when solving this problem is to detect the dangerous objects in good time and to take every conceivable precaution. However, liquid explosive compounds, which can be prepared in advance or directly before using from corresponding reagents, have been used nowadays as well. Therefore the elaboration of the methods of the operative determination of the type of the liquid is a current problem.

The method of nuclear magnetic resonance is widely used for studying the liquid and solid compounds [1]. The attractiveness of low magnetic fields for solving this problem is in the low cost of the devices themselves and of their operation, and the relatively low energy inputs for the maintenance of the magnetic field.

In this work, it was shown that it is possible to elaborate the methodology of the differentiation of liquid compounds by the magnetic resonance images in low magnetic fields. The most reliable determination of the type of the unknown liquid is possible, when its three parameters are measured: longitudinal and transverse relaxation times, and the self-diffusion coefficient. These parameters can be measured directly in low and ultra-low magnetic fields. On the basis of the above study, it is possible to state that the methodology of the detection of liquid explosive and hazardous compounds using NMR in low and ultra-low fields can be elaborated and successfully introduced for providing security in crowded places.

1. Rameev B.Z., Mozzhukhin G.V., Khusnutdinov R.R., Aktas B., Konov A.B., Gabidullin D.D., Krylatykh N.A., Fattakhov Y.V., Salikhov K.M.: Proc. SPIE **8357**, 83570Z (2012); <http://dx.doi.org/10.1117/12.923625>. Online Publication Date: May 10, 2012.

EPR of the Narrow-Gap Semiconductor PbS Doped Highly by Manganese Ions

V. A. Ulanov^{1,2}, A. M. Sinitsyn², R. R. Zainullin², and E. R. Zhiteytssev¹

¹ Zavoiisky Physical-Technical Institute, Russian Academy of Sciences, Kazan 420029, Russian Federation, ulvlad@inbox.ru

² Kazan State Power Engineering University, Kazan 420066, Russian Federation

PbS belongs to the family of A^{IV}B^{VI} narrow gap semiconductors. Among them the lead chalcogenides (PbSe, PbTe and PbS) attract a great interest as an important class of materials for electronic devices. These materials have small band gaps, high dielectric constants, and a variety of very unusual thermodynamic, vibrational, electronic and infrared properties. Relative to family of the widespread A^{II}B^{VI} narrow gap semiconductors which have a direct gap at the Γ point in the Brillouin zone, the direct gap for lead chalcogenides occurs at the L point. Besides, the order of band gap $E_G(\text{PbS}) > E_G(\text{PbTe}) > E_G(\text{PbSe})$ and the valence band maximum energies $E_{\text{VBM}}(\text{PbS}) > E_{\text{VBM}}(\text{PbSe}) > E_{\text{VBM}}(\text{PbTe})$ are anomalous compared to that of A^{II}B^{VI} semiconductors. Furthermore, the band pressure coefficient is negative in contrast to A^{II}B^{VI}. All these physical properties give the lead chalcogenides very many interesting possibilities for their technical applications in infrared and thermoelectric devices. The progress in the nanoscale technology has made possible the fabrication of new type of lead salt semiconductor nanostructures whose characteristics change with respect to the geometry of them (such as quantum dots, quantum wires and quantum wells).

For a number of last years, many investigations have been directed to study the doping-induced modification of energy spectrum of the lead chalcogenide semiconductors. The behaviour of magnetic impurities in lead salts also has been a subject of considerable interest in the studies of physical properties of these materials (see, for instance, [1–5]). It was found that in some cases the energy spectrum of a host material remains unchanged, but doping results in an appearance of a deep impurity level with a high density of states that pins the Fermi level. But rather a little information was got for these materials with very high concentrations of magnetic impurities ($x > 0.01$).

In the present work we performed EPR study of $\text{Pb}_{1-x}\text{Mn}_x\text{S}$ single crystals which were grown using the Bridgeman method under well-known growth conditions. Manganese was introduced into the charge in a form of metallic powder. Crystals thus obtained were then used for investigation of peculiarities in the EPR line shapes and spectral characteristics of crystalline pieces which were cut from along the ingots. X-band measurements were performed at temperatures from 1.8 to 300 K. The magnetic ion content was varied from $x = 0.001$ to $x = 0.03$. The best resolved EPR spectra were observed in the samples with $x = 0.001$ at temperature $T = 4.2$ K. These spectra contained six lines arisen due to hyperfine splitting of Mn ($I_{\text{Mn}} = 5/2$) and could be characterized by $g = 1.987 \pm 0.001$

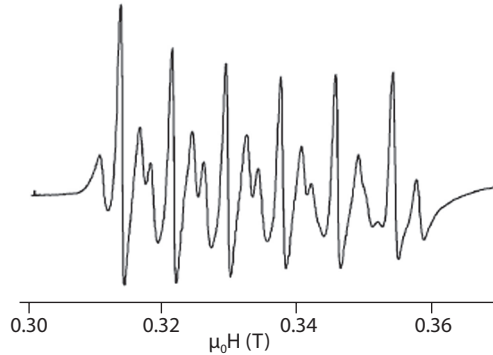


Fig. 1. EPR spectrum of $\text{Pb}_{0.99}\text{Mg}_{0.01}\text{S}$ ($f = 9337$ GHz, $T = 4.2$ K, $H \parallel \langle 111 \rangle$).

and $A_{\text{Mn}} = 212 \pm 1$ MHz. No superhyperfine structure (SHFS) and fine structure (FS) splittings were observed in the EPR spectra of the samples $\text{Pb}_{1-x}\text{Mn}_x\text{S}$ with $0.001 < x < 0.005$. The first fact can be explained by low natural abundance of the ^{33}S isotope and the second – by a negligibly small cubic crystal-field acting in the positions of manganese spins $S = 5/2$ in the PbS lattice. Two satellite lines on each side of the hyperfine lines were registered in the samples with $x > 0.005$ when the internal magnetic field vector was parallel to the crystal axes (111) (Fig. 1). The same lines were observed by authors of the article [4] in the $\text{Pb}_{1-x}\text{Mn}_x\text{Te}$ samples and were interpreted as fine structure lines of cubic Mn^{2+} impurity centers being in the ^6S ground state. But angular dependencies obtained in our experiments speak about dynamic trigonal distortions of the crystal field acting in the positions of the manganese ions. Probably, these distortions arise due to an interaction of impurity ions with conduction electrons populating the energetic valleys at L points of the Brillouin zone.

Investigating the $\text{Pb}_{1-x}\text{Mn}_x\text{Te}$ samples with $x > 0.015$, in each case we observed a single broad unresolved line. Its line width was dependent on temperature and on content of manganese in the sample. These dependencies were analyzed and their nature considered.

The work was supported by Foundation for Basic Research (grant 12-02-31148).

1. Łusakowski A., Bogusławski P., Radzyński T.: Phys. Rev. B **72**, 035216 (2011)
2. Das R.K., Tripathi G.S., Misra P.K.: Phys. Rev. B **83**, 115206 (2011)
3. Story T., Swüste C.H.W., Eggenkamp P.J.T., Swagten H.J.M., de Jonge W.J.M.: Phys. Rev. Lett. **77**, 2802 (1996)
4. Lattenmayr H., Jantsch W., Palmetshofer L.: Solid State Commun. **64**, 1253 (1987)
5. Korczak S.Z., Korczak W., Subotowich M., Wasicwicz H.: Phys. Stat. Sol. B **153**, 361 (1980)

Light-Induced EPR Study of Charge Recombination in P3HT/PC70BM Composite

E. A. Lukina^{1,2}, A. G. Popov^{1,2}, M. N. Uvarov², and L. V. Kulik²

¹ Novosibirsk State University, Novosibirsk 630090, Russian Federation, kataluk@yandex.ru

² Institute of Chemical Kinetics and Combustion, Novosibirsk 630090, Russian Federation

This work is devoted to study of charge recombination in poly(3-hexylthiophene)/[6,6]-phenyl-C₇₁-butric acid methyl ester (P3HT/PC70BM) composite and comparison of the results with literature data about poly(3-hexylthiophene)/[6,6]-phenyl-C₆₁-butric acid methyl ester (P3HT/PC60BM). P3HT/PC70BM and P3HT/PC60BM composites are used as active layers in organic solar cells. It is known that charge recombination in P3HT/PC60BM composite is a complex process which can not be described by simple Langevin bimolecular recombination model. Much less is known about P3HT/PC70BM, although it is more effective in solar cells. Furthermore, light-induced EPR signal in P3HT/PC70BM can be observed at a room temperature. Thus the recombination in P3HT/PC70BM can be studied by light-induced EPR at the conditions, which are close to normal operating conditions of solar cell.

The film of P3HT/PC70BM composite (1:1 by weight) was cast from toluene solution and then annealed at 150 K for 10 min. Recombination order was determined from light-induced CW EPR signal intensity dependence on light intensity and from charge recombination kinetics. Results were explained using the model proposed in [1, 2] for P3HT/PC60BM composite. Bimolecular recombination is trap-limited and thermally activated delocalization of localized charge carriers is required for free charges recombination. In this case bimolecular recombination rate constant k depends from charge carrier concentration n . It is possible to assume $k = k_0 n^\beta$; β is strongly influenced by sample morphology [1].

Temperature dependence of recombination rate constant k_0 was measured at 80–300 K. At temperatures higher than 150 K the recombination activation energy was determined: $E_0 = 0.16 \pm 0.01$ eV. Presumably this value is determined by energies required for detrapping of a trapped charge carrier and for crossing the bound between donor and acceptor phases. At a temperature lower than 150 K k_0 is temperature independent, thus the tunneling is assumed.

The work was supported by RFBR grant №12-03-31190-mol-a.

1. Guo J., Ohkita H., Yokoya S., Benten H., Ito S.: J. Am. Chem. Soc. **132**, 9631 (2010)
2. Clarke T.M., Jamieson F.C., Durrant J.R.: J. Phys. Chem. **113**, 20934 (2009)

Abnormal Lines in EPR Spectra of Sportsmen's Serum Blood

**M. I. Ibragimova¹, A. I. Chushnikov¹, G. V. Cherepnev²,
V. Yu. Petukhov¹, and E. P. Zheglov¹**

¹ Zavoiisky Physical-Technical Institute, Russian Academy of Sciences, Kazan 420029,
Russian Federation, ibragimova@kfti.knc.ru

² Tatarstan Republic Clinical Hospital №2, Kazan 420043, Russian Federation,
rkb2_rt@mail.ru

As well known the standard EPR spectrum of human serum blood consists of signals from Fe^{3+} in transferrin, Cu^{2+} in ceruloplasmin and free radicals. The appearance of new signals in blood spectra allows detecting the subtle dysmetabolic deviation, and these signals can serve as diagnostic markers of various metabolic disorders. In this work we studied 26 blood serum samples collected from professional sportsmen using EPR in combination with hematological and biochemical laboratory tests. Only 23% of EPR spectra ($n = 6$) were practically normal while in the rest spectra the different types of abnormal absorption lines were detected. Presumably, the significant portion of new signals may be caused by different cytochromes. In particular, the part of them can be identified as signals from cytochrome c-oxidase. The appearance of these abnormal paramagnetic centers in serum might be caused by excessive muscular exercise and sports trauma, or the use of metabolically active substances. Moreover, it is known that the majority of cytochromes are harbored by cells with intense metabolism, *e.g.* myocytes and hepatocytes. Another anisotropic signal with $g_1 \cong 2.02$, $g_2 \cong 1.94$ and $g_3 \cong 1.86$ registered in 50% of EPR spectra (in ~25% cases concomitantly with cytochrome signals) was identified as a signal from sulfur-iron centers. This center can also indicate excessive muscular exercise and trauma. The presence of abnormal paramagnetic centers in blood of sportsmen correlates with increased levels of such (non-specific) enzyme as creatine kinase, high activity of which being common for traumatic lesions, intake of high doses of psychotropic drugs, and for any types of shock. However, further studies are required for determining the possible correlations between the EPR measurements and the biochemical data. It should be mentioned that the presence of cytochrome and sulfur-iron centers is not detectable by routine biochemical analyses. The results obtained point to a necessity for a more detailed study of sportsmen blood by EPR, since routine biochemical and hematological tests sometimes fail to detect subtle pathologic changes under intensive physical exercises.

The work is supported by RFFR Grant №13-02-97065.

EPR of Chromium Precipitates in BaF₂ Crystals

E. R. Zhiteytshev¹, R. R. Zainullin², A. M. Sinitsyn², and V. A. Ulanov^{1,2}

¹Zavoisky Physical-Technical Institute, Russian Academy of Sciences, Kazan 420029, Russian Federation, evg@kfti.knc.ru

²Kazan State Power Engineering University, Kazan 420066, Russian Federation, ulvlad@inbox.ru

The fluorite matrices doped with transition metals have been extensively studied in the last four decades. Now the interest in these crystals is due to their ability to accommodate large molar fractions of some impurities that form solid solutions within the fluorite structure. It is important that in most cases no incoherent precipitates have been detected. In such cases the X-ray diffraction data only show a distortion of the lattice whose sign and magnitude vary as a function of the ratio of the radii of the dopant to that of the host matrix.

In this work we studied a possibility to form chromium nanostructures in bodies of the BaF₂ crystals which characterized as the most accommodative matrices among the fluorite type crystals. Chromium impurity ions attracted our attention because of their orbitally degenerate ground state on cation sites in fluorite-type crystals. In such state an impurity center usually displays a strong static distortion due to the JT interaction of the ground state with vibrations of symmetry τ_{2g} and ϵ_g . If a concentration of the Jahn-Teller impurity ions is large enough, the incoherent precipitates can be formed in a crystalline matrix.

BaF₂ crystals used in these experiments as matrices were grown by the Bridgman technique in a helium atmosphere containing some quantity of fluorine gas. A graphite of high chemical purity was used as a material for crucibles. Chromium was introduced in the BaF₂ single crystals by diffusion from a crystal surface at temperatures $T = 1200\text{--}1300$ K. The EPR measurements were performed at X-band frequencies and $T = 4.2$ K. Practically isotropic EPR spectrum observed consisted of two very broad lines and had a powder-like outline. It was found by theoretical description of the EPR spectrum that in the BaF₂ crystalline matrices chromium impurity ions stimulated a formation of microscopic crystallites with low symmetry lattices. These paramagnetic crystallites are oriented randomly regarding to host lattice. Their magnetic properties and structures are discussed.

The present work was supported by Foundation for Basic Research (grant 12-02-31148).

Spin Dynamics of ZnTPP in Room-Temperature Ionic Liquids [bmim]PF₆ and [bmim]BF₄ Studied by Time-Resolved EPR

M. Ivanov, S. L. Veber, and M. V. Fedin

International Tomography Center, Novosibirsk State University, Novosibirsk 630090,
Russian Federation, michael.ivanov@tomo.ncs.ru

Room temperature ionic liquids (RTILs) have drawn a significant attention of scientific community during last few decades. This interest is caused by unique properties exhibited by RTILs on macro- and microscopic scales, including their thermo-stability, negligible vapor pressure, high viscosity and ability to form micro-ordered structures in supercooled state. One of the interesting applications of ILs concerns their influence on the formation of chemical induced electron polarization (CIDEP) in photo-excited triplet molecules and during photochemical reactions. Up to date, only one study of CIDEP in photo-excited triplet molecules in ILs using time-resolved electron paramagnetic resonance (TR EPR) has been reported [1].

In this work we have studied CIDEP of zinc tetraphenylporphyrin (ZnTPP) in two ILs ([bmim]PF₆ and [bmim]BF₄) of significantly different viscosity. It has been assumed that high micro-viscosity of IL should affect the rotational motion of ZnTPP and, consequently, the electron relaxation times between triplet sublevels. We used X-band (9 GHz) TR EPR as one of the most appropriate methods for studying spin dynamics of triplet molecules. The temperature dependence of micro-viscosity of [bmim]PF₆ and [bmim]BF₄ in the range of 230–294 K has been preliminarily studied by EPR of nitroxide spin probes. Inhomogeneous freezing and micro-structuring phenomena have been found in IL [bmim]PF₆. Remarkably, owing to the high viscosity of ILs used, the photo-excited triplet state of ZnTPP has been detected even at room temperature, in agreement with [1]. The detailed analysis of temperature-dependent TR EPR kinetics has been performed, which revealed crucial influence of micro-ordered structure of RTILs on the electron relaxation rates in photo-excited triplet ZnTPP.

1. Kawai A., Hidemori T., Shibuya K.: *Molecular Physics* **104**, no. 10-11, 1573–1579 (2006)

Quantum Phase Transition in Eu-Zn Pnictides on the ESR Date

Y. V. Goryunov¹ and A. N. Nateprov²

¹ Zavoiyskiy Physical-Technical Institute, Russian Academy of Sciences, Kazan 420029, Russian Federation, goryunov@kfti.knc.ru

² Institute of Applied Physics, Kishinev 2028, Moldova, nateprov@mail.md

Ternary Eu- and Yb-pnictides with CaAl_2Si_2 -type structures attract attention because of their unusual and very promising magnetic and thermoelectric properties. We have studied the magnetic properties of the $\text{EuZn}_2(\text{P, As, Sb})_2$ compounds by ESR (electron spin resonance) method. The ESR in powder samples was measured for X-band in TE_{102} rectangular cavity in the range from 4.2 to 300 K. Above 150 K we observed the symmetric resonance lines Eu^{2+} with ideal a Lorentzian lineshape. At the temperature decreasing well before the antiferromagnetic (AFM) ordering temperature T_N we have observed an increasing of linewidth δH and a decreasing of the resonance fields H_0 , which in our case very good described by Landau's theory of magnetic fluctuations with the contribution of type $(T-\theta)^{-1/2}$ ($\theta > 0$ and $\theta = T_N$ or $\theta = \theta_{\text{cw}}$ (θ_{cw} – Curie-Weiss temperature). At $T = \theta$ we observed singularity in behavior of H_0 and δH . Well known, that intensity of the ESR spectrum is proportional to magnetic susceptibility of a spin systems. The intensity of the ESR line changed with temperature in full corresponding to a typical temperature dependence of the susceptibility of an antiferromagnet. However, it should be emphasized that, unlike the typical for antiferromagnet negative paramagnetic Curie-Weiss temperature we obtained positive θ_{ESR} . This fact of positiveness paramagnetic Curie-Weiss temperature for the antiferromagnet is confirmed by direct measurements of the dc susceptibility. The obtained values of paramagnetic temperatures θ_{ESR} and θ_{cw} are quite close. For example, the Neel's temperatures T_N and paramagnetic Curie-Weiss temperatures from the ESR data θ_{ESR} for the EuZn_2Sb_2 : $T_N = 12.0$ K, $\theta_{\text{ESR}} = 1.9$ K, (DC measurement: $T_N = 13.3$ K, $\theta_{\text{cw}} = 6.65\text{--}8.8$ K weakly anisotropic antiferromagnetic state [1]). Fig. 1 demonstrates these temperatures T_N and θ_{cw} depending on composition of compounds using lattice constant as a tuning parameter. Similarly, the positive Curie-Weiss law for antiferromagnets have been observed for other compounds of europium with the same structure [2] and the ThCr_2Si_2 -type structure (for EuRh_2As_2 [3] $T_N = 47$ K and $\theta_{\text{cw}} = +12$ K.) According to the theory of spin fluctuations T. Moriya, the deviations of the susceptibility from an ideal Curie law $\chi = C/T$ are described by the Curie-Weiss law $\chi = C[T - \theta_{\text{cw}}]^{-1} = C[T - (\theta_{\text{mag}} - T_{\text{fluct}})]^{-1}$. Here, the Curie-Weiss temperature θ_{cw} is the difference between the valence fluctuation temperature $T_{\text{fluct}} > 0$, and θ_{mag} , presenting magnetic correlations; θ_{mag} , is usually negative for antiferromagnetic and positive for ferromagnetic order. Therefore, without valence fluctuation ($T_{\text{fluct}} = \hbar\nu = 0$, ν – frequency of fluctuations) the susceptibility is enhanced for ferromagnetism and reduced for antiferromagnetism. The valence fluctuation results in a reduction of the susceptibility.

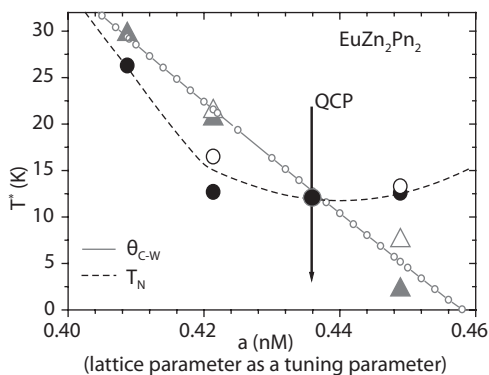


Fig. 1. Comparison of the behavior of the Curie temperature (triangles) and the Neel temperature (circles) with changing of the composition of the compounds indicate on the presence of quantum critical point in this ternary system.

As Fig. 1 shows spin fluctuations have the main influence on the paramagnetic Curie temperature for the defined composition of the investigated compounds and we observe the characteristic temperature of spin fluctuations is greater than the Neel temperature. This means that the system goes to special magnetic state at such compositions.

Thus, the above indicates that there is a special class of compounds of europium, in which the electronic instability leads to a new type of magnetic behavior and, consequently, to the possible existence of new magnetic phases and quantum phase transitions. Comparison of the behavior of the Curie temperature and the Neel temperature with changing of the composition of the compounds indicate on the presence of quantum critical point in this ternary system. In such behavior is seen a certain analogy of observed magnetic phase in pnictides system with the behavior of the A phase of MnSi, which associated with skyrmion phase.

1. Weber F., Cosceev A., Drobnik S., Faisst A. *et al.*: Phys. Rev. B **73**, 014427 (2006)
2. Schellenberg C.I., Pfannenschmidt U. *et al.*: Z. Anorg. Allg. Chem. **637**, 1863 (2011)
3. Michels G., Roepke M., Niemöller T. *et al.*: J. Phys.: Condens. Matter **8**, 4055 (1996)

The Dependence of 4-Styrylpyridine Photoisomerization on Wavelength Radiation and on the Solvent. UV, NMN, and DFT Studies

L. G. Gafiyatullin, L. I. Savostina, O. I. Gnezdilov, O. A. Turanova, I. V. Ovchinnikov, and A. N. Turanov

Zavoisky Physical-Technical Institute, Russian Academy of Sciences, Kazan 420029, Russian Federation, sasha_turanov@rambler.ru

There are intensive work on the synthesis of organic photochromic compounds to create photoswitchable devices at the present time. 4-Styrylpyridines are of interest as a photoisomerizing ligands having ethylenic groups in the structure [1]. Coordination compounds with paramagnetic metal ions, containing these ligands let to create new spin-crossover materials with photocontrollable magnetic properties [2].

At this study, the photoisomerization of 4-styrylpyridine has been investigated depending on the selection of photoirradiation wavelength ($\lambda = 365$ or 254 nm) and solvent by UV and ^1H NMR spectroscopy methods. The photoisomerization occurs by follows scheme: *trans*- \rightarrow *cis*- \rightarrow cycle A without the formation of dehydrated cyclic photoisomer B (benzo[h]isoquinoline) upon light irradiation with $\lambda = 365$ nm of 4-styrylpyridine organic solution (acetonitrile, hexane, chloroform, and liquid crystal). Upon light irradiation with $\lambda = 254$ nm of similar solutions, the result depends on the solvent: cyclic isomer A is formed in acetonitrile, cyclic isomer B is formed in hexane, a halogenation of ethylene bond occurs in chloroform, as a result of the solvent decomposition with formation of a new dichlorosubstituted product.

The recording technique of UV spectra of 4-styrylpyridine dissolved in liquid-crystalline films on the frame with free surfaces has been suggested.

The DFT calculations results of optimal conformation of investigated molecules, their energy, electron density, and the UV absorption spectra, which correlate well with the experimental data, has been presented. The obtained information will be useful in selection of synthetic strategy of photocontrollable magneto-optical coordination compounds with photoisomerized 4-styrylpyridine as ligands.

The work was supported by RFBR (grant №12-03-97090-r)

1. Bradamante S., Facchetti A., Pagani G.A.: J. Phys. Org. Chem. **10**, 514 (1997)
2. Boillot M.-L., Zarembowich A.: Sour in "Spin Crossover in Transition Metal Compounds" (Gutlich P., Goodwin H.A., eds.), V. II, p. 261. Springer, 2004.

FMR Investigation of Iron Silicide Films Ion Beam Synthesized in Magnetic Field

**G. G. Gumarov, A. V. Alekseev, M. M. Bakirov,
V. Yu. Petukhov, and V. F. Valeev**

Zavoisky Physical-Technical Institute, Kazan 420029, Russian Federation
gumarov@kfti.knc.ru

The modification of magnetic properties in thin films by ion irradiation is especially useful as it can be used to locally alter magnetic properties like saturation magnetization, magnetic anisotropy and etc. Earlier we used magnetic-field-assisted ion-beam synthesis to produce thin films of ferromagnetic silicide Fe_3Si in single-crystal silicon substrates [1]. It was shown that application of the magnetic field during the high-dose Fe ion implantation led to the pronounced in-plane magnetic anisotropy in the synthesized films. The goal of the present work is to investigate the magnetic properties of ion-beam synthesized thin iron silicide films using the method of ferromagnetic resonance.

The FMR signal is found to be dependent on the film orientation in the magnetic field similar to that found for the FMR in thin magnetic films. It was revealed that FMR line for anisotropic samples considerably narrower than for isotropic ones. Moreover the nonmonotonic temperature dependence of FMR linewidth was observed both for isotropic and anisotropic samples (Fig. 1). Such dependence is explained on the basis of model of magnetic resonance in an assembly of single-domain uniaxially anisotropic particles [2]. As the temperature rises, the orientational fluctuations of the magnetic moment weaken the inhomogeneous broadening of the FMR line arising from the distribution in the

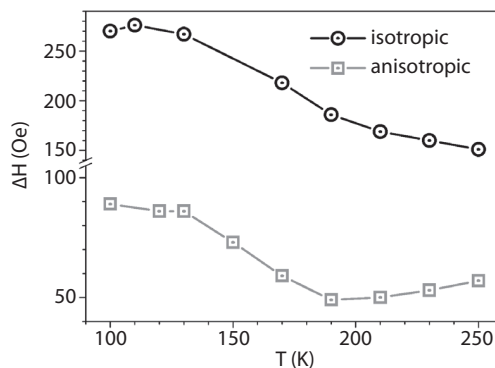


Fig. 1. Temperature dependence of FMR linewidth for isotropic and anisotropic samples.

directions of anisotropy axes of the particles. The origins of the differences in the linewidth for the isotropic and anisotropic samples are discussed.

The work was supported by grant of Nanotechnology and Information Technology Division of RAS №3, project №1.12 and grant of Physical Sciences Department of RAS II.5, project B24.

1. Gumarov G.G. *et al.*: Nucl. Instr. Meth. Phys. Res. B **267**, 1600 (2009)
2. Raikher Yu.L., Stepanov V.I.: Sov. Phys. JETP **75**, 764 (1992)

Unusual Anisotropy of the $\{g\}$ -Tensor in Dimer Dysprosium (III) Complex. EPR Study

**R. T. Galeev¹, A. A. Sukhanov¹, R. M. Eremina¹, V. K. Voronkova¹,
A. Baniodeh², and A. K. Powell²**

¹Zavoisky Physical-Technical Institute, Russian Academy of Sciences,
Kazan 420029, Russian Federation

²Karlsruhe Institute of Technology, University of Karlsruhe, Karlsruhe D-76131, Germany

Complexes containing dysprosium ions attracted interest as perspective candidates for the synthesis of new SMMs because of the large single-ion magnetic anisotropies. There are examples of dysprosium compounds showing SMM behavior [1, 2].

In this report we present EPR study compound consist of Dy-Dy dimers. Dysprosium ions have low symmetry, nine-coordinate surroundings. The EPR measurements were made on a Bruker EMX/plus spectrometer equipped ER4102ST X-band resonator and a 4116DM dual mode resonator and on Bruker Elexsys E-580 in Q-band. We carried out measurements of the temperature dependence of EPR spectra from 4 to 290 K and the numerical calculations of the EPR spectra for X- and Q-bands. Simulations allow us to find the spin-Hamiltonian parameters. For anisotropy of g -factor of the ground states of dysprosium ions unusual values were obtained.

Calculations of the crystalline field with consideration of the nearest environment of dysprosium ions have shown that this anisotropy can be due to the varying of the electron density on the ligands.

This research is supported in part by the Russian Foundation for Basic Research (project no. 13-02-01157) and the President of the Russian Federation (grant no. NSh-5602.2012).

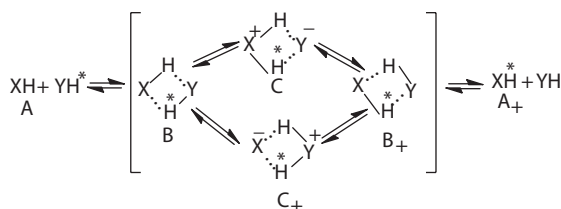
1. Ishikawa N.: Polyhedron **26**, 2147 (2007)
2. Feltham H.L.C., Lan Y., Klöwer F., Ungur L., Chibotaru L.F., Powell A.K., Brooker S.: Chem. Eur. J. **17**, 4362 (2011)

The Kinetic EPR Spectroscopy of Diamines Protolytic Reactions

A. S. Masalimov, A. A. Tur, and S. N. Nikolskiy

Chemical Department, Karaganda State University, Karaganda 100028,
Republic of Kazakhstan, masalimov-as@mail.ru

The stable semiquinone radical 3,6-di-tert.buthyl-2-oxyphenoxyl (XH) was used as acid spin probe for EPR-spectroscopic determination the rate constants of the fast intermolecular proton exchange (IPE) reactions with different diamines (YH) in toluene medium. In the scheme of IPE reaction H* indicates the acid proton with inverted nuclear spin.



The experimental data presented in Table 1 show that diamines have two times more values of IPE rate constants than diethylamine, containing only one NH-acid proton. But the existence of the second NH₂-group in diamines brings to increasing activation energy of IPE reactions in comparison with diethylamine. Probably, the second NH₂-group of diamines makes the process of IPE reactions intermediate B and B₊ formation. At low temperatures proceed the deceleration of IPE reaction and in system XH-diamine go only protonation with formation of ionic pair C₊. This ionic pair can associate to a dimer in toluene solutions. The specific geometry of protonated hexamethyldiamine brings to formation of the chelate molecular structure in corresponding ionic pair C₊.

Figure 1 shows the evolution of acid-base interaction in the protolytic system XH-PEI at different temperatures. Triplet of doublets **a** is the EPR spectra of semiquinone spin probe XH at 293 K. Protonation of PEI with XH gives an ionic pair

Table 1. Kinetic parameters of the fast IPE-reactions between radical XH and different diamines in toluene solutions.

No	Diamines	k_{ex} (293 K) (l/mol·c)	E_a (kJ/mol)
1	diethylamine	$(3.1 \pm 0.7) \cdot 10^9$	4.0 ± 0.4
2	ethyldiamine	$(6.8 \pm 0.1) \cdot 10^9$	10.4 ± 0.2
3	2,3-diaminobutane	$(6.1 \pm 0.1) \cdot 10^9$	9.8 ± 0.8
4	hexamethyldiamine	$(7.2 \pm 0.1) \cdot 10^9$	8.7 ± 0.9

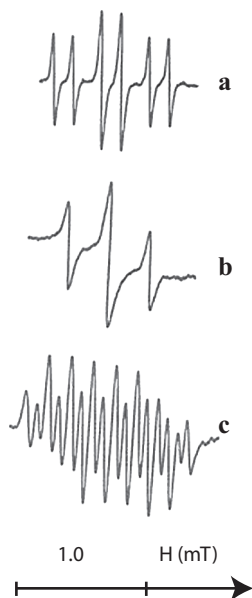


Fig. 1. The EPR spectra of chelate structure with hyperfine splitting of two nitrogens atomic nucleus take place also in reactional system XH and polyethyleneimine (PEI).

C_+ which was described with triplet **b** at 253 K. The proton separation from XH involves disappearance of the hydroxylic hyperfine splitting in EPR spectra **a** of semiquinone radical. Triplet **b** form by hyperfine interaction of unpaired electron with two benzene rings protons of 3,6-di-tert.buthyl-orthosemiquinones anion-radical. The EPR-spectra **c** indicates formation of the chelate in system XH-PEI at room temperature.

EPR Study of Nitric Oxide Production in Heart and Spinal Cord of Rats under Hypokinesia and Condition of Spinal Cord Injury

**Kh. L. Gainutdinov^{1,2}, V. V. Andrianov^{1,2}, V. S. Iyudin¹,
I. I. Shaikhutdinov³, F. G. Sitdikov², R. F. Tumakaev³, G. G. Yafarova^{1,2,3},
R. Kh. Yagudin³, R. I. Zaripova², and T. L. Zefirov²**

¹ Zavoisky Physical-Technical Institute, Russian Academy of Sciences, Kazan 420029, Russian Federation, kh_gainutdinov@mail.ru

² Kazan Federal University, Kazan 420008, Russian Federation

³ Republican Clinical Hospital of the Tatarstan Republic, Kazan 420064, Russian Federation

Nitric oxide (NO) is known to be an important signaling molecule modulating the physiological functions of the organism and the cell metabolism. The literature provides evidence of two opposing modes of NO influence on the physiology of various tissues: (1) positive, stimulatory, versus (2) toxic, damaging action that may lead to cell death [1]. Hence it can be asserted that the “sign” of effect depends on the amount of NO, yet it is not clear what amounts should be regarded as low, normal, or elevated. A very topical medico-social problem is hypokinesia/hypodynamia, associated with the way of life, occupation, prolonged inactivity caused by illness, etc. Hypokinesia (HK) incurs reduced load on the musculature, leading to alteration of tissue function and morphology, up to pathological states depending on its duration and degree [2]. So problems arise also under a spinal pathology. In this context, here we assessed the changes in NO production in the tissues of rats grown under restrained motility and after spinal cord injury.

Experiments were carried out on little outbred albino rats. The animals were divided into 2 groups (10 per group), control and experimental. Controls were kept under standard vivarium conditions. Experimental animals were subjected to 30-day HK. Exposure to HK started from the age of 21 days. By day 25 of HK, the animals spent 23 h in penal cages every day and the duration of ex-

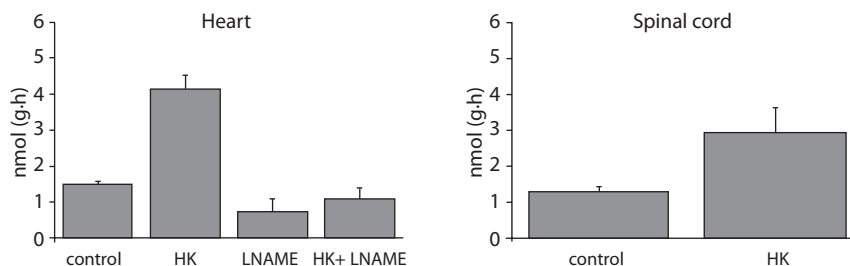


Fig. 1. Changes in NO production in heart and spinal cord tissues in rats subjected to 30-day HK and effect of NOS inhibitor L-NAME on the NO content in rat heart tissue, control and after 30-day HK.

posure remained unchanged until the end of the experiment. The levels of NO were measured in heart and spinal cord tissues. The samples for measurements of EPR spectra were prepared for measurements by the spin trap method, detecting NO in low concentrations [3]. Exposure of rats to HK for 30 days led to a 3-fold increase of NO content in the heart and 2-fold increase in spinal cord tissues (Fig. 1). It should be admitted that the model used here does not allow explicitly distinguishing the NO related effects of HK proper and those of the attending immobilization stress (though the latter was unlikely to be dramatic in gradual adaptation at young age). In terms of 3–7 days after spinal cord injury we observed the increase of NO production in spinal cord in 3 times more than the level of control.

As shown in the brain, NO is continuously produced from arginine by constitutive NO synthases (NOS). However, NO can be produced in the body via another pathway involving nitrite reductase. In order to discern the origin of surplus NO in HK, we used a nonspecific NOS inhibitor L-NAME. As evident from Fig. 1, administration of L-NAME to rats upon 30-day HK and not long before measurements decreased the amount of NO trapped in heart tissue to a level even lower than that in untreated controls but not significantly different from L-NAME treated controls.

The financial support of the Foundation for Basic Research (grant 12-04-97035_r_Povolj'e_a) is gratefully acknowledged.

1. Boehning D., Snyder S.H.: *Annu. Rev. Neurosci.* **26**, 105 (2003)
2. Kozlovskaya I.B., Kirenskaya A.V.: *Rus. Fiziol. Zh.* **89**, 247 (2003)
3. Mikoyan V.D., Kubrina L.N., Serezhnikov V.A. *et al.*: *Biochim. Biophys. Acta* **1336**, no. 2, 225–234 (1997)

ESR Study of Critical Fluctuations at N-Sa Phase Transition

B. M. Khasanov

Institute of Physics, Kazan Federal University, Kazan 420008, Russian Federation,
bulat.khasanov@ksu.ru

Magnetic resonance relaxation experiments have been very useful in the study of the dynamical properties of liquid crystals. Pretransitional effects which are manifested as critical anomalies in relaxation measurements, are caused by long-rang cooperative modes, associated with the quasicritical fluctuations in the ordering at phase transitions.

Several electron spin resonance (ESR) relaxation studies at nematic-isotropic (N-I), and nematic-smectic A (N-Sa) phase transitions were performed using different nitroxide spin probes dissolved in *nO.m* homologous liquid crystal series [1, 2, 3]. The ESR spectra were motionally narrowed. This permits a linewidth analysis as a function of the ^{14}N nuclear spin quantum number m , $T_2^{-1} = A + Bm + Cm$. Critical type divergences were observed at N-I and N-Sa transitions for all the hyperfine lines.

The fluctuations in the nematic order parameter can result in a slowly fluctuating orientational potential at the site of the probe molecule, thus modulating the rotational reorientation of the probe. Such modulations lead to anomalous effects in spin relaxation and divergences for the hyperfine lines [1]. Near the N-Sa phase transition ESR probes typically undergo partial expulsion from the orientationally well ordered aromatic cores of the liquid crystal molecules toward less ordered aliphatic regions. The formation of smectic clusters is described by density fluctuations and the movement of the probe molecules affects the order parameter and rotational correlation time of the probe. Thus density fluctuations modulate the molecular dynamics and spin relaxation of the probe [2].

However, the P-probe (2,2',6,6'-tetramethyl 4-(butyloxy) benzylamino-piperidine N-oxide), which is similar in structure to a liquid crystal molecule and exhibits the ordering and dynamics similar to that expected for the host molecules do not expelled from core region. The observation of significant divergences for the P-probe in 7O.5 liquid crystal with a very narrow ($\sim 4\text{C}$) nematic range, suggests that the direct coupling between orientational and positional order parameters can play a significant role when the orientational order parameter is not saturated.

In a smectic *A* phase molecules are arranged in a one dimensional periodic structure. For a monolayer phase the molecular length gives the period of the one dimensional mass density wave $\rho(z) = \rho_0(1 + |\psi|\cos 2\pi z/d)$, where ρ_0 – is the average density, d – its periodicity, $|\psi|$ is the amplitude of the complex smectic order parameter. The coupling term of the nematic order parameter to the smectic order parameter of the type $s\psi^2$, as well as a Gauss approximation $\chi^{-1}s^2$ term are included in free energy expression. In the Landau mean field theory the susceptibility χ diverges near N-I phase transition. This term permits

larger deviations in s from its equilibrium value near the N-I transition than deeper into the nematic phase. However, here we predict the increase in χ also close to N-Sa transition, which is due to above nematic-smectic coupling and strong smectic order parameter fluctuations. We call it reentrant enhancement of orientational susceptibility, that is, a universal behavior of the non-order parameter orientational field near the N-Sa phase transition. We show that the inverse nematic susceptibility develops a finite drop near the N-Sa transition and lead to the rather strong divergence in B and C parameters in the linewidth. Thus our predictions seem to reproduce well the general features of experimental data [3] when the former, expulsion model, do not play a role in influencing relaxation near the N-Sa transition.

1. Nayeem A., Rananavare S.B., Sastry V.S.S., Freed J.H.: J. Chem. Phys. **96**, 3912 (1992)
2. Zager S.A., Freed J.H.: Chem. Phys. Lett. **109**, 270 (1984)
3. Rananavare S.B., Pisipati V.G.K.M., Freed J.H.: Liquid Crystals **3**, 957 (1988)

Electron Spin Resonance in Thin Film $\text{GdMnO}_3/\text{SrTiO}_3$

**T. P. Gavrilova¹, I. V. Yatsyk¹, R. M. Eremina¹, D. V. Mamedov²,
I. I. Fazlizhanov¹, A. A. Rodionov², V. I. Chichkov³,
N. V. Andreev³, and Ya. M. Mukovskii³**

¹Zavoisky Physical-Technical Institute, Russian Academy of Sciences, Kazan 420029, Russian Federation, tapa_left@mail.ru

²Kazan (Volga Region) Federal University, Kazan 420008, Russian Federation

³National University of Science and Technology MISiS, Moscow 119049, Russian Federation

We studied the magnetic properties of GdMnO_3 thin films of thickness about 100 nm deposited onto the SrTiO_3 substrates using the electron paramagnetic resonance technique. EPR measurements in thin film $\text{GdMnO}_3/\text{SrTiO}_3$ were performed at 9.4 GHz frequencies. The EPR spectrum of a GdMnO_3 single crystal consists of only one broad exchange narrowed line [1], unusual magnetism is observed at the interface between the GdMnO_3 thin film and substrates SrTiO_3 . ESR spectra in GdMnO_3 single crystal, $\text{GdMnO}_3/\text{LaAlO}_3$ thin film, $\text{GdMnO}_3/\text{SrTiO}_3$ thin film in X-band are presented in Fig. 1. The EPR spectrum of the single crystal GdMnO_3 in X-band consists from one exchange narrowed line with $g \sim 2$ (Fig. 1, curve 1). The EPR spectrum of $\text{GdMnO}_3/\text{LaAlO}_3$ thin film consists from Gd^{3+} fine structure (Fig. 2, curve 2) [1] and the thin film $\text{GdMnO}_3/\text{SrTiO}_3$ – both exchange narrowed line and Gd^{3+} fine structure (Fig. 2, curve 3).

The temperature dependence of the EPR spectra in $\text{GdMnO}_3/\text{SrTiO}_3$ is presented in Fig. 2. With increasing the temperature from 200 to 340 K the intensity of the fine-structure line $|7/2\rangle \rightarrow \langle 5/2|$ decreases and at 350 K almost disappears. Of the observed the linewidth at $g \sim 2$ ($\Delta H \approx 340$ Oe) is narrower

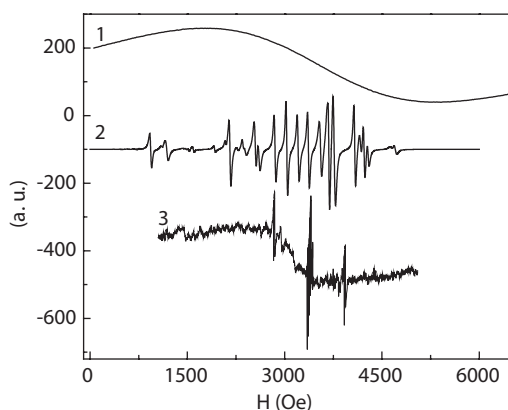


Fig. 1. Electron paramagnetic resonance spectrum in the X-band at $T = 300$ K for: 1, GdMnO_3 single crystal; 2, $\text{GdMnO}_3/\text{LaAlO}_3$ thin film; 3, $\text{GdMnO}_3/\text{SrTiO}_3$ thin film.

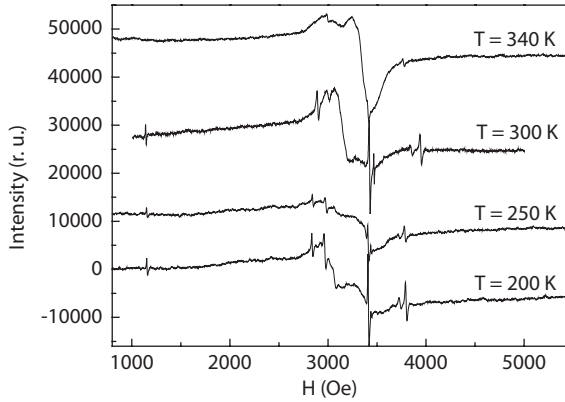


Fig. 2. The temperature dependency of the EPR spectra in $\text{GdMnO}_3/\text{SrTiO}_3$.

than in the single crystal GdMnO_3 ($\Delta H \approx 2700$ Oe), but wider than the lines of the fine structure of the Gd^{3+} ($\Delta H \approx 40$ Oe).

The angular dependence of the electron paramagnetic resonance spectrum in thin film $\text{GdMnO}_3/\text{SrTiO}_3$ in X-band at $T = 300$ K is presented in Fig. 3. The paramagnetic Gd^{3+} has the electron configuration $4f^7$ and belongs to the $^8S_{7/2}$ state. The combined effect of the spin-orbit interaction, crystal field, and

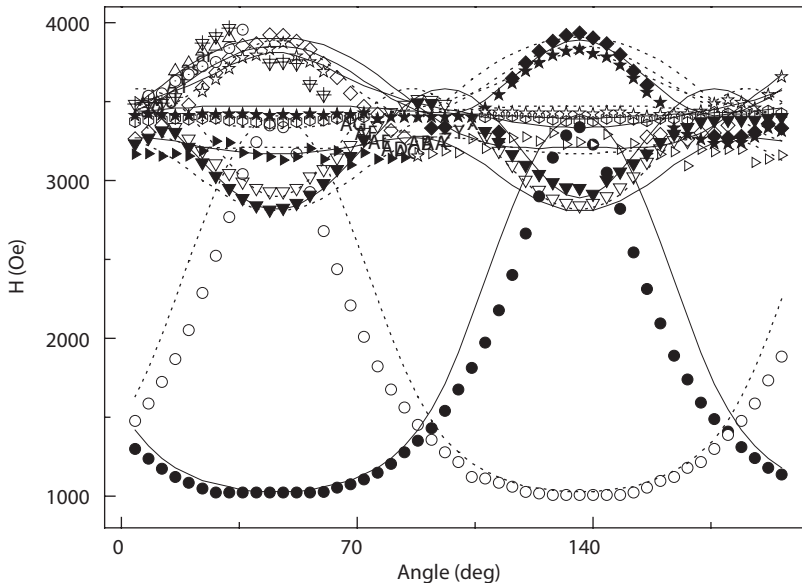


Fig. 3. The angular dependence of the EPR spectrum in thin film $\text{GdMnO}_3/\text{SrTiO}_3$ in X-band at $T = 300$ K.

magnetic dipole-dipole interaction between $4f$ electrons leads to the splitting of the 8S state, which is described by the spin Hamiltonian [2]:

$$H_{\text{cr}} = \frac{1}{3} \sum_m (b_2^m O_2^m + c_2^m \Omega_2^m) + \frac{1}{60} \sum_m (b_4^m O_4^m + c_4^m \Omega_4^m) + \frac{1}{1260} \sum_m (b_6^m O_6^m + c_6^m \Omega_6^m),$$

where b_n^m and c_n^m are the parameters characterizing the fine structure and O_n^m and Ω_n^m are the spin Stevens operators. The fine structure parameters for the paramagnetic center with the monoclinic symmetry corresponding to the gadolinium ion, which are determined by the analysis of the angular dependence for the resonance values of the applied magnetic field for the EPR spectra measured at room temperature in the X-band, and have the following values (in units of 10^{-4} cm^{-1}): $c_2^2 = -132$; $c_4^2 = -12.5$; $c_4^4 = -38$; $c_6^6 = -1$; $b_2^0 = -22$; $b_2^2 = 94$; $b_4^0 = 12.5$; $b_4^2 = 12$; $b_4^4 = 90$; $b_6^0 = -24$; $b_6^2 = -2$; $b_6^4 = 4$; $b_6^6 = 10$; $g_x = 1.99$, and $g_z = 1.98$. We took into account that there exist two types of paramagnetic centers with the axes directed at an angle of 90° with respect to each other.

1. Yatsyk I.V., Mamedov D.V., Fazlizhanov I.I. *et al.*: JETP Lett. **96**, 416 (2012)
2. Al'tshuler S.A., Kozyrev B.M.: Electron Paramagnetic Resonance in Compounds of Transition Elements. Moscow, Nauka, 1972; New York, Halsted, 1975.

Electron Spin Echo of Light-Induced Spin Correlated Radical Pairs in PCBM/P3HT Composite

A. A. Popov¹ and **L. V. Kulik²**

¹ Novosibirsk State University, Novosibirsk 630090, Russian Federation, rastopyakin@gmail.com

² Institute of Chemical Kinetics and Combustion, Novosibirsk 630090, Russian Federation, chemphy@kinetics.nsc.ru

The composite of [6,6]-phenyl C₆₁ butyric acid methyl ester (PCBM) and poly(3-hexylthiophene) (P3HT) is a perspective material for active layer of organic solar cells. After light absorption the charge transfer occurs in this material with quantum yield close to unity. Short-living spin-correlated radical pairs PCBM⁻/P3HT⁺ are formed [1], which can be further separated to free charge carriers.

In this work the spin dynamics of photoinduced radicals PCBM⁻ and P3HT⁺ was studied by pulse EPR spectroscopy (also called Electron Spin Echo or ESE). The radicals were generated by laser flashes with 532 nm wavelength. Two-pulse sequence $\pi/2-t-\pi$ -echo was used to perform ESE experiment.

Computer modeling of ESE signal allows to interpret experimental data and to estimate parameters of spin Hamiltonian of photoinduced radical pairs. For laser flash-generated radical pairs PCBM⁻/P3HT⁺ the temporal shape of ESE signal is quite unusual, but it is well reproduced in numerical calculation based on the model of spin-correlated radical pairs.

Calculations were performed using a density matrix formalism on the assumption of absence of any interaction between species in radical pair except for exchange interaction. Averaging over spectral positions and spatial orientation of both species in radical pair were executed by Monte Carlo procedure.

The strength of exchange interaction in photoinduced radical pair PCBM⁻/P3HT⁺ was estimated during computer modeling of the experimental ESE signal. The average magnitude of exchange interaction was approximately 1 MHz. Also it was normally distributed with distribution width approximately equal to 0.5 MHz.

1. Behrends J., Sperlich A., Schnegg R. *et al.*: Phys. Rev. B. **85**, 125206 (2012)

The Synthesis, EPR and Magnetic Properties of Fe(III) Complexes with Tetradentate N₂O₂ Donating Schiff-Base Ligand Bridged by Pirazine

**T. A. Ivanova¹, L.V. Mingalieva¹, I. V. Ovchinnikov¹, I. F. Gilmutdinov²,
O. A. Turanova¹, and G. I. Ivanova¹**

¹ Zavoiisky Physical-Technical Institute, Russian Academy of Sciences, Kazan 420029,
Russian Federation, alex@kfti.knc.ru

² Kazan Federal University, Kazan, Russian Federation

Iron (III) complexes bridged by pirazine $[\text{Fe}(\text{Salen})(\text{Pyr})_n]\text{BPh}_4$, where Salen = N,N'-ethylenebis(salicylideneamine), Pyr = pyrazine, BPh_4 = tetraphenylborate, have been prepared and investigated by means of the temperature dependent (4–290 K) EPR spectroscopy and magnetic susceptibility. The integrated intensity of the EPR spectra has a complex nonmonotonic temperature dependence (Fig. 1.) It has been interpreted in assumption that the Fe^{3+} ions are connected by pyr molecules, have antiferromagnetic interaction and form antiferromagnetic chains and binuclear complexes. The fine structure in the EPR spectra appears at the temperatures below 50 K (Fig. 2). It is caused by transitions between energy levels in the multiplets with $S = 3, 2, 1$ of dimers $\text{Fe}^{3+}\text{-Fe}^{3+}$ with $S = 5/2$. The temperature dependence of the magnetic susceptibility is in agreement with the results obtained from the analysis of the integrated intensity of the EPR spectra. Detection of the magnetization hysteresis in a low temperature range and the

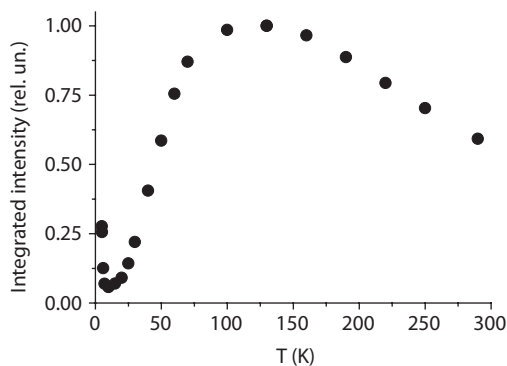


Fig. 1. The temperature dependence of the integrated intensity of the EPR spectra of $[\text{Fe}(\text{Salen})(\text{Pyr})_n]\text{BPh}_4$.

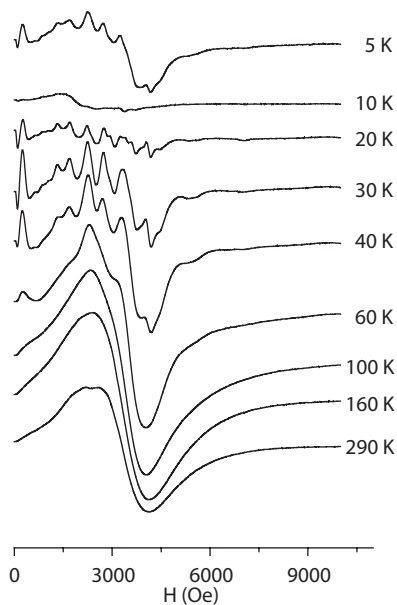


Fig. 2. The EPR spectra of $[\text{Fe}(\text{Salen})(\text{Pyr})_n]\text{BPh}_4$; $\nu = 9.3$ GHz.

difference of magnetization measured in FS and ZFS modes indicate that the studied compound has a weak ferromagnetism at liquid helium temperatures. This feature is in accordance with the integrated intensity of the ESR spectrum increasing below 10 K.

The work was supported by RFBR (grant №12-03-97090-r)

EPR Investigation of Cu (II) Complexes with Hyperbranched Polyesterpolyols Modified by Amines

**S. V. Yurtaeva¹, I. V. Ovchinnikov¹, M. P. Kutyreva², A. R. Gataulina²,
N. A. Ulakhovich², and V. I. Muravyev²**

¹ Zavoiisky Physical-Technical Institute, Russian Academy of Sciences, Kazan 420029,
Russian Federation, yurtaeva@mail.knc.ru

² Department of Inorganic Chemistry, Butlerov Institute of Chemistry, Kazan (Volga Region) Federal
University, Kazan 420008, Russian Federation, Marianna.Kutyreva@ksu.ru

Hyperbranched polyesterpolyols (HBPP) are the new class of multifunctional platforms which demonstrate their biological activity. The availability of ester fragments and biological similarity of structure course their low toxicity. Such characteristics make them attractive for future applications as drug platforms. The present research concerns the investigation of new synthesized complexes of polyesterpolyamines with Cu(II) ions. The aim of the research was to define Cu(II) coordination and probable localization of Cu(II) in polymer structure and to analyze the influence of geometry and composition of Cu(II) coordination site on the biological activity of synthesized complexes.

The second and third generation polymers HBPP H-20, H-30 (Fig. 1) modified by amine reagents were studied. Complexes of Cu(II) with HBPP H-20 platform modified by six reagents (3-(Dimethylamino)-1-propylamine, (3-Aminopropyl) triethoxysilane, N-(2-aminoethyl)-3-aminopropyltrimethoxysilane, Diethylamine, Ethylenediamine (1,2-Diaminoethane) and complexes of Cu(II) with HBPP H-30 modified by two reagents (Diethylamine and 3-(Diethylamino)propylamine) were synthesized and investigated by EPR.

When constructing the model of copper coordination site in polyesterpolyols the question arises of a number of nitrogen and oxygen atoms coordinating copper ion. IR-investigations of the synthesized copper metal-polymer complexes showed that in complexation of the majority complexes nitrogen atoms of aminogroups are present. To estimate the geometry and composition of copper site in polyesterpolyamines in details the electron paramagnetic resonance (EPR) spectroscopy and UV-Vis optic spectroscopy were used. By means of EPR and UV-Vis spectroscopy the concentrated samples of polyesterpolyamines with Cu(II) ions (powders and resins) and 1% and 0.1% solutions in DMSO were studied.

The EPR spectra of the majority of the concentrated samples demonstrated the presence of copper clusters. The EPR spectra of solutions constituted of signals corresponding to isolated copper paramagnetic centers. In polymer platforms modified by Diethylamine the clusters were not formed. The EPR spectra of isolated copper centers were described by spin Hamiltonian with axial symmetry.

The parameters of Cu(II) hyperfine interactions (HFI) were evaluated from the EPR spectra. The models of composition and structure of copper complexation sites based on the coordination in elongated octahedral were proposed. Cu (II) sites composition in different complexes were defined as CuO_4L_2 , $\text{CuN}_2\text{O}_2\text{L}_2$,

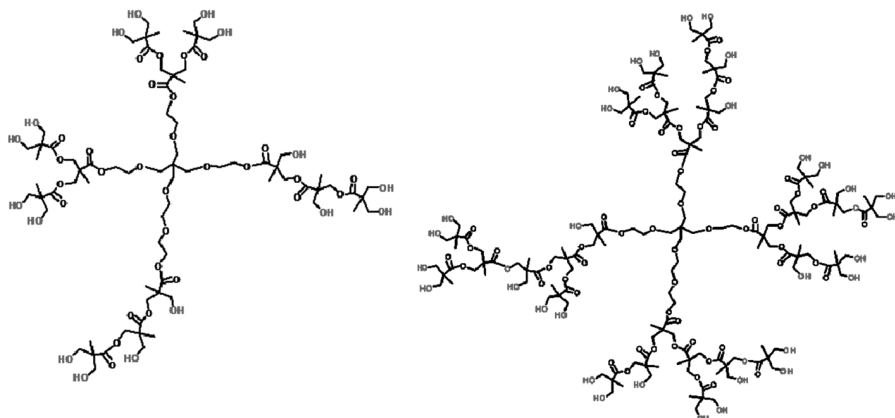


Fig. 1. The structure of hyperbranched polyesterpolyols H-20 and H-30 of the second and third generations.

CuN_4L_2 ($\text{L} = \text{H}_2\text{O}$, DMCO). It was determined that the majority of coordination sites is characterized by rotational isomerization.

UV-Visible optic spectra were studied for the solutions of all types of Cu(II) -HBPP complexes. Copper titration curves were also studied for different values of HBPP: metal ratio. UV-Visible spectra also demonstrated the manifestation of special features of copper coordination. Obtained EPR data correlate with the data of UV-Vis spectroscopy.

All the synthesized and investigated complexes demonstrated the biological activity to *Aspergillus* and *Candida albicans* cultures. The study found the correlation between the values of HFI parameter A_{\parallel} and the level of biological activity estimated as the percent amount of suppressed cell culture in the presence of copper HBPP complexes. Correlation between biologic activity and HFI parameter A_{\parallel} was estimated as -0.92 . It is supposed that biological activity of Cu(II) -HBPP complexes depends on equatorial ligand rotation.

Electron Magnetic Resonance in Biological Systems

S. V. Yurtaeva¹ and V. N. Efimov²

¹ Zavoisky Physical-Technical Institute, Russian Academy of Sciences, Kazan 420029, Russian Federation, yurtaeva@mail.knc.ru

² Institute of Physics, KFU, Kazan 420008, Russian Federation, vefimov.51@mail.ru

Up to recently many experimental facts of observation of electron magnetic resonance (EMR) signals in biological systems are accumulated in scientific literature. The wide anisotropic signals were detected for the first time in the late 1950's and early 1960's in DNA samples. Lately such signals were observed in cultures of synchronized dividing cells, in samples of magnetotactic bacteria, in tissues in which the organs of navigation and magnetoreception locate in insects (bees, ants, termites), birds and fish, in mammal and human tissues (nerve tissues and brain, heart, liver, placenta, blood etc.) in extracted DNA samples, in culture of cancer cells, in tumor tissues and others.

Up to now the origin of such signals is not known exactly and the nature of such signals is not quite clear despite of heated discussions. The data about EMR in such biosystems are dispersed and rather uncomplete, but the understanding of the origin of these signals is very important for many medical-biological problems such as the understanding of the molecular mechanisms of brain functioning, the origin of neurodegenerative transformations, the mechanisms of different pathologies of different tissues and mechanisms of cell division.

Magnetic resonance characteristics of such signals are widely investigated only in magnetotactic bacteria. It is known the origin of the signal: the chains of interacting magnetite nanoparticles of 20–150 nm size. TEM microscopic images were obtained. Concerning the other systems listed before the scientific discussion is being continued.

Previously we have conducted the investigation of EMR signals characteristics for the samples of human tumors [2] and nervous tissues in laboratory models [3]. Our research data and literature data allowed us to determine the following characteristics of the signals.

1) One or two line components with g -value higher than 2.1 of symmetric or asymmetric Lorentz shape (in different temperature intervals) are usually observed.

2) Characteristic nonmonotonic behavior of temperature dependencies of resonance field (H_{res}), linewidth (ΔH) and integral intensity (I) with maximum for H_{res} , I and local minimum for ΔH near the temperatures 120–130 K is observed.

3) Anisotropic behavior of H_{res} of EMR signals was detected, which is character for ferrimagnetic resonance of magnetite crystals and which disappears near 130 K.

4) The correlations between the temperature behavior of the $H_{\text{res}}(T)$ and $\Delta H(T)$ and temperature dependence of magnetocrystalline constant $|K_1|$ in magnetite are detected. To our opinion all the enumerated characteristics correspond to crystalline magnetite characteristics.

Except for the referred signals with g about 2.1, sometimes rather wide EMR signals with g about 5 and very intensive zero field signals are observed.

It is determined that EMR characteristics in different tissues and cells are very similar to the characteristics of the signals in the samples of extracted DNA [4]. Coincidence of EMR characteristics for very different biologic systems allows us to suppose, that there is any universal phenomenon in all these cases.

Till nowadays there are heated discussions about the interpretation of wide EMR signals in the literature. But there is not the only one point of view about this question. There are two schools with different opinions. On the one hand there are many facts demonstrating that EMR signals are from magnetic impurities of biogenic magnetite, produced in the process of biomineralization in living systems [5], but on the other hand, magnetism of biological systems may be connected with the intrinsic structural characteristics of DNA, in which mesoscopic ring currents occur, that may produce magnetic moments and lead to resonant microwave absorption [6]. Moreover there are experimental data demonstrating the feasibility of synthesis of ordered arrays of iron oxide nanoparticles using DNA [7].

The present report represents a review of experimental results in EMR investigation of biological systems. The main approaches in interpretation of the results are also discussed.

1. Fischer H., Mastrogiacomo *et al.*: Earth and Planetary Science Letters **270**, 200–208 (2008)
2. Yurtaeva S.V., Efimov V.N., Silkin N.I. *et al.*: Appl. Magn. Res. **42**, no. 2 (2012)
3. Yurtaeva S.V., Efimov V.N., Iyudin V.S. *et al.*: KFTI Annual. 29–33 (2013) (in Russian)
4. Omerzu A., Anzelak B. *et al.*: Phys. Rev. Lett. **104**, 156804(1–4) (2010)
5. Kirschvink J.L. *et al.*: Magnetite Biomineralization and Magnetoreception in Organisms Plenum press, New York, 1985.
6. Kwon J.W., Lee C.H., Do E.D. *et al.*: Bull. Corean Chem. Soc. **29**, 1233–1242 (2008)
7. Chernichko D.I., Khomutov G.B.: Inorganic Materials **45**, 1283–1288 (2009)

Asymmetric Stochastic Resonance in a System of Ferromagnetic Nanoparticles

A. G. Isavnin and I. I. Mirgazov

Kazan (Volga Region) Federal University, Kazan 420008, Russian Federation, isavnin@mail.ru

Stochastic resonance phenomenon has been well investigated in various areas, including magnetic nanoparticles systems. In some previous papers the effect was considered as application to superparamagnetic particles, with noise intensity measure being temperature of the sample and external periodic signal being weak radiofrequency field [1, 2]. The influence of additional permanent magnetic field, applied at different angles to the “easy axis”, to dynamic magnetic susceptibility was also thoroughly explored before [3, 4] in the framework of the two-state model.

Here we present our calculations for output signal-to-noise ratio (SNR) of the system of fine ferromagnetic (iron) nanoparticles with auxiliary permanent magnetic field applied at arbitrary angle. Along with dynamic magnetic susceptibility, SNR is the most important characteristic of stochastic resonance. As usually we consider thermal switches of the particle magnetic moment as internal noise of the system, and output signal is assumed to be regular part of the magnetic moment motion at frequency of external weak radiosignal. We obtained analytical expressions for the SNR as a dependence on some parameters of the system, including temperature.

1. Sadykov E.K., Isavnin A.G.: *Phys. of the Solid State* **36**, 1843 (1994)
2. Sadykov E.K., Isavnin A.G.: *Hyperfine Interact.* **99**, 415 (1996)
3. Isavnin A.G.: *Russ. Phys. J.* **48**, 511 (2005)
4. Isavnin A.G.: *Russ. Phys. J.* **49**, 308 (2006)

Magnetic Resonance and Optical Spectroscopy of Yb³⁺ in the CsCaF₃ and CaF₂ Single Crystals

M. L. Falin^{1,2}, K. I. Gerasimov^{1,2}, and V. A. Latypov¹

¹ Zavoisky Physical-Technical Institute, Russian Academy of Sciences, Kazan 420029, Russian Federation

² Kazan (Volga Region) Federal University, Kazan 420008, Russian Federation

Crystals of the perovskite ABF₃ (A = Cs⁺, B = Ca²⁺) and fluorite MeF₂ (Me = Ca²⁺) type are promising materials for practical applications and convenient model systems for studying the magneto-optical properties of impurity dopant ions. In these matrices it is possible to substitute two various cations being inequivalent positions. This enables one to carry out investigations of impurity dopant ions in sixfold or twelfold coordinations. Previously we presented results on the study of Yb³⁺ in CsCaF₃ crystals [1, 2]. This report is concerned with the further investigation of impurity paramagnetic centers formed by Yb³⁺ ions by EPR and optical methods.

The crystals were grown using the Bridgman-Stockbarger method. The concentration of the impurity ions was 0.1–1.0 w%. EPR was carried out using an X-band spectrometer ERS-231 at $T = 4$ K. Optical spectra were registered on a homebuilt multifunctional spectrometer at $T = 2, 77$ and 300 K.

From angular dependences of EPR lines in the (001) and (110) planes it was found that Yb³⁺(I) and Yb³⁺(II) centers form structurally-inequivalent complexes of cubic symmetry. Depending on the conditions of crystal synthesis, one observes the redistribution of EPR spectra intensities.

The complete coincidence of optical and EPR spectra of new centers Yb³⁺(II) in CsCaF₃ and Yb³⁺ of cubic symmetry in CaF₂ were discovered. This implies the existence in crystals CsCaF₃ self-organized fluorite nanocrystals, the concentration of which may vary arbitrarily. The given supposition rejects a possibility of positioning Yb³⁺ on a place of Cs, as the crystal field of twelfold coordinated complexes can not coincide with eightfold coordination in CaF₂ nanocrystal.

The parameters of the corresponding spin Hamiltonians, the ground states and their wave functions were determined. Structural models of the new observed complexes were proposed.

This work was supported by the grant NSh-5602-2012.2 and the Russian Foundation for Basic Research (grant 13-02-97031r_Volga region_a).

1. Falin M.L., Anikeenok O.A., Latypov V.A., Khaidukov N.M., Callens F., Vrielinck H., Hoefstaetter A.: Phys. Rev. B **80**, 174110 (2009)
2. Falin M.L., Gerasimov K.I., Latypov V.A., Leushin A.M., Hoefstaetter A.: Appl. Magn. Res. **40**, 65 (2011)

Separation of the Contributions of Dipole-Dipole and Exchange Interactions to the Shape of Epr Spectra of Free Radicals in Diluted Solutions

M. M. Bakirov, K. M. Salikhov, and R. T. Galeev

Zavoisky Physical-Technical Institute, Russian Academy of Sciences, Kazan 420029,
Russian Federation

Nitroxide radicals are widely used in physics, biology, and pharmacology. The high sensitivity of the EPR spectra of nitroxide radicals to their chemical structure, the presence of paramagnetic additives, solvent polarity makes method of EPR spin labels an effective tool. EPR of radicals are widely known, but the description of the EPR of nitroxide radicals often use simplified algorithms that do not take into account all the processes due to exchange and dipole-dipole interactions.

In paper [1] the contributions of the dipole-dipole and Heisenberg exchange interactions to the width and shape of the EPR lines is considered in detail and new approaches to separate the contributions of these interactions is suggested.

In this report, using the algorithm proposed in paper [1] we made separation of the contributions of the exchange and dipole-dipole interactions. The study was carried out for radical solutions of tempon, in depending on the viscosity of the solvent. The sample was dissolved in 60% water glycerol solution. The study was made on the CW EMX EPR spectrometer at temperatures of 283, 288, 293, 298 and 328 K.

This research is supported in part by the Russian Foundation for Basic Research (project no. 12-03-97071) and the President of the Russian Federation (grant no. NSh-5602.2012).

1. Salikhov K.: Appl. Magn. Reson. **38**, 237–256 (2010)

Modeling of PELDOR Signal for Three Spin Systems

I. T. Khairuzhdinov and K. M. Salikhov

Zavoisky Physical-Technical Institute, Russian Academy of Sciences, Kazan 420029,
Russian Federation, semak-olic@mail.ru

Pulse Electron Double Resonance signals depend on the dipole-dipole interaction between paramagnetic centers. This effect can be used for the measuring distances between paramagnetic centers [1].

The methodology of the distance measurements is well elaborated in case of the correlated pairs of paramagnetic centers which are randomly distributed in a sample. However, the spatial design of paramagnetic centers in groups (clusters) can be of importance [2].

Keeping this fact in mind we have performed computer simulating of PELDOR signals for nitroxide biradicals and three radicals with hyperfine structure of ESR spectra. We calculated PELDOR signals for isolated three spin systems with different ratios of the distances between paramagnetic centers and the Euler angles in triads. The radical systems in a sample assumed to be randomly oriented relative to the external magnetic field.

The results obtained are compared with those available in literature.

1. Milov A.D., Salikhov K.M., Schirov M.D.: *Solid State Physics* **23**, 975 (1981)
2. Tsvetkov Y.D., Milov A.D.: *Electron Paramagnetic Resonance: from Fundamental Research to Pioneering Applications @ Zavoisky Award* (Salikhov K.M., ed.), p. 170–171. New Zealand, AXAS, 2009.

Tunable High-Frequency EPR Spectroscopy of the Clay and Plasticine

G. S. Shakurov and **V. A. Shustov**

Zavoisky Physical-Technical Institute, Russian Academy of Sciences, Kazan 420029,
Russian Federation, shakurov@kfti.knc.ru

The EPR spectrum of natural clay usually represents a wide line, which is sum of the EPR signal from different paramagnetic centers. However if the transition ions have fine structure, there are possibility to study them separately using tunable EPR spectroscopy method. We investigated the natural Cambrian blue clay and several types of plasticine. The plasticine includes the clay and it was interesting to compare their EPR spectra. The chemical analysis of clay shows that it contains Mn and Fe. For mineral composition analysis we undertook X-ray measurements using diffractometer DRON-7. EPR spectra were carried out on the home made spectrometer where backward wave oscillators were used as the tunable microwave power sources. EPR spectra of plasticine are presented on the Fig. 1. EPR line has the maximum intensity and regular shape in the zero magnetic field when the resonance frequency is equal to ZFS. As the resonance frequency shifts from ZFS, intensity is decrease and line became irregular shape. Nevertheless it is possible to measure field-frequency dependencies and to define the values of g -factors. The clay and one of the types of plasticine have identical EPR spectra. The other plasticines have similar spectra. The origin of EPR signals on the high frequency presumable associated with Al_2O_3 . All samples contains the alumina, besides the spectra of excitation of $\text{Al}_2\text{O}_3:\text{Fe}$ and of our samples have very close values of ZFS and g -factors. Another possible nature of the EPR signals at high frequency also discussed in the report.

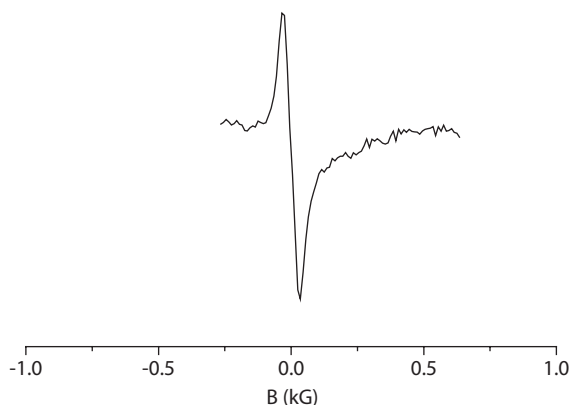


Fig. 1. EPR spectrum of plasticine. 114.8 GHz.

Chiral Spin-Liquid State in $\text{Mn}_{1-x}\text{Fe}_x\text{Si}$ Solid Solutions

V. V. Glushkov¹, S. V. Grigoriev², S. V. Demishev¹, T. V. Ischenko¹,
I. I. Lobanova¹, A. N. Samarin¹, A. V. Semeno¹, and N. E. Sluchanko¹

¹ Prokhorov General Physics Institute of RAS, Moscow 119991, Russian Federation,
demis@lt.gpi.ru

² Petersburg Nuclear Physics Institute, Gatchina, Saint-Petersburg 188300, Russian Federation

A characteristic feature of quantum helimagnets consists in forming of the chiral spin liquid (CSL) magnetic phases characterized by short-range order [1]. These materials can be driven into CSL phase either by weakening of the electron-electron interactions [2] or by disorder effects [3]. Basing on the electron spin resonance (ESR) evidence of Heisenberg magnetism in MnSi [4, 5] we developed a model, where magnetic phase with short-range order is controlled by characteristic lengths describing classical (R_{f1}) and quantum (R_{f2}) fluctuations. In weak magnetic field ($B \rightarrow 0$) the short-range magnetic order phase appears when fluctuations of the order parameter in paramagnetic (P) phase (“chiral gas” [1]) freeze due to the condition $R_{f1,2} = R_s$ (R_s is some characteristic length in the considered material). The disorder effects may be taken into account by supposition that R_s is given by correlation length R_c , so that

$$\begin{aligned} R_{f1} &= \frac{a_1}{[1 - T/T_c(x)]^\delta}; & R_{f2} &= a_2 \frac{T_0}{T}; \\ R_s = R_c &= \frac{l}{(1 - x/x_c)^\nu}. \end{aligned} \quad (1)$$

Here x denotes some parameter, which determines quantum criticality. Non-trivial physical behavior can be obtained when critical point corresponding to change of the topology of the magnetic subsystem x_c does not coincide with the “underlying” critical point x^* at which transition temperature into the spiral phase (SP) with long-range order $T_c(x)$ turns to zero: $T_c(x^*) = 0$. If $x^* < x_c$ the CSL “tail” is formed and a new crossover line dividing areas with dominating classical (P1) and quantum fluctuations (P2) appears in the paramagnetic phase (Fig. 1). Using model equations (1) we have computed magnetic phase diagram of $\text{Mn}_{1-x}\text{Fe}_x\text{Si}$ solid solutions where driving parameter x is given by iron concentration. The calculations are in good agreement with the results of magnetic measurements, which show sequence of quantum critical points at x^* (QCP1) and x_c (QCP2). The model can be extended to the case of high magnetic fields up to $B \sim 8$ T and allows consistent explanation of the magnetic phase diagram subtracted from the magnetoresistance data.

Basing on the obtained magnetic phase diagram of $\text{Mn}_{1-x}\text{Fe}_x\text{Si}$ solid solutions we have carried out high-frequency (60 GHz) ESR probing of the chiral spin-liquid. It is found that entering into CSL results in strong broadening of the ESR line width, which can be explained by enhancement of the spin fluctuations.

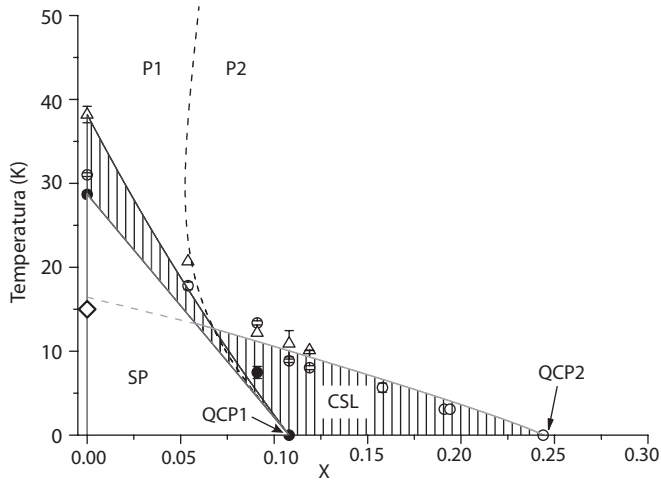


Fig. 1. Magnetic phase diagram of $\text{Mn}_{1-x}\text{Fe}_x\text{Si}$ solid solutions. Points denote experimental data; lines are theoretical calculations. The phases with short-range magnetic order are shaded.

The obtained experimental data indicates a possibility of a crossover between Heisenberg-type and itinerant magnetism induced by increase of iron content.

This work is supported by Program of RAS “Strongly correlated electrons” and by RFBR grant 13-02-00160.

1. Tewari S., Belitz D., Kirkpatrick T.R.: Phys. Rev. Lett. **96**, 047207 (2006)
2. Kruger F., Karahasanovic U., Green A.G.: Phys. Rev. Lett. **108**, 067003 (2012)
3. Vojta T., Sknepnek R.: Phys. Rev. B **64**, 052404 (2001)
4. Demishev S.V. *et al.*: JETP Lett. **93**, 213 (2011)
5. Demishev S.V. *et al.*: Phys. Rev. B **85**, 045131 (2012)

EPR Study on Mechanism of *ipso*-Nitration of Arylboronic Acids

H. Yang, Y. Li, M. Jiang, and H. Fu

Department of Chemistry, Tsinghua University, Beijing 100084, P. R. China,
cyhj@tsinghua.edu.cn

Nitroarenes are key starting materials for the manufacture of various chemical products, such as pharmaceuticals, dyes and materials [1–3]. The traditional method for synthesis of nitroarenes is from mixed-acid ($\text{H}_2\text{SO}_4/\text{HNO}_3$) strategy. However, the products with the isomeric mixtures from the nitration of substituted arenes are often unavoidable, and the weak functional group tolerance is usually observed. In addition, the nitration reactions have met great challenge from green chemistry because of use of large quantities of hazardous acids. Herein, the mechanism of nitration of arylboronic acids was studied by EPR. Base on the results of EPR studies, we developed a simple, efficient and practical *ipso*-nitration of arylboronic acids with 0.5 equiv of iron nitrate without addition of any other additive.

EPR was used to monitor the reaction process of nitration of arylboronic acids. As a model reaction, 4-methyl boronic acid and iron nitrate were added to toluene under a nitrogen atmosphere. Both Fe^{3+} and the free radicals could be monitored via EPR. It was found that the Fe^{3+} signal were disappeared in EPR spectra when the temperature was increased from room temperature to the reaction temperature (80 °C). It was shown that Fe^{3+} was transformed to Fe^{2+} with the temperature increasing. At the same time, strong radical signal was observed in EPR spectra (Fig. 1) at the reaction temperature. It was found that every triple peaks were split into numerous peaks in EPR spectra. It suggested that the radical containing nitrogen atom was connect to the boron atom because there exist two main isotopes of boron ($I = 3$ for ^{10}B and $I = 3/2$ for ^{11}B). Each peak would be split by two different boron atoms and hydrogen atoms in the aryl ring.

The mechanism for *ipso*-nitration of arylboronic acids with iron nitrate is proposed in Fig. 2. $\text{Fe}(\text{III})(\text{NO}_3)_3$ produces $\text{Fe}(\text{II})(\text{NO}_3)_2$ (I) and free radical II

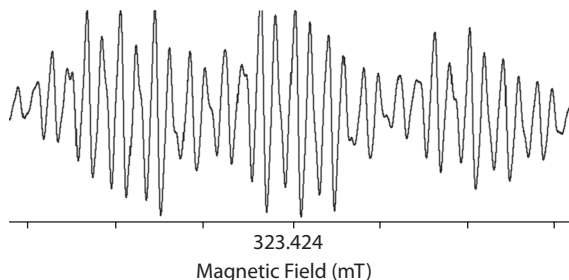


Fig. 1. EPR spectra of 4-methyl boronic acid and $\text{Fe}(\text{NO}_3)_3 \cdot 9\text{H}_2\text{O}$ in toluene under N_2 atmosphere at 80 °C.

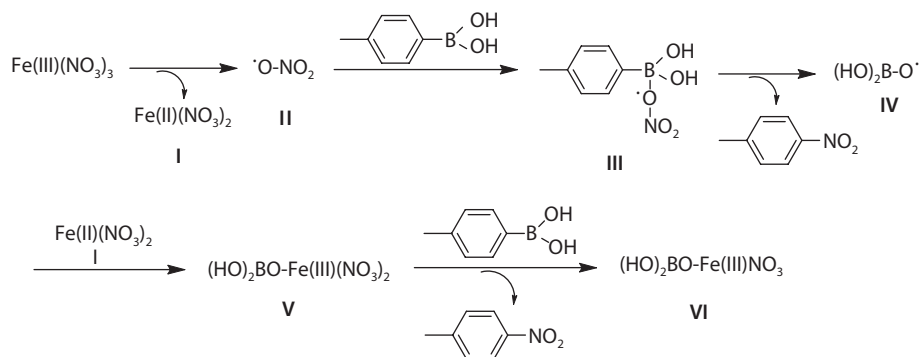


Fig. 2. Possible mechanism for *ipso*-nitration of arylboronic acids with iron nitrate.

under heating condition, and reaction of **II** with 4-methyl boronic acid leads to aryl free radical **III**. Reaction of **III** provides the target product leaving boronic acid free radical (**IV**), and reaction of **I** with **IV** affords Fe(III) salt (**V**). **V** containing NO_3^- can further react with 4-methyl boronic acid to give the target product freeing Fe(III) salt (**VI**).

The financial support of the National Natural Science Foundation of China (Grant No. 21105054) is gratefully acknowledged.

1. Prakash G.K.S., Olah G.A.: *Org. Lett.* **13**, 2205 (2004)
2. Manna S., Maiti D.: *Org. Lett.* **14**, 1736 (2012)
3. Seiple I.B., Sun S., Baran P.S. *et al.*: *J. Am. Chem. Soc.* **132**, 13194 (2010)

Magnon BEC in CsMnF₃

R. Gazizulin

Kazan (Volga Region) Federal University, Kazan 420008, Russian Federation

Measurement of the g -factors of Ground and Excited States in the Zero dc Magnetic Field by the Photon Echo Method

V. N. Lisin and A. M. Shegeda

Zavoisky Physical-Technical Institute, Russian Academy of Sciences, Kazan 420029, Russian Federation

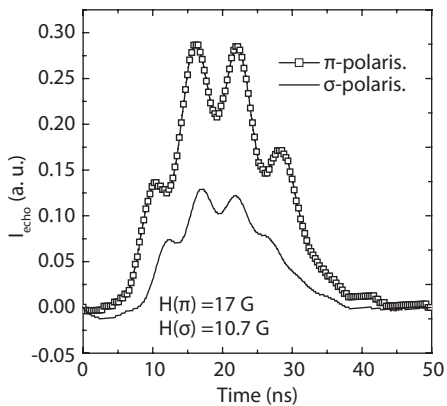
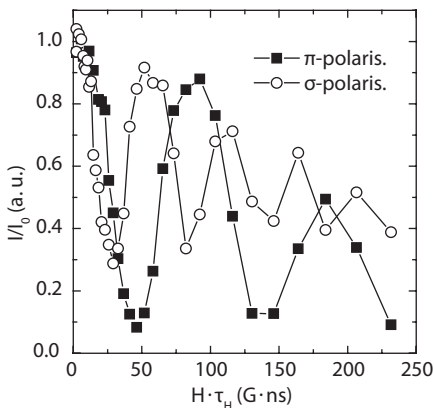
The g -factors of the ground $^4I_{15/2} g_{g\parallel}$ and excited $^4F_{9/2} g_{e\parallel}$ states of the Er^{3+} ion in the LuLiF_4 and YLiF_4 in the zero dc magnetic field are determined from measurement of Zeeman splitting of the σ and π optical lines in a weak pulse magnetic field use precision method [1, 2]. The intensity of two-pulse photon echo qualitatively can be described by the expression [1, 2]

$$I(t) = I_0(t)(1 + \cos\varphi(t))/2, \quad \varphi_1 = Z\tau_H, \quad \varphi_2 = Z(t - t_0),$$

$$Z = (g_{e\parallel} \pm g_{g\parallel})\beta H/\hbar$$

and the phase $\varphi(t) = \varphi_1$ [1] if magnetic pulse is applied in the intervals between the first and second laser pulses or between the second laser pulse and the echo signal and $\varphi(t) = \varphi_2(t)$ [2] in a case of a weak pulsed magnetic field acting during the time of the radiation of the photon echo pulse. Here $I_0(t)$ is echo intensity without magnetic pulse, τ_H is a duration and H is an amplitude of a pulse magnetic field, t_0 is the time of the beginning of pulse action, β is the Bohr magneton, \hbar is the Planck constant, the plus and minus signs correspond to the σ and π laser polarizations. The pulse magnetic field is directed along the crystal axis C .

The experimental dependence of the intensity of two-pulse photon echo versus the magnetic pulse area $H\tau_H$ is shown in the left figure (the case $\varphi(t) = \varphi_1$). In



the right figure it is shown photon echo signal versus the time of detection in the case ($\varphi(t) = \varphi_2$) of a weak pulsed magnetic field acting during the time of the radiation of the photon echo pulse. Defining from both figures periods of oscillations and equating phase $\varphi_1 = 2\pi$ and $\varphi_2 = 2\pi$, you can find the values of g -factors by two different methods. The accuracy of determination of g -factors by these methods is discussed.

1. Lisin V.N., Shegeda A.M., Gerasimov K.I.: JETP Lett. **95**, 61 (2012)
2. Lisin V.N., Shegeda A.M.: JETP Lett. **96**, 298 (2012)

EPR Study of New Spin Labels Based on 2,5-Bis(Spirocyclohexane)-Substituted Nitroxides of Pyrroline and Pyrrolidine Series

**O. A. Krumkacheva¹, I. A. Kirilyuk², Y. F. Polienko², I. A. Grigor'ev²,
R. K. Strizhakov³, E. S. Babailova³, A. V. Ivanov³, M. A. Vorobjeva³,
A. G. Venyaminova³, A. A. Malygin³, G. G. Karpova³,
M. V. Fedin¹, and E. G. Bagryanskaya^{1,3}**

¹ International Tomography Center SB RAS, Novosibirsk 630090, Russian Federation

² Institute of Chemical Biology and Fundamental Medicine SB RAS, Novosibirsk 630090, Russian Federation

³ N. N. Vorozhtsov Novosibirsk Institute of Organic Chemistry SB RAS, Novosibirsk 630090, Russian Federation

It has been found recently that piperidine nitroxides with spirocyclic moieties at α -carbons of nitroxide group may have advantages over 2,2,6,6-tetramethyl analogues in structural studies using PELDOR [1]. In this work [2] we investigated chemical and spectral properties of new 2,5-bis(spirocyclohexane)-substituted nitroxides of pyrroline and pyrrolidine. New spin labels demonstrate advantages over 2,2,5,5-tetramethylpyrroline nitroxides with respect to electron spin relaxation rates, which should favor PELDOR distance measurements at liquid nitrogen temperature range. Moreover, new nitroxides demonstrate much higher stability toward reduction by ascorbate than spirocyclohexane-substituted nitroxides of piperidine series and showed 1.3–3.1 times lower reduction rates compared to corresponding 2,2,5,5-tetramethyl nitroxides.

For the first time we used new spirocyclohexane-substituted spin label with advanced relaxation properties and high stability toward reduction by ascorbate to measure distances for oligonucleotides using Q-band PELDOR. To test this spin label, we applied it to model RNA duplex with known distances between corresponding residues and compared results with standard 2,2,5,5-tetramethyl-substituted nitroxides. The obtained distance distributions correspond well to the expected ones. It implies that novel spirocyclohexane-substituted nitroxides are promising spin labels for distance measurements by PELDOR, including structural investigation of RNA and DNA in cell.

This work was supported by the Russian Foundation for Basic Research (12-03-33010, 12-04-01435).

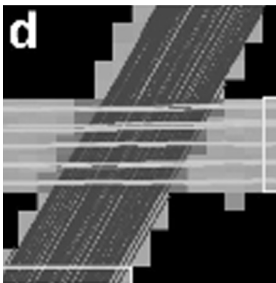
1. Rajca A., Kathirvelu V., Roy S.K., Pink M., Rajca S. *et al.*: Chem. Eur. J. **16**, 5778 (2010)
2. Kirilyuk I.A., Polienko Y.F., Krumkacheva O.A., Strizhakov R.K., Gatilov Y.V., Grigor'ev I.A., Bagryanskaya E.G.: J. Org. Chem. **77**, 8016 (2012)

Validation of the MRI Based Fiber Tracking Results on a Numerical Phantom

O. V. Nedopekin, L. V. Konopleva, and K. A. Il'yasov

Institute of Physics, Kazan University, Kazan 420008, Russian Federation

Diffusion measurements with Magnetic Resonance Imaging (MRI) gives possibility to investigate the structure of biological tissues *in vivo*. Mean diffusion distance of water molecules during the measurement time is of the same scale as size of cells, therefor the method is very sensitive to any tissue microstructure changes. Diffusion in brain tissues and muscles is anisotropic – it is more restricted across fibers that along of them, what gives possibility to detect the local direction of axonal or muscle fibers. Fiber tracking algorithms (FT) use this local information to find out fiber pathways, and so connectivity between different regions of brain can be noninvasively determined [1], what opens new possibilities for neuroscience and clinical diagnostics. However spatial resolution of MRI is limited to a few millimeters, what is by several orders of magnitude larger than fiber diameter. Such averaging over voxel gives correct directional information for fiber bundles with diameter of several millimeters and for fibers with different directions within a voxel only averaged direction can be found. Lack of correct directional information in crossing regions, partial volume effects and noise in measured data lead to different errors in FT.



Fragment of numerical phantom with fiber crossing. Streamline FT is more prone to noise in the raw MRI data and even for parallel fibers more hops to neighbor fibers is observed.

In this work a numerical fiber tracking phantom has been used to validate the results of FT with streamline, global tracking and probability tracking methods [2, 3]. It has been observed that the global tracking method is more stable than streamline method against errors caused by noise in the measured MRI data. Modifications of probability tracking method were done to get better measure of quality and probability of the existence for the detected fiber tracks.

1. Conturo T.E., Lori N.F., Cull T.S. *et al.*: Proc Nat Acad Sci USA. **96**, 10422 (1999)
2. Kreher B.W., Schnell S., Il'yasov K.A. *et al.*: Neuroimage. **43**, 81(2008)
3. Il'yasov K.A., Aganov A.V., Kreher B.W.: Tech. of living systems (Russ.) **6**, 3 (2012)

CPMG Echo Amplitudes with Arbitrary Refocusing Angle: Explicit Expressions, Asymptotic Behavior, Approximations

M. V. Petrova¹, A. B. Doktorov², and N. N. Lukzen¹

¹ International Tomography Center SB RAS, Novosibirsk 630090, Russian Federation, petrovamv@tomo.nsc.ru

² Institute of Chemical Kinetics and Combustion SB RAS, Novosibirsk 630090, Russian Federation

Carr-Purcell-Meiboom-Gill (CPMG) periodic pulse sequence with arbitrary excitation and refocusing angles and resonance offset of RF pulses was considered. Exact explicit analytical formula for echo magnetization amplitudes was obtained. The echo amplitudes are expressed in term of Legendre polynomials. The dependence of asymptotic behavior of CPMG echoes on RF pulse refocusing angle was studied, analytical approximation for echoes was also obtained. It was shown that the form of the asymptotic curve depends dramatically on the sequence parameters; and if the refocusing angle $\alpha \neq \pi$ the echo amplitudes decay is determined not only by spin-spin relaxation time T_2 as usually, but also by spin-lattice relaxation time T_1 and the refocusing angle. It was also found that the CPMG echo signals can decay with or without oscillation; the threshold between the two cases was found to depend on the ratio of spin-spin and spin-lattice relaxation rates and the refocusing angle. Accuracy of all approximate expressions obtained was tested by comparison with exactly calculated echo amplitudes, showing a promise for practical use.

The work was supported by Foundation for Basic Research (grant 14-02-31210).

Comparison of X-, Q- and G-band Stimulated Electron Spin Echo Data on Molecular Motions of Spin Labels

**N. P. Isaev¹, M. V. Fedin², V. Denysenkov³, T. Prisner³,
and S. A. Dzuba^{1,4}**

¹ Institute of Chemical Kinetics and Combustion, Novosibirsk 630090, Russian Federation

² International Tomography Center, Novosibirsk 630090, Russian Federation

³ Institute of Physical and Theoretical Chemistry, Center of Biomolecular Magnetic Resonance,
Goethe University Frankfurt, Frankfurt 60438, Germany

⁴ Novosibirsk State University, Novosibirsk 630090, Russian Federation,
isaev@kinetics.nsc.ru

A few years ago new method of investigation of molecular motion was proposed [1], which is based on analyzing transverse relaxation in stimulated electron spin echo experiment ($\pi/2-\tau-\pi/2-T-\pi/2-\tau$ -echo), when T is constant and τ is varying. The extraction of the anisotropic part of transverse relaxation, which is done by comparing relaxation in hyperfine components of different anisotropy, allows investigating independently nanosecond librations and microsecond small-angle reorientations of nitroxide spin probes and labels in organic glasses [2] and lipid bilayers [1, 3, 4]. So far, these experiments have been done at X-band (9 GHz) only [1–4].

Q-band (35 GHz) also seems to be convenient for these studies, because here EPR spectrum possesses a low-field narrow hyperfine component that is almost isotropic, which facilitates extraction of the relaxation anisotropy.

Nitroxide G-band (180 GHz) spectrum has much higher anisotropy what allows one to study the symmetry of molecular motions in contrast to X-band. Also high-field EPR machines have much lower “dead time”, what is extremely required for stimulated echo relaxation investigation.

In this work, comparative X-, Q- and G-band stimulated echo investigations of molecular motions of spin-labeled lipids in model membranes are performed. The results are discussed with involving several models of molecular motion.

1. Isaev N.P., Dzuba S.A.: *J. Phys. Chem. B* **112**, 13285–13291 (2008)

2. Isaev N.P., Kulik L.V., Kirilyuk I.A. *et al.*: *J. Non-Cryst. Solids* **356**, 1037–1042 (2010)

3. Isaev N.P., Syryamina V.N., Dzuba S.A.: *J. Phys. Chem. B* **114**, 9510–9515 (2010)

4. Syryamina V.N., Isaev N.P., Peggion C. *et al.*: *J. Phys. Chem. B* **114**, 12277–12283 (2010)

Pulsed ENDOR Study of the Nitrogen Donors in 6H SiC Crystals Grown under Carbon-Rich Conditions

**D. Savchenko^{1,2}, E. Kalabukhova², A. Pöppl³, B. Shanina²,
and E. Mokhov⁴**

¹ Department of Analysis of Functional Materials, Institute of Physics AS CR, Prague 18221, Czech Republic, dariyasavchenko@gmail.com

² Department of Semiconductor Heterostructures, V. E. Lashkaryov Institute of Semiconductor Physics NASU, Kyiv 03028, Ukraine, katia@i.kiev.ua

³ Institute of Experimental Physics II, Leipzig University, Leipzig D-04103, Germany, poeppl@physik.uni-leipzig.de

⁴ Laboratory of Electronics of Semiconductors with the Strong Binding Energy, A. F. Ioffe Physical Technical Institute RAS, St. Petersburg 194021, Russian Federation, mokhov@rednet.ru

In the present work X-band field-sweep electron spin echo (FS ESE) and pulsed electron nuclear double resonance (ENDOR) were used to study n-type carbon-rich 6H-SiC crystals (with low and high compensation level) with the aim to verify the recently proposed new conception that nitrogen (N) donors substitute both carbon (C) and silicon (Si) sites and may occupy 3 inequivalent positions at Si site in n-type 6H SiC by properly varying of the Si/C ratio during crystal growth [1]. We have found that besides the N ENDOR spectra substituting quasi-cubic "k1" and "k2" positions in 6H SiC lattice (N_{k1} and N_{k2}), six spectra (N_1 – N_6) due to ^{14}N nuclei were observed in ENDOR spectrum of high compensated n-type C-rich 6H SiC. From the analysis of obtained hyperfine coupling (HFC) constants (see Table 1) the N_2 center with the smallest HFC was attributed to the N substituting hexagonal "h" position at Si site ($N_{h,\text{Si}}$) while N_6 center was assigned to $N_{k1,\text{Si}}$. The presence of N_1 , N_3 , N_4 , N_5 spectra was explained by the local strains, which may cause the small reduction of the HFC for the N donors located in the vicinity of the strain [4]. By comparing the number of FS ESE and ENDOR spectra observed in n-type C-rich 6H SiC with different compensation

Table 1. The g -values and HFC for N donors obtained in low and high compensated n-type C-rich 6H SiC with $(N_D - N_A) \sim 10^{16} \text{ cm}^{-3}$ from FS ESE and ENDOR data.

Center	N_{k2}	N_3	N_{k1}	N_5	N_2	N_1	N_6	N_4
g_{\parallel}	2.0037	2.0037	2.0040	2.0038	2.0038	2.0039	2.0038	2.0038
g_{\perp}	2.0030	2.0030	2.0026	2.0030	2.0030	2.0030	2.0030	2.0030
$A_{\parallel} \sim A_{\perp}$ (MHz)	33.32	29.77	33.60	32.20	25.94	21.58	34.66	30.36
Ref.	[1, 2]	[3]	[1, 2]	This work	[3]	[3]	This work	This work
$x \cdot A_{\text{HFC}}$		$0.89 \cdot N_{k2}$		$0.97 \cdot N_{k1}$		$0.83 \cdot N_2$		$0.87 \cdot N_6$
Compensation level	High, low	High, low	High, low	High	High, low	High, low	High	High, low
Model	N_{k2}, Si	N_{k2}, Si^*	N_{k1}, C	N_{k1}, C^*	N_h, Si	N_h, Si^*	N_{k1}, Si	N_{k1}, Si^*

degree the $N_{k2, Si}$ was found to be occupied (in paramagnetic state) only in the high compensated samples indicating that $N_{k2, Si}$ corresponds to the deeper donor center in 6H SiC and among other “k” positions at C and Si sites it shows the highest HFC. At the same time the $N_{h, Si}$ was found to be in paramagnetic state both in the low and highly compensated C-rich 6H SiC indicating that it has relatively shallow energy level in the band gap but deeper than that of $N_{h, C}$ which was not observed in the compensated 6H SiC.

As a result, the incorporation of nitrogen on Si sites over 3 inequivalent positions can be achieved by properly varying of the C/Si ratio towards C excess during crystal growth. $N_{h, Si}$ and $N_{k1, Si}$ cannot be observed in stoichiometric 6H SiC, where the N donor at Si site is occupied only one “k” position ($N_{k2, Si}$). Residual distortion for N donors at C and Si atoms is different due to their different covalent radius. The reduction of HFC for N donors at Si site in vicinity of the strain is larger than that for N donors at C site. The obtained data are consisted with the known fact that the N-doping concentration is very sensitive to C/Si ratio and it decreases with increasing C/Si ratio. It was concluded that the C-excess in 6H SiC inhibits the site competition process between nitrogen and carbon for C sites proposed in [5] and provokes the nitrogen incorporation on Si site.

The work was supported by large infrastructure SAFMAT (project CZ.2.16/3.1.00/22132) and Grant Agency of Czech Republic (project 13-06697P).

1. Savchenko D., Kalabukhova E., Pöpl A., Shanina B.: Phys. Status Solidi B **249**, 2167 (2012)
2. Savchenko D., Kalabukhova E., Kiselev V., Hoentsch J., Pöpl A.: Phys. Status Solidi B **246**, 1908 (2009)
3. Savchenko D., Kalabukhova E., Lukin S., Mokhov E., Hoentsch J., Pöpl A.: Physica B **404**, 4735 (2009)
4. Wilson D., Feher G.: Phys. Rev. **124**, 1068 (1961)
5. Larkin D., Neudeck P. *et al.*: Appl. Phys. Lett. **65**, 1659 (1994)

AUTHOR INDEX

Abdulmalic, M. A.	72
Adachi, T.	61
Aksu, P.	64
Aktaş, B.	64
Alekseev, A. V.	127
Aliabadi, A.	72
Alloul, H.	60
Aminov, L. K.	87
Anashkin, V. N.	117
Andreev, N. V.	136
Andrianov, V. V.	132
Artyomov, M. Yu.	100
Astakhov, G. V.	82
Ates, L.	108
Augustyniak-Jabłokow, M. A.	26, 115
Babailova, E. S.	158
Bagryanskaya, E. G.	30, 158
Bakirov, M. M.	127, 148
Bakkal, G.	107
Baniodeh, A.	28, 129
Baranov, P. G.	82
Barbon, A.	46
Bayazitov, A. A.	109
Belov, V. V.	68
Bennati, M.	55
Berendyaev, V.	113
Berezin, A. S.	104
Biktagirov, T. B.	93
Bordignon, E.	5
Böttcher, R.	87
Bowman, M. K.	13, 51
Brustolon, M.	46
Büchner, B.	59, 72, 91
Bychkova, A. V.	113
Chakour, M.	42
Chakraborty, R.	42
Chasovskaya, T. E.	68

Chen, C.	42
Cherepnev, G. V.	121
Chichkov, V. I.	136
Chushnikov, A. I.	121
Demishev, S. V.	11, 151
Denysenkov, V.	161
Dereli, Ö.	112
Dietz, C.	5
Doktorov, A. B.	160
Dolinenkov, F. N.	65
Domracheva, N. E.	102
Drozdyuk, I. Yu.	30
Dultseva, G. G.	73
Dyakonov, V.	82
Dzuba, S. A.	32, 161
Efimov, V. N.	144
Eremina, R. M.	110, 129, 136
Eremin, M. V.	25
Ergun, E.	107
Evstigneeva, M. A.	91
Fakhrutdinov, A. R.	117
Falin, M. L.	52, 147
Fattakhov, Ya. V.	109, 117
Fazlizhanov, I. I.	136
Fedin, M. V.	30, 123, 158, 161
Fedorova, O. S.	7
Fokin, A. V.	100
Fuchs, F.	82
Fu, Hua	38, 153
Gafiyatullin, L. G.	126
Gafurov, M. R.	93
Gainutdinov, Kh. L.	132
Galeev, R. T.	129, 148
Gataulina, A. R.	142
Gavrilova, T. P.	136
Gazizulin, R.	155
Gerasimov, K. I.	80, 147
Geru, I.	23
Gilmutdinov, I. F.	140
Glushkov, V. V.	11, 151
Gnezdilov, O. I.	126
Golbeck, J.	15
Golubeva, E. N.	33
Gorlov, A. D.	70
Goryunov, Y. V.	124

Grafe, H.-J.	59
Grampp, G.	33
Grigor'ev, I. A.	158
Grigoriev, S. V.	151
Gubskaya, V. P.	43
Gumarov, G. G.	127
Gündoğdu, S.	112
Hinderberger, D.	42
Ibragimova, M. I.	121
Il'yasov, K. A.	159
Indu, S.	42
Isaev, N. P.	161
Isavnin, A. G.	146
Ischenko, T. V.	151
Ivanova, G. I.	140
Ivanova, T. A.	140
Ivanov, A. V.	158
Ivanov, K. L.	54
Ivanov, M.	123
Iyudin, V. S.	40, 132
Jeschke, G.	5
Jiang, Min	38, 153
Joseph, B.	5
Kalabukhova, E.	162
Kandrashkin, Yu. E.	40
Karpova, G. G.	158
Kataev, V.	10, 59, 72
Khabipov, R. Sh.	117
Khairuzhdinov, I. T.	149
Khaliullin, G.	58
Khasanov, B. M.	134
Khitrin, A. K.	103
Khramtsov, V. V.	17
Kirilyuk, I. A.	158
Kiryutin, A. S.	54
Klauss, H.-H.	86
Klimashina, E. S.	93
Kobzeva, T. V.	73
Kochelaev, B. I.	20
Koike, Y.	61
Kokorin, A. I.	33
Kolokolov, D. I.	30
Komarovskikh, A. Y.	74
Konopleva, L. V.	159
Korkhov, V.	5

Kothe, G.	79
Kovaleva, E. G.	66
Kovarski, A. L.	113
Krumkacheva, O. A.	158
Krupskaya, Y.	59
Krylatykh, N. A.	117
Kulik, L. V.	35, 120, 139
Kupriyanova, G. S.	64, 65
Kupriyanov, I. N.	74
Kurkin, I. N.	87
Kutyreva, M. P.	142
Kuznetsov, D. A.	50
Kuznetsov, N. A.	7
Latypov, V. A.	52, 147
Lavrenova, L. G.	104
Lide, E. V.	104
Likhtenshtein, G. I.	21
Link, G.	79
Lin, T.-S.	79
Lisin, V. N.	156
Li, Yong	38, 153
Lobanova, I. I.	11, 151
Lubitz, W.	3, 98
Lukaschek, M.	79
Lukina, E. A.	35, 120
Lukzen, N. N.	54, 160
Maćkowiak, M.	115
Maltseva, E. L.	68
Malygin, A. A.	158
Mambetov, A. E.	43
Mamedov, D. V.	136
Mamin, G. V.	93
Maryasov, A. G.	13, 51
Masalimov, A. S.	130
Mikhalitsyna, E. A.	40
Milov, A. D.	7
Mingalieva, L. V.	110, 140
Mirgazov, I. I.	146
Mladenova-Kattinig, B. Y.	33
Möbius, K.	8, 15
Moiseev, S. A.	80
Mokhov, E.	162
Möller, A.	59
Molochnikov, L. S.	66
Morosov, V. I.	80

Morozov, V. A.	89
Mozzhukhin, G. V.	64
Mukhamedshin, I. R.	60
Mukovskii, Ya. M.	136
Muravyev, V. I.	142
Nadolinny, V. A.	74, 104
Nadtochenko, V.	15
Nalbandyan, V. B.	91
Nateprov, A. N.	124
Nedopekin, O. V.	159
Nikolskiy, S. N.	130
Noji, T.	61
Nuretdinov, I. A.	43
Nurmamyatov, I. A.	117
Ohmichi, E.	4
Ohta, H.	4
Okubo, S.	4
Orlinskii, S. B.	93
Ovcharenko, V. I.	30
Ovchinnikov, I. V.	126, 140, 142
Ozmen, A.	107, 108
Palali, L.	107
Palmina, N. P.	68
Pal'yanov, Y. N.	74
Paulsen, H.	5
Petr, A.	72
Petrova, M. V.	160
Petukhov, V. Yu.	121, 127
Polienko, Y. F.	158
Polyhach, Ye.	5
Popov, A. A.	35, 139
Popov, A. G.	120
Pöppl, A.	87, 162
Potapov, A. P.	100
Powell, A. K.	28, 129
Prisner, T.	161
Putlayev, V. I.	93
Pyataev, A. V.	102
Rakhmatullin, R. M.	87
Rameev, B. Z.	64
Reichenwallner, J.	42
Rodionov, A. A.	93, 136
Rosenfeld, M.	113
Rüffer, T.	72

Saenko, N. S.	88
Sakhin, V. O.	61
Sakurai, T.	4
Salakhutdinov, L. F.	61
Salikhov, K. M.	43, 47, 148, 149
Samarin, A. N.	11, 151
Savchenko, D.	162
Savitsky, A.	15
Savostina, L. I.	98, 126
Saxena, S.	95
Sayin, U.	107, 108
Sayin, Z.	107
Schäpers, M.	59
Selmke, B.	42
Semenov, A. V.	11, 151
Semenov, A. Yu.	15
Sen, S.	87
Shagalov, V. A.	117
Shaikhutdinov, I. I.	132
Shakurov, G. S.	150
Shanina, B.	162
Shapiro, A. V.	113
Sharipov, K. P.	110
Shegeda, A. M.	156
Sheveleva, A. M.	30
Shimokawa, T.	4
Shukaev, I. L.	91
Shustov, V. A.	150
Sinitsyn, A. M.	118, 122
Sinyavsky, N. Ya.	65
Sitdikov, F. G.	132
Sluchanko, N. E.	11, 151
Solovarov, N. K.	53
Soltamova, A. A.	82
Soltamov, V. A.	82
Sorokina, O. N.	113
Stepanov, A. G.	30
Stratan, M. I.	91
Strizhakov, R. K.	158
Strzelczyk, R.	115
Sukhanov, A. A.	28, 53, 129
Tadyszak, K.	115
Takui, T.	78
Talanov, Yu. I.	61

Tapramaz, R.	107
Tararkov, A. N.	76
Tarasov, V. F.	53
Taşdemir, H. U.	108, 112
Tcherepanov, A. N.	76
Theison, S.	42
Tkach, I.	55
Tormyshev, V. M.	13
Tretyakov, E. V.	30
Trommer, W. E.	42
Tsvetkov, Yu. D.	2, 7, 51
Tumakaev, R. F.	132
Tur, A. A.	130
Turanov, A. N.	103, 126
Turanova, O. A.	126, 140
Türkkan, E.	108, 112
Tyurin, V. S.	40
Ulakhovich, N. A.	142
Ulanov, V. A.	118, 122
Uvarov, M. N.	35, 120
Valeev, V. F.	127
van Gastel, M.	98
Varadarajan, R.	42
Vasilchikova, T. M.	91
Vasiliev, A. N.	91
Vavilova, E. L.	59
Vazhenin, V. A.	100
Veber, S. L.	30, 123
Venyaminova, A. G.	158
Vieth, H.-M.	54
von Hagens, T.	5
Vorobeva, V. E.	102
Vorobjeva, M. A.	158
Voronkova, V. K.	28, 40, 43, 129
Weidner, J.-U.	79
Wolter-Giraud, A. U. B.	59
Yafarova, G. G.	132
Yago, T.	79
Yagudin, R. Kh.	132
Yang, Haijun	38, 153
Yatsyk, I. V.	136
Yavkin, B. V.	93
Yulikov, M.	5
Yurkovskaya, A. V.	54
Yurtaeva, S. V.	142, 144

Zainullin, R. R.	118, 122
Zaripova, R. I.	132
Zaripov, M. M.	52
Zaripov, R. B.	43, 53, 80
Zefirov, T. L.	132
Zharikov, E. V.	53
Zheglov, E. P.	121
Zhiteytsev, E. R.	118, 122
Ziatdinov, A. M.	88
Zueva, E. M.	102
Zvereva, E. A.	91

© Казанский физико-технический институт, 2013

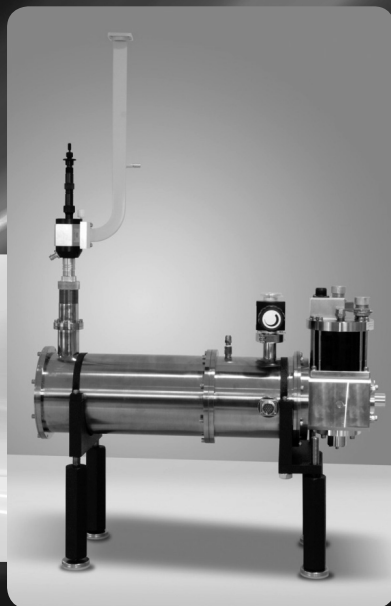
Ответственный редактор В. К. Воронкова; редакторы: С. М. Ахмин, Л. В. Мосина; технический редактор О. Б. Яндуганова. Издательство КФТИ КазНЦ РАН, 420029, Казань, Сибирский тракт, 10/7, лицензия № 0325 от 07.12.2000.

CryoFree EPR VT Systems

Cryogen-free EPR sample cryostats for variable temperature operation are now available for X-Band waveguide cavities and for Flexline probes with base temperature options down to 4 K



Flexline cryostat



Waveguide cavity cryostat

- All systems allow rapid sample exchange
- Variable temperature range: base – 300K
- Rapid cool down (<60 min to base temperature)
- Optical access
- Vibration isolation for CW Spectroscopy
- Compatible with ER 073, ER 075 and ER 077 magnets

Explore our leading range of EPR systems and accessories:
www.bruker.com/epr

